Superconducting RF cavities for accelerators

Fritz Caspers
all slides by: Wolfgang Weingarten
CERN
JUAS lecture 2012
Archamps/Haute-Savoie

ACKNOWLEDGMENT

- A lot of 'material' from CERN will be used but this does not mean that 'material' from other institutions is considered inferior.
- Other material was taken from contributions to the CERN Accelerator Schools, CAS [1] (CERN-2006-002, CERN-2005-03, CERN-2005-04, CERN-2004-08, CERN-1996-03, CERN-1992-03, as well as earlier ones and other sources mentioned).
  - R. P. Feynman et al., Lectures on Physics Vol. II
  - P. Schmüser et al.; The Superconducting TESLA Cavities; Phys. Rev. Special Topics - AB 3 (9) 092001
  - A. W. Chao & M. Tigner, Handbook of Accelerator Physics and Engineering, World Scientific
  - Alexey Ustinov, Lecture on superconductivity, University Erlangen-Nürnberg (from which I used some slides w.r.t. Superconductivity)

(http://www.pi.uni-karlsruhe.de/ustinov/group_hp/fluxon.physik.uni-erlangen.de/pages/lectures/WS_0708/Superconductivity-2007-01.pdf)

- and an excellent textbook of the field: H. Padamsee, J. Knobloch, and T. Hays, RF Superconductivity for accelerators & H. Padamsee, RF Superconductivity, Weinheim 2008, resp.

[1] http://cdsweb.cern.ch/collection/CERN%20Yellow%20Reports

Last but not least I thank my colleagues E. Haebel and J. Tuckmantel for many discussions, clarifications, and presentation material.

OUTLINE OF LECTURE

- Introduction
- Basics of superconductivity
- Basics of RF cavities
- Interaction of cavity with beam
- Technological issues
- Applications and outlook

Basics of superconductivity

- Recommended Literature
- Historical remarks
- Meissner effect
- Two kinds of superconductors
- Materials
- Two fluid model
- Basics of RF superconductivity
  - The surface resistance
  - Critical fields
  - Field limitations
  - Superheating field
- Summary

Recommended literature

Literature

W. Buckel and R. Kleiner, « Superconductivity: Fundamentals and applications, Wiley VCH 2004

V. V. Schmidt « The physics of superconductors », Springer 1997

M. Tinkham, « Introduction to superconductivity », McGraw-Hill 1996, and many others

Nobel lectures (http://nobelprize.org/nobel_prizes/physics/laureates/)

Historical remarks 1/4

Nobel prize for « his investigations on the properties of matter at low temperatures which led, inter alia, to the production of liquid helium »

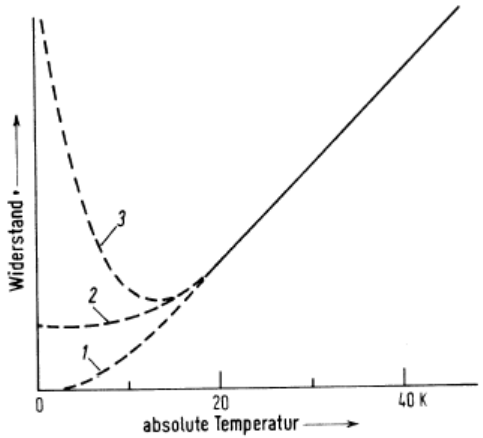

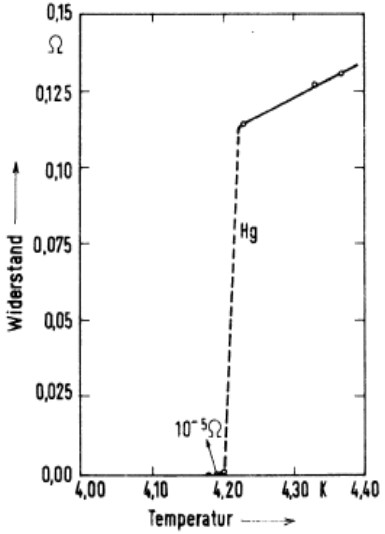

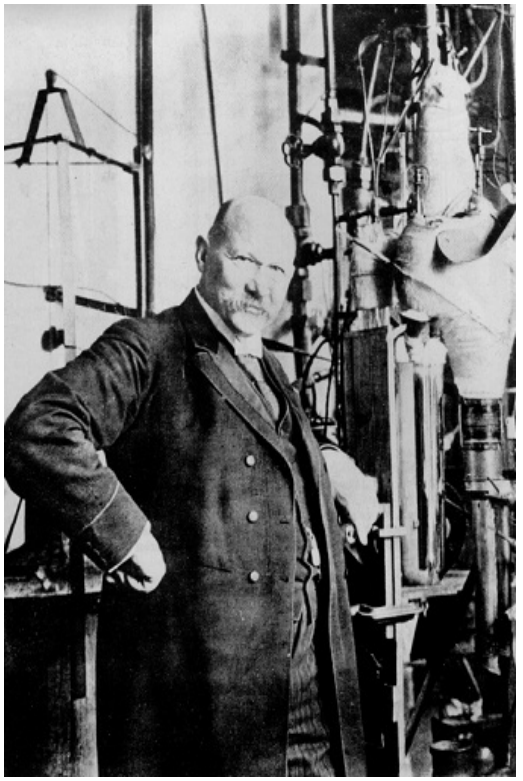

H. Kamerling – Onnes in his laboratory at Leiden (NL)

Historical remarks 2/4

- 1908 Liquefaction of helium (4.2 K)
- 1911 Zero resistance
- 1933 Meissner effect
- 1935 Phenomenological theory of H & F. London
- 1950 Ginzburg – Landau theory
- 1951 – 2 TYPE II superconductors (Abrikosov)
- 1957 Bardeen – Cooper – Schrieffer theory
- 1960 Magnetic flux quantisation
- 1962 Josephson effect
- 1986 High temperature superconductors (Bednorz – Müller)


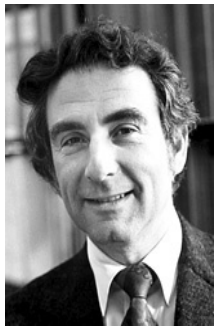
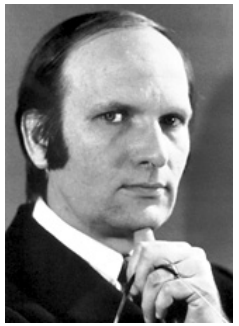

Bardeen – Cooper – Schrieffer (BCS)

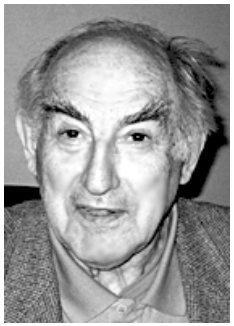

Ginzburg

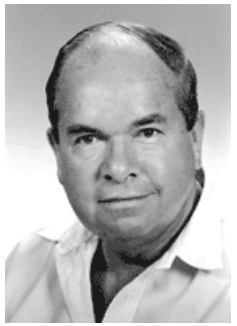

Abrikosov

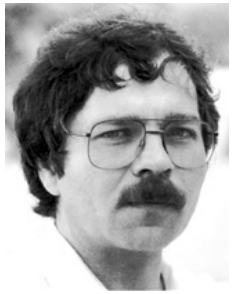

Bednorz

Müller

Historical remarks 3/4

- Zero resistivity
- Meissner effect

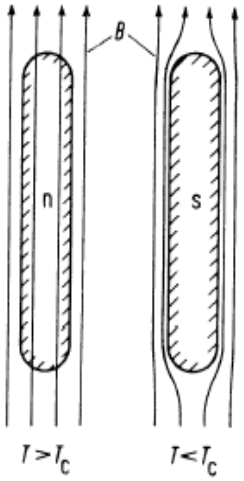

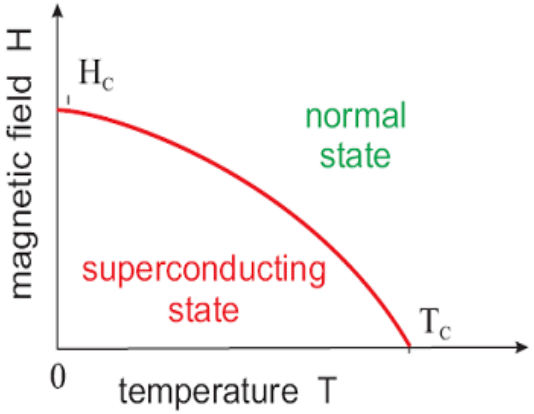

H – *T* diagram for the superconducting state

Superconductivity is destroyed:

- by increasing temperature at $T > T_c$
- by large magnetic field $H > H_c$

$$\frac{H_c(T)}{H_c(0)} = \left[1 - \left(\frac{T}{T_c}\right)^2\right]$$

Historical remarks 4/4

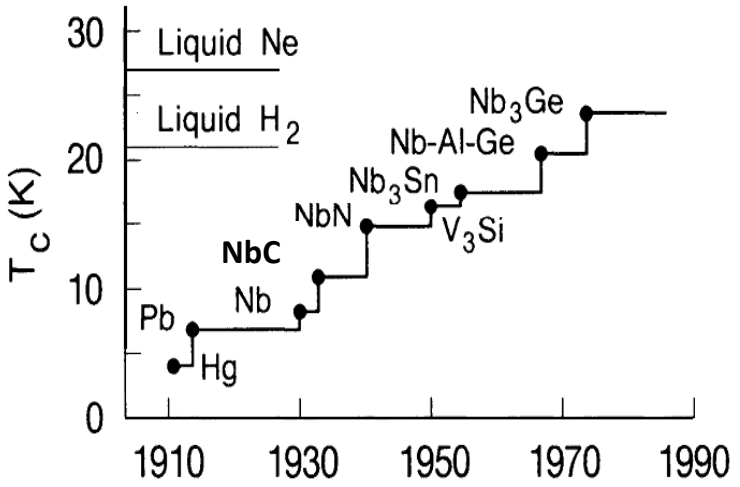

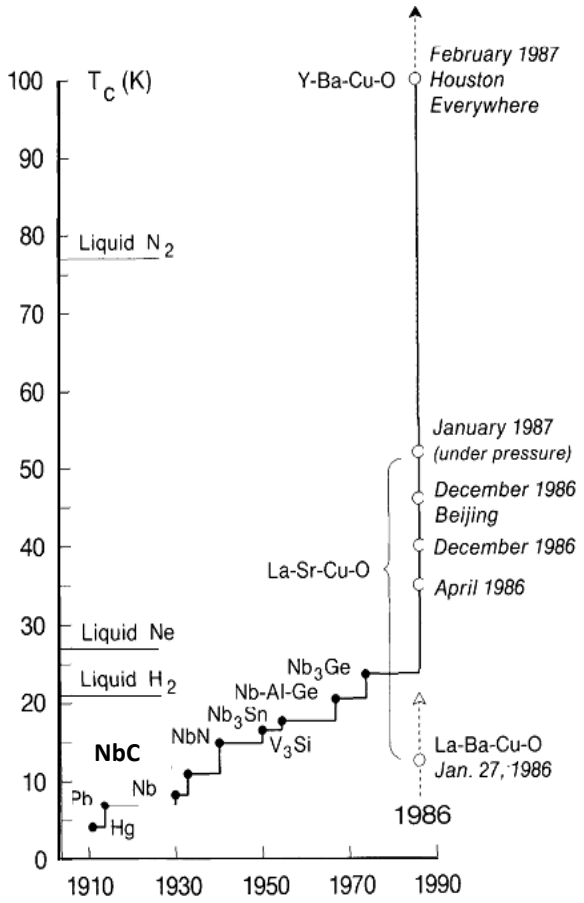

Development of the superconducting transition temperatures after the discovery of the phenomenon in 1911. The materials listed are metals or inter-metallic compounds and reflect the respective highest T_c's - Adapted from G. Bednorz – Nobel lecture

Figure 1.13. Evolution of the superconductive transition temperature subsequent to the discovery of the phenomenon. From [1.29], © 1987 by the American Association for the Advancement of Science.

Meissner effect 1/3

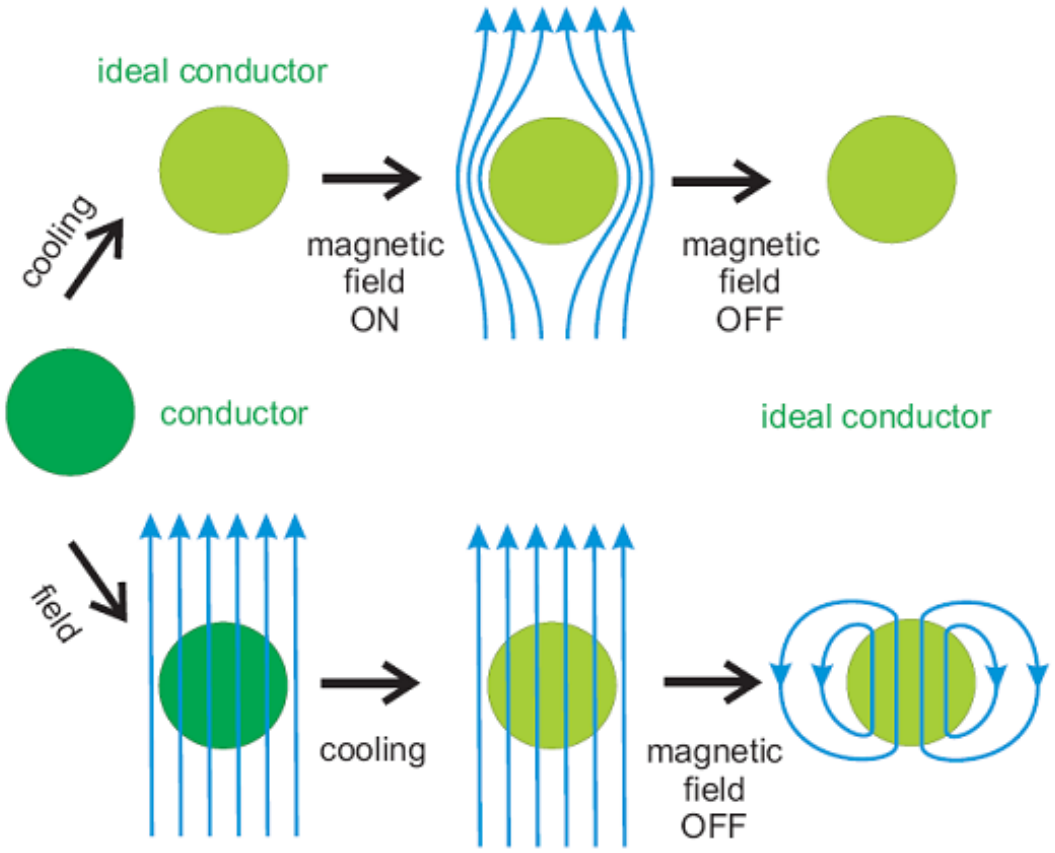

An ideal conductor in magnetic field

Meissner effect 2/3

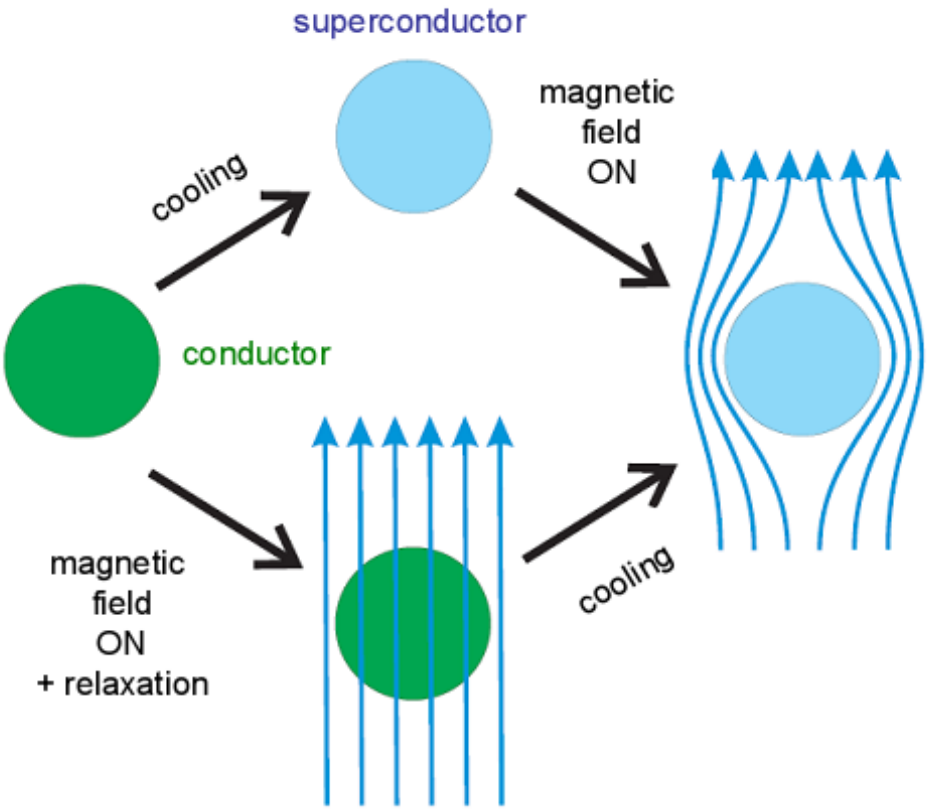

A superconductor in magnetic field

Meissner effect 3/3

1. Magnetic lines of force outside a superconductor are always tangential to its surface

$$\operatorname{div}\vec{B} = 0;$$

$$\text{Since } \vec{B}_n^{(i)} = 0 \Rightarrow \vec{B}_n^{(e)} = 0$$

2. A superconductor in an external magnetic field always carries an electric current near its surface

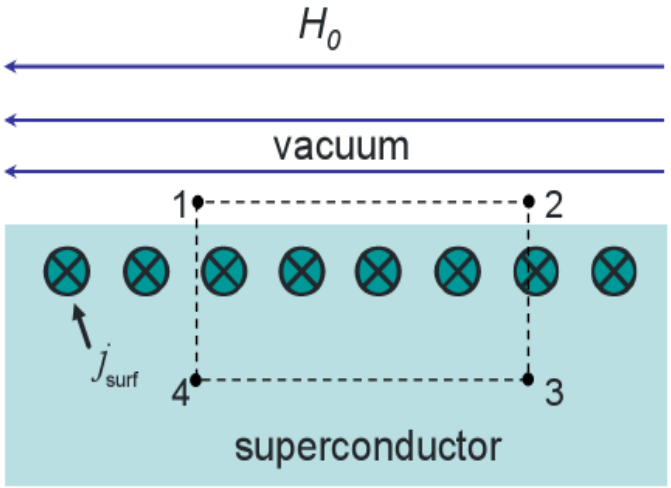

$$\vec{\nabla}\times\vec{B} = \mu_0\vec{j} \Rightarrow \vec{j} = 0 \text{ inside the superconductor}$$

$$\oint \vec{B}\cdot \mathrm{d}\vec{l} = \mu_0 j_{\text{surf}} \cdot l_{1-2}$$

$$\oint \vec{B}\cdot \mathrm{d}\vec{l} = \mu_0 H_0 \cdot l_{1-2} \Rightarrow \vec{j}_{\text{surf}} = \vec{n}\times\vec{H}_0$$

Thus, the surface current is completely defined by the magnetic field at the surface of a superconductor.

Two kinds of superconductors 1/3

Magnetic properties of a **type I superconductor**

Magnetic properties of a superconducto can be derived from $\rho = 0$ and $B = 0$

Type I superconductors are all elemental superconductors (except niobium)

$$\vec{B} = \mu_0 \cdot \left(\vec{H}_0 + \vec{M} \right)$$

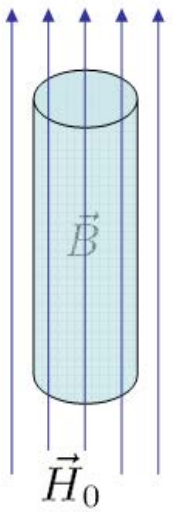

Magnetization curve

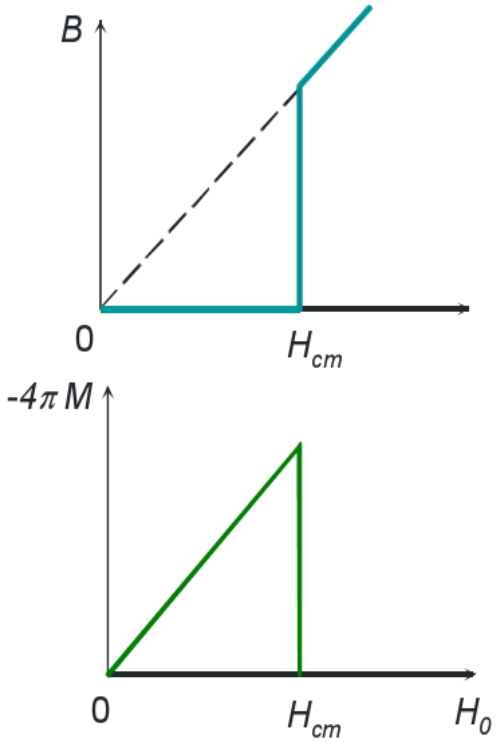

Two kinds of superconductors 2/3

- Type II superconductor

  Magnetic properties of a **type II superconductor**

  Above the 1st critical field H_{c1} magnetic flux penetrates into the bulk

  Above the 2nd critical field H_{c2} the material is normal conducting (except for a thin surface layer that remains superconducting until the 3rd critical field H_{c3})

$$\vec{B} = \mu_0 \cdot \left(\vec{H}_0 + \vec{M} \right)$$

Magnetization curve

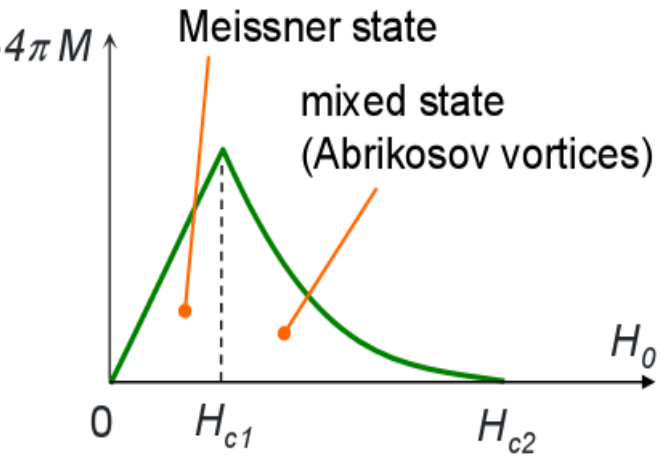

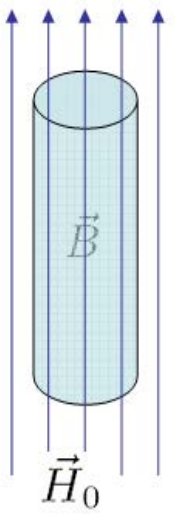

Two kinds of superconductors 3/3

Mixed state of a type II superconductor

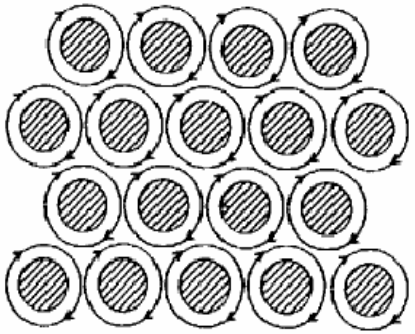

Mixed state (Shubnikov phase) of a type II superconductor consists of a regular lattice of Abrikosov vortices.

Magnetic decoration image of a vortex lattice

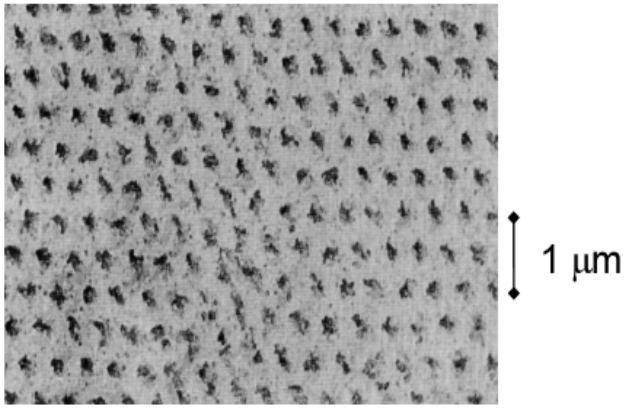

Surface tension at nc-sc interface 1/2

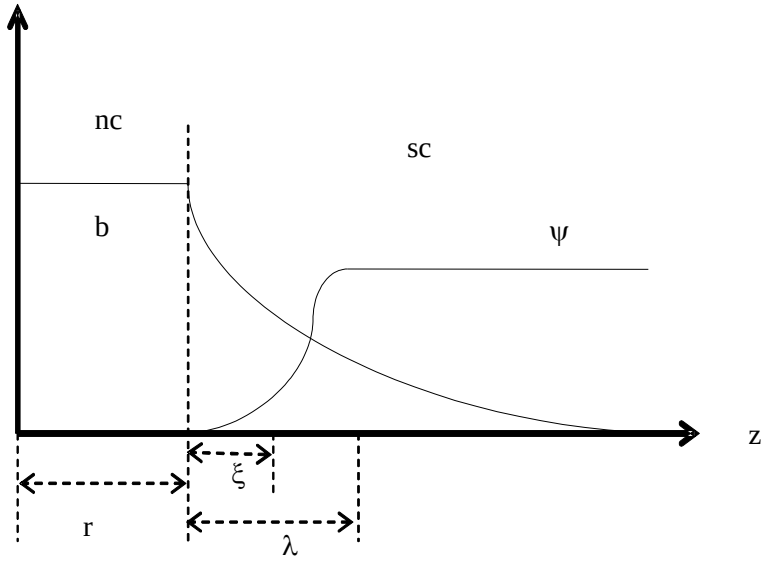

Fig. 1: Interface between normal to superconducting metal for a type II superconductor with $\lambda > \xi$. b denotes the (microscopic) magnetic field and ψ describes the wave function of the superconducting condensate.

Inspecting Fig. 1, the energy balance DE between the condensation energy E_c and the diamagnetic energy E_B for a planar interface area A and an applied magnetic field B, is

$$\Delta E = \Delta E_c - \Delta E_B =$$

$$= \frac{1}{2\mu_0} B_{th}^2 A(r+\xi) - \frac{1}{2\mu_0} B^2 A(r+\lambda)$$

Surface tension at nc-sc interface 2/2

For a type II superconductor, as the penetration of magnetic fields starts from small filaments of cylindrical shape located parallel to the interface, a more realistic way to describe the energy balance is based on a small half-cylinder of radius r instead of a plane, which will become normal:

$$\Delta E = \Delta E_c - \Delta E_B = \frac{1}{2\mu_0}\cdot B_{th}^2 \cdot \frac{\pi}{2}\cdot(r+\xi)^2 - \frac{1}{2\mu_0}\cdot B^2 \cdot \frac{\pi}{2}\cdot(r+\lambda)^2 < 0\,,$$

from which the threshold B^*_{c1} of the magnetic field for penetration is defined as

$$B^*_{c1} \geq \frac{r+\xi}{r+\lambda}\cdot B_{th} \xrightarrow{r\to 0} \frac{\overbrace{\xi}^{1/\kappa}}{\lambda}\cdot B_{th} = \frac{1}{\kappa}\cdot B_{th}\,.$$

In a type II superconductor, the lowest value of the applied magnetic field B which induces penetration as filaments of magnetic field into the bulk is called the lower critical field B_{c1}, for which the microscopic theory gives as exact result:

$$B_{c1} = \frac{\ln\kappa}{\sqrt{2}\cdot\kappa}\cdot B_{th}\,,$$

very close to the previous one. In a type I superconductor, the lowest value of the applied magnetic field B which induces bulk penetration of magnetic field is called the thermodynamic critical field B_{th}

Materials 1/2

pure metals

material	T_c,K	H_c,Oe	year
Al	1.2	105	1933
In	3.4	280	
Sn	3.7	305	
Pb	7.2	803	1913
Nb	9.2	2060	1930

alloys

NbN	15	$1.4\ 10^5$	1940
Nb_3Ge	23	$3.7\ 10^5$	1971

ceramics

material	T_c,K	year
$La_{1.85}Ba_{0.15}CuO_4$	35	1986
$YBa_2Cu_3O_7$	93	1987
$Bi_2Sr_2CaCu_2O_{8+x}$	94	1988
$Ta_2Ba_2Ca_2Cu_3O_{10+x}$	125	1988

Cold liquids required for reaching low temperatures:

helium ^4He (4.2 K)
hydrogen H_2 (20 K)
neon Ne (27 K)
nitrogen N_2 (77 K)

Materials 2/2

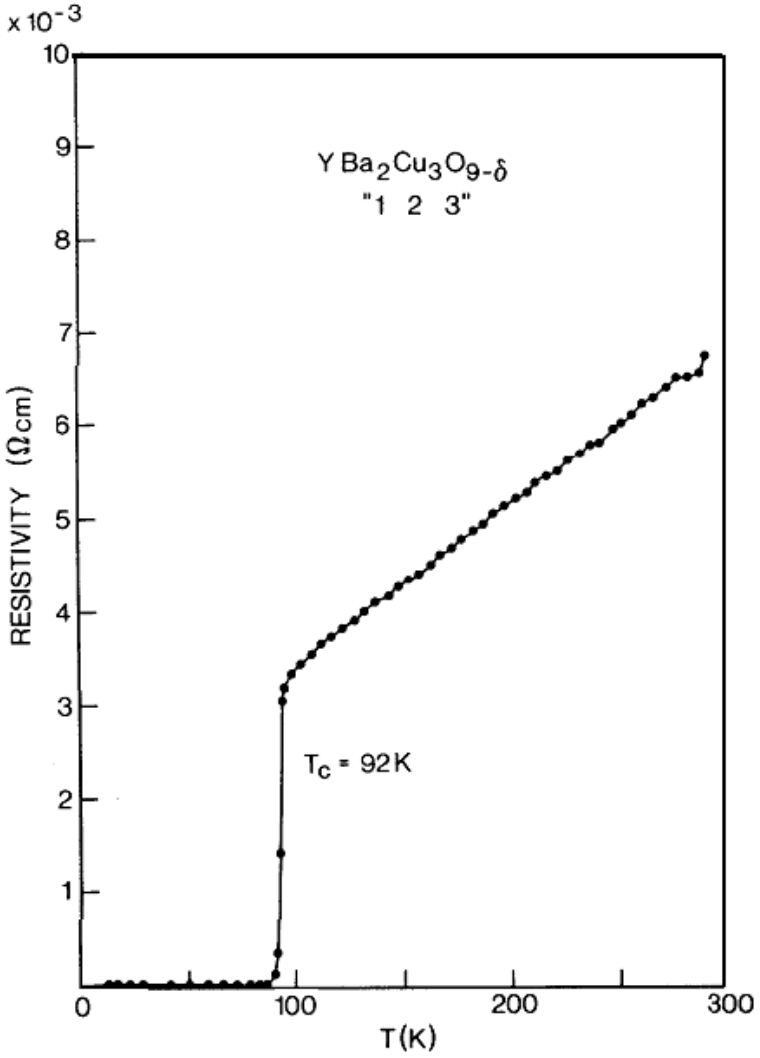

Resistivity of a single-phase $YBa_2Cu_30_7$ sample as a function of temperature.

Two fluid model

Basic ingredients for RF superconductivity

- Two fluid model (Gorter-Casimir)
- Maxwell electrodynamics

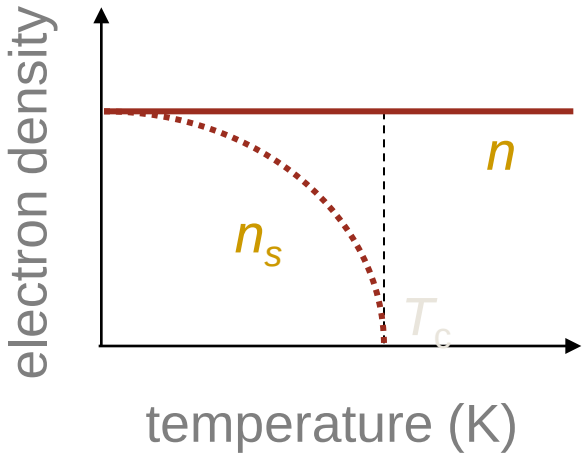

Basic assumptions of two fluid model

- all free electrons of the superconductor are divided into two groups
  - superconducting electrons of density n_s
  - normal electrons of density n_n

The total density of the free electrons is

$n = n_s + n_n$.

As the temperature increases from 0 to T_c, the density n_s decreases from n to 0.

$$n_s/n = 1-(T/T_c)^4$$

RF Superconductivity

1st London equation (Newton's force law without friction)

$$n_s m \frac{\mathrm{d}\vec{v}_s}{\mathrm{d}t} = n_s e \vec{E} \qquad \vec{j}_s = n_s e \vec{v}_s$$

$$\vec{E} = \frac{\mathrm{d}}{\mathrm{d}t}(\Lambda \vec{j}_s) \qquad \Lambda = m/n_s e^2$$

In the stationary state $dj_s/dt = 0$ and hence E = 0 everywhere in the superconductor.

2nd London equation (Meissner effect)

$$\vec{\nabla} \times \vec{E} - \Lambda \cdot \vec{\nabla} \times \frac{d}{dt} \vec{j}_s = 0$$

$$\vec{\nabla} \times \vec{E} = -\frac{d}{dt}\vec{B} \Rightarrow \frac{d}{dt}\vec{B} + \Lambda \cdot \vec{\nabla} \times \frac{d}{dt} \vec{j}_s = 0$$

After integration and taking the integration constant = 0)

$$\Rightarrow \vec{B} = -\Lambda \cdot \vec{\nabla} \times \vec{j}_s$$

Penetration depth 1/2

On introducing the vector potential ***A*** via $\vec{B} = \vec{\nabla} \times \vec{A}$ one obtains a relationship between the supercurrent and the vector potential, very similar to Ohm's law $\vec{j} = \sigma \vec{E}$

$$\Rightarrow \vec{j}_s = -\frac{1}{\Lambda}\vec{A} = -\frac{n_s e^2}{m}\vec{A}$$

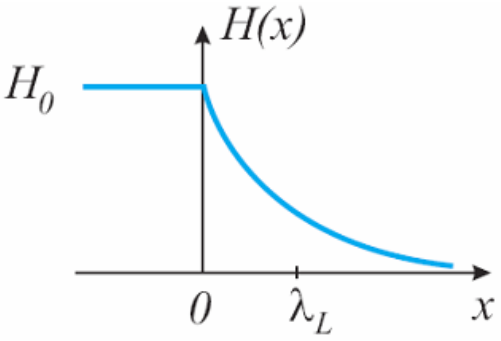

London penetration depth:

Starting from the 2nd London equation

$$\vec{B} + \Lambda \vec{\nabla} \times \vec{j}_s = 0 \Rightarrow \vec{B} + (\Lambda/\mu_0) \underbrace{\vec{\nabla} \times \vec{\nabla} \times}_{\vec{\nabla}\vec{\nabla}\cdot\vec{B} - \Delta\vec{B}} \vec{B} = 0$$

$$\vec{B} - (\Lambda/\mu_0)\Delta\vec{B} = 0 \Rightarrow \vec{B} = \vec{B}_0 \exp(x/\lambda_L)$$

with the London penetration depth $\lambda_L^2 = \Lambda/\mu_0 = m/(n_s e^2 \mu_0)$

Element	Al	Nb (crystal)	Nb (film)	Pb	Sn	YBCO
λ(0), Å	500	470	900	390	510	1700

Penetration depth 2/2

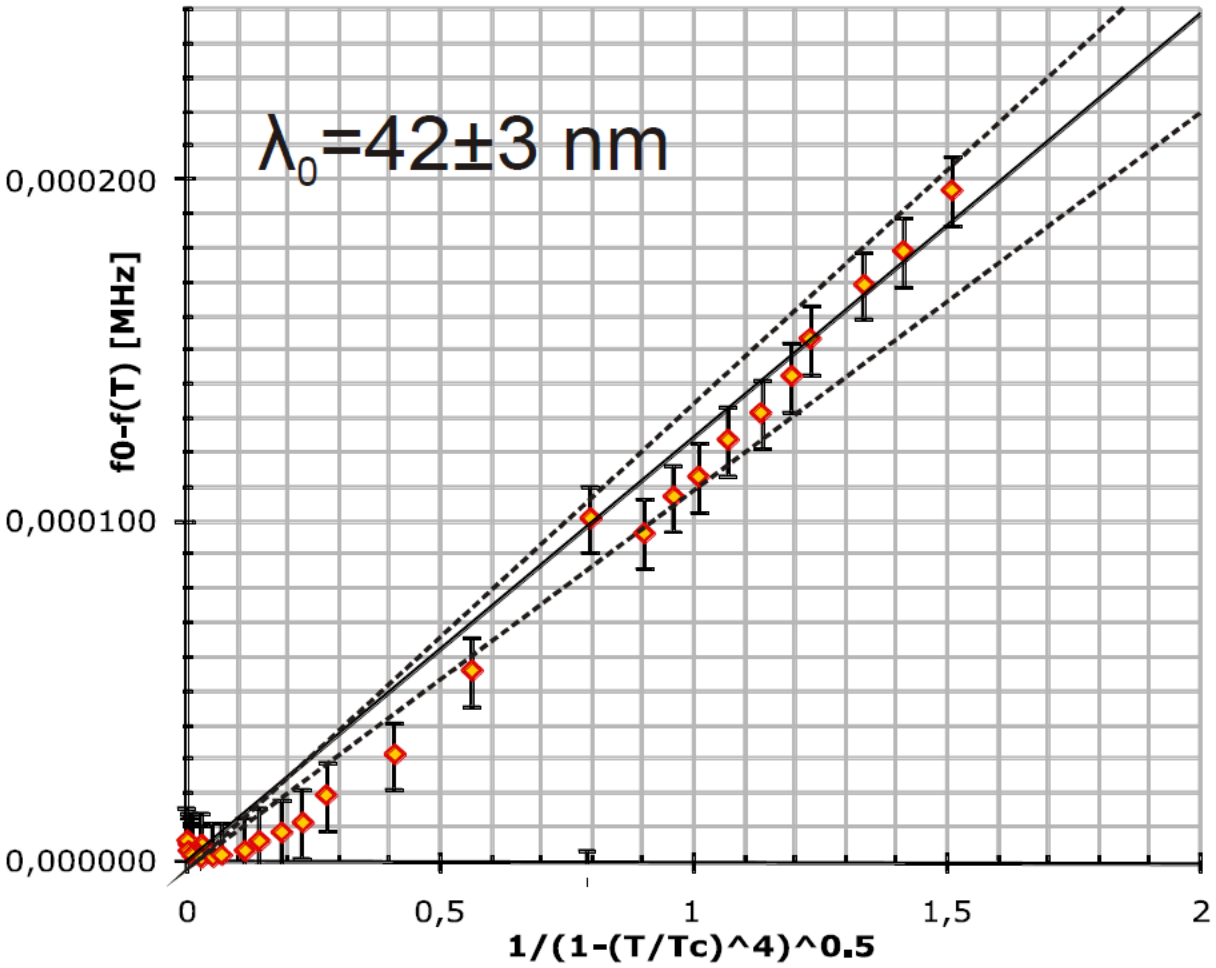

- Measurement and analysis by T. Junginger (CERN Quadrupole Resonator)

Comparison nc-sc

Comparison of superconductor (two-fluid model) with normal conductor

Superconducting metal	Normal-conducting metal
$\text{curl}\ \boldsymbol{H} = \boldsymbol{j} + \varepsilon_0 (\mathrm{d}/\mathrm{d}t)\boldsymbol{E}$ $\text{curl}\ \boldsymbol{E} = -\mu_0 (\mathrm{d}/\mathrm{d}t)\boldsymbol{H}$ $\text{div}\ \boldsymbol{H} = 0$ $\text{div}\ \boldsymbol{E} = 0$	
$(\mathrm{d}/\mathrm{d}t)\,\boldsymbol{j} = \boldsymbol{E}/(\mu_0 \lambda_L^2) + \sigma_n (\mathrm{d}/\mathrm{d}t)\boldsymbol{E}$ $\text{curl}\,\boldsymbol{j} = -\boldsymbol{H}/\lambda_L^2 - \sigma_n \mu_0 (\mathrm{d}/\mathrm{d}t)\boldsymbol{H}$	$\boldsymbol{j} = \sigma_n \boldsymbol{E}$
$\Delta\,\boldsymbol{E} = -K^2 \boldsymbol{E}$ $\Delta\,\boldsymbol{H} = -K^2 \boldsymbol{H}$	
$K^2 = -\lambda_L^{-2}\,(1 + \mathrm{i}\sigma_n \mu_0 \omega \lambda_L^2 - \varepsilon_0 \mu_0 \omega^2 \lambda_L^2)$ $Z_{ssc} = (1/2)\omega^2 \mu_0^2 \lambda_L^3 \sigma_n - \omega \mu_0 \lambda_L$, $\varepsilon_0 \mu_0 \omega^2 \lambda_L^2 \ll \sigma_n \mu_0 \omega \lambda_L^2 \ll 1$.	$K^2 = \varepsilon_0 \mu_0 \omega^2 (1 - \mathrm{i}\sigma_n/(\omega \varepsilon_0))$ $Z_{snc} = (\omega \mu_0 \delta/2)(1 - \mathrm{i}) =$ $\sqrt{[\omega \mu_0/(2\sigma_n)]}(1 - \mathrm{i}),\ \omega \varepsilon_0/\sigma_n \ll 1$.

Effective electron mass m

Electron mean free path l

Conductivity of the nc electrons $\sigma_n = l n_n e^2/(m v_F)$

London penetration depth $\lambda_L = \sqrt{[m/(n_s e^2 \mu_0)]}$

Surface impedance $Z_s = (E_z/H_y)|_{x=0} = \mu_0 \omega/K$

Skin depth $\delta = \sqrt{[2/(\mu_0 \sigma_n \omega)]}$

Fermi velocity v_F

Density of nc electrons n_n

Density of sc electrons n_s

The surface resistance 1/3

The RF magnetic field penetrates this sheet to within the penetration depth λ_L.

According to the Maxwell equation curl $\boldsymbol{E} = -\mathrm{d}\boldsymbol{B}/\mathrm{d}t$, the RF magnetic field is accompanied by an electric field

$E_y = j\omega\lambda_L B_z = j\omega\lambda_L \mu_0 H_z = j\omega\lambda_L\mu_0 H_{z0} \exp(-x/\lambda_L)$.

The electric field interacts with the nc electrons (still present at non-zero temperatures) and gives rise to a power dissipation per square meter

$$P_c = (\sigma_n/2)\int_0^\infty E_y^2(x)\mathrm{d}x = (1/4)\lambda_L \sigma_n E_{y0}^2 = (1/4)\omega^2\mu_0^2\lambda_L^3\sigma_n H_{z0}^2$$

with $\sigma_n = \sigma_0(T/T_c)^4$, σ_0 being the conductivity of the nc electrons just above T_c, By definition, $P_c = (1/2)\, R_s\, H_z^2$, and we obtain for the surface resistance R_s in the two-fluid model approximation,

$$R_s = \frac{1}{2}\omega^2\mu_0^2\lambda_L^3\sigma_n = \frac{1}{2}\omega^2\mu_0^2\lambda_L^3\sigma_0\left(\frac{T}{T_c}\right)^4$$

which can be approximated for $T<T_c/2$

$$R_s = (A/T)\omega^2 \exp(-\Delta/kT),\ 2\Delta \approx 3.5kT_c$$

$$R_s^{BCS}[\mathrm{n\Omega}] \approx 10^5 \cdot (f[\mathrm{GHz}])^2 \cdot \frac{\exp\left(-\frac{18}{T[\mathrm{K}]}\right)}{T[\mathrm{K}]}$$

The surface resistance 2/3

- Dependence of R_s on T and f

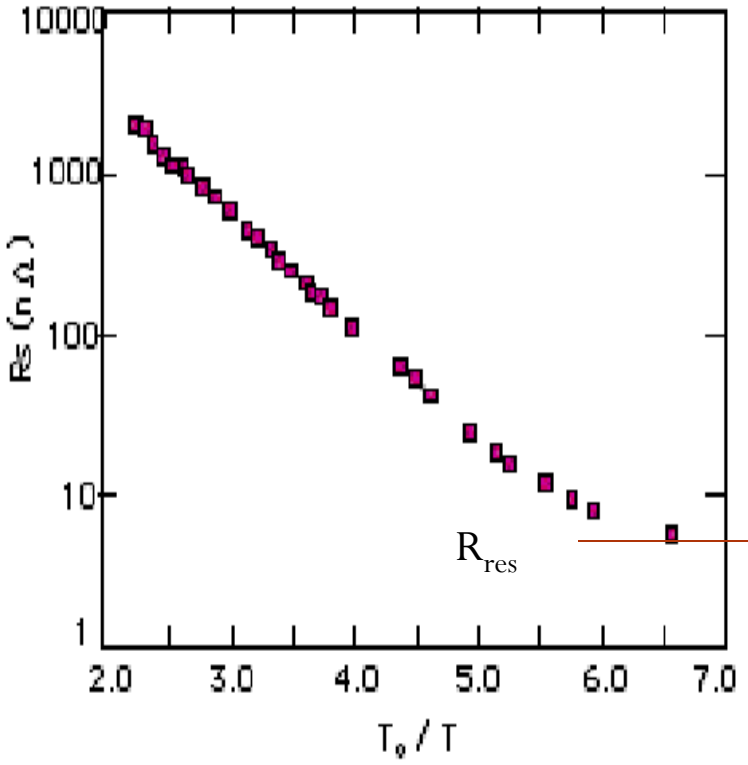

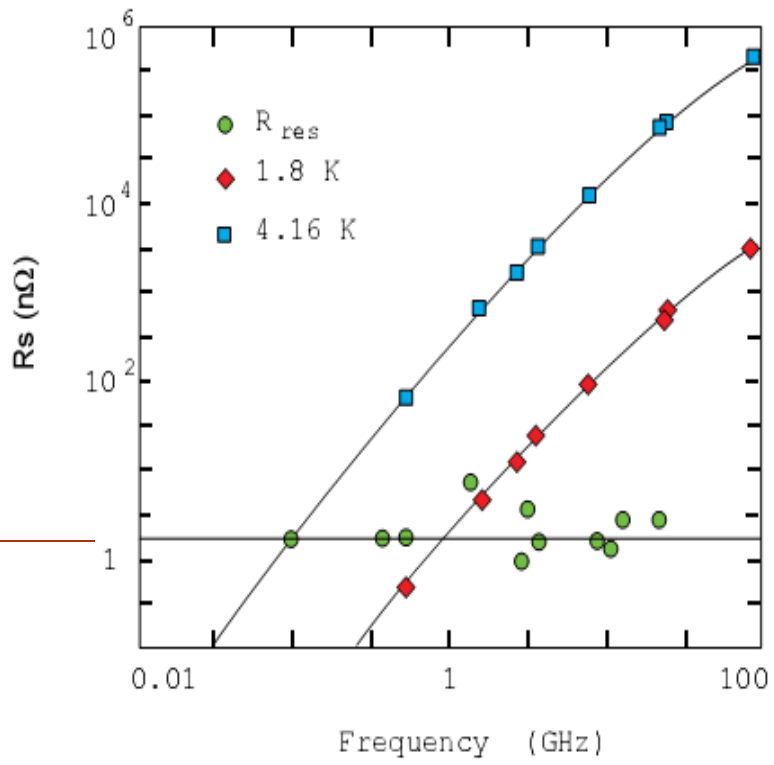

The surface resistance 3/3

- Material parameter dependence of $R_s\,(T, f)$

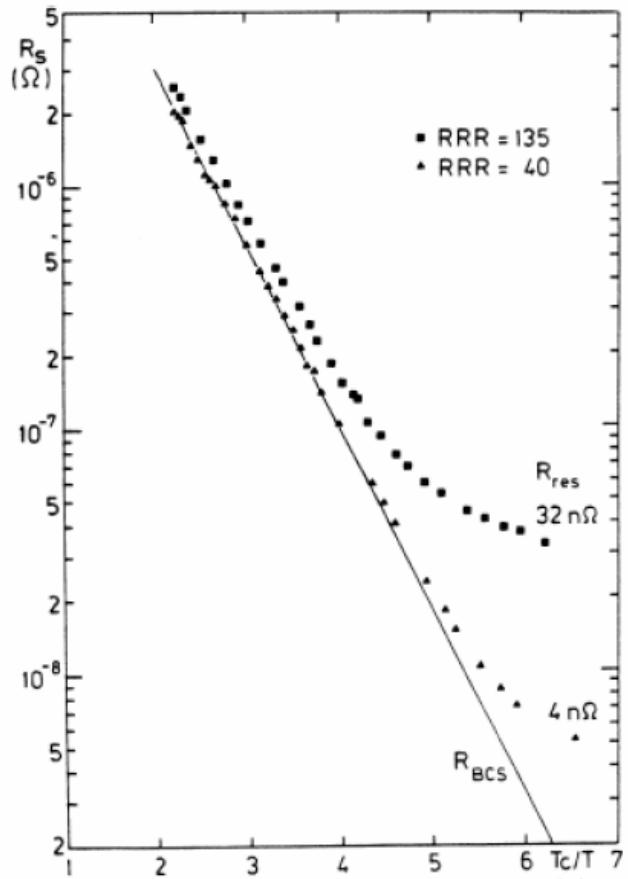

Fig. 2: Surface resistance $R_s(T)$ of two 3 GHz cavities, fabricated from niobium of different purity. $R_s(T)$ is the sum of the temperature dependent part R_{BCS} and the residual resistance R_{res}.

$$R_s^{BCS}(\omega, T) = \frac{A}{T}\omega^2 \exp\left(-\frac{\Delta}{kT}\right)$$

$$2\Delta \approx 3.5 \cdot kT_c$$

A depends on the material

$$R_s = R_s^{BCS} + R_{res}$$

Critical field (s)

Critical field of superconductors studied for RF

Material	T_c [K]	B_{cth0} [mT]	B_{c10} [mT]	B_{c20} [mT]	B_{sh0} [mT]	B_{exp0} [mT]
Sn	3.7	30.9	–	–	68	30.6
In	3.4	29.3	–	–	104	28.4
Pb	7.2	80.4	–	–	105	112
Nb	9.2	200	185	420	240	160
Nb_3Sn	18.2	535	≈ 20	2400	400	106

Critical fields in DC and RF superconductivity

B_c	Critical magnetic field of type-I superconductor
B_{c1}	Lower critical magnetic field of type-II superconductor
B_{c2}	Upper critical magnetic field of type-II superconductor
B_{cth}	Thermodynamic critical field
B_{sh}	Superheating critical field
B_{exp}	Experimentally obtained maximum field in RF

An index "0" following any of the above symbols refers to the temperature T = 0 K, tacitly assuming $B(T) = B_0 [1 - (T/T_c)^2]$.

Superheating field

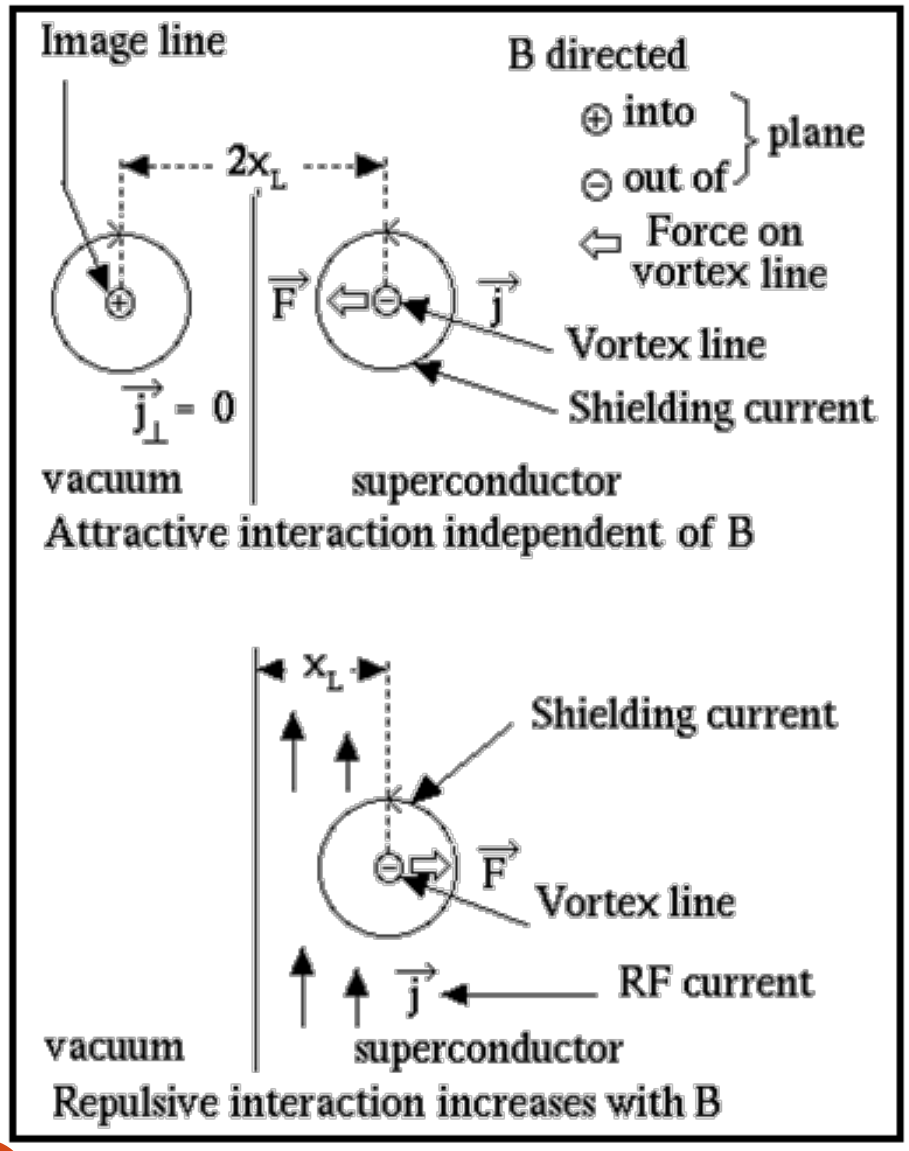

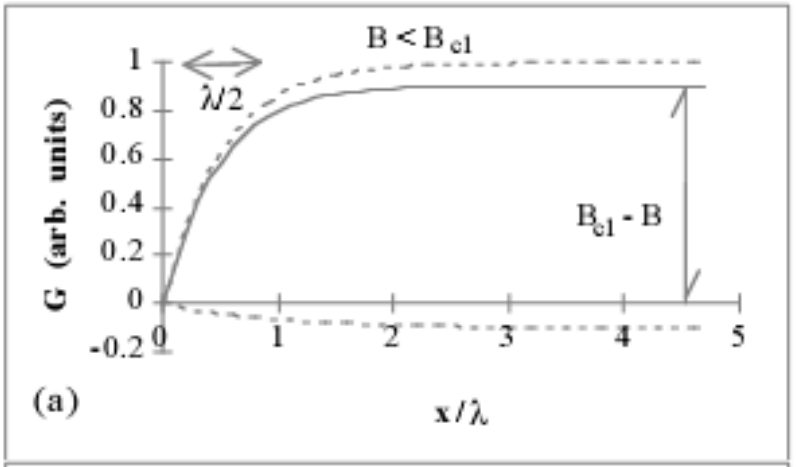

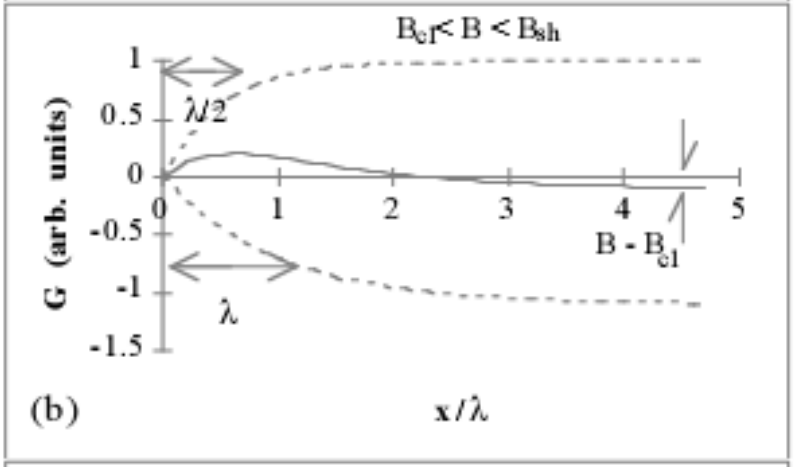

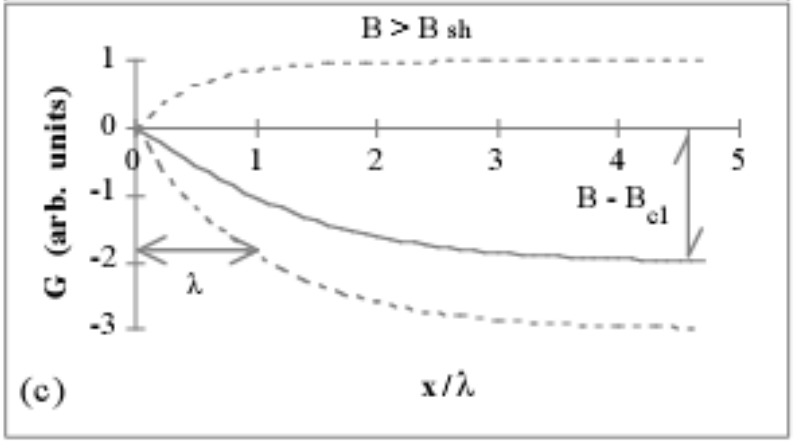

Field limitations in RF 1/3

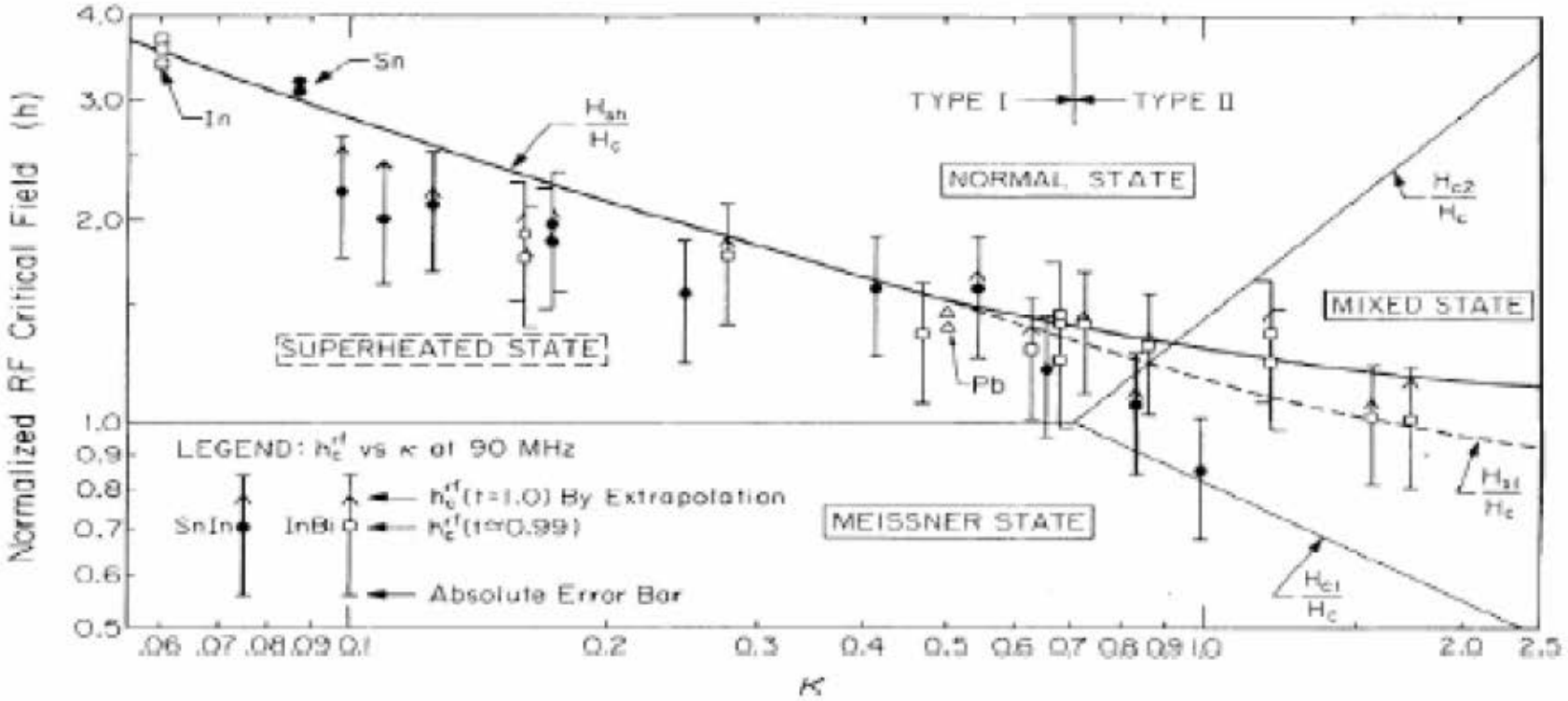

Figure 7: Measurements on the radiofrequency critical magnetic field in different superconducting alloys (SnIn, InBi) as a function of the Ginzburg-Landau parameter κ for temperatures near T_c [Yogi et al. 1977]. The curve $\frac{H_{sh}}{H_c}$ denotes the calculation by [Matricon and Saint-James 1967].

Field limitations in RF 2/3

There is experimental evidence that the **super-heating field** is the ultimate limitation in RF

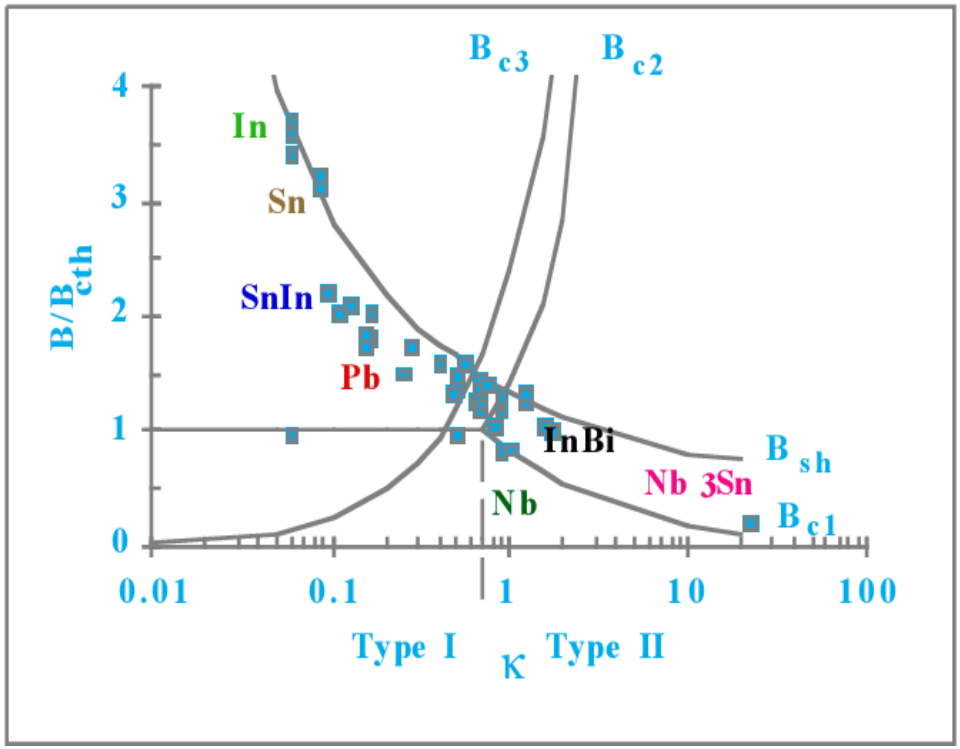

Mate-rial	κ	B_{cth0} [mT]	B_{exp}/B_{cth}
Sn	0.086	30.9	3.11 3.24
In	0.06	29.3	3.41 3.61 3.72 0.953
Pb	0.5	80.4	0.98 1.38 1.46
Nb	0.9	~ 200	0.815 1.17 1.96
Nb_3Sn	22.8	~ 535	0.199
SnIn	0.1- 1.0		2.2 - 0.85
InBi	0.16- 1.74		1.84- 1.01

B_{cth} thermodynamic critical field
B_{exp} experimentally obtained maximum field in RF
The index '0' refers to the temperature $T = 0$ K.

Field limitations in RF 3/3

- Measurements at CERN with "Quadrupole Resonator"

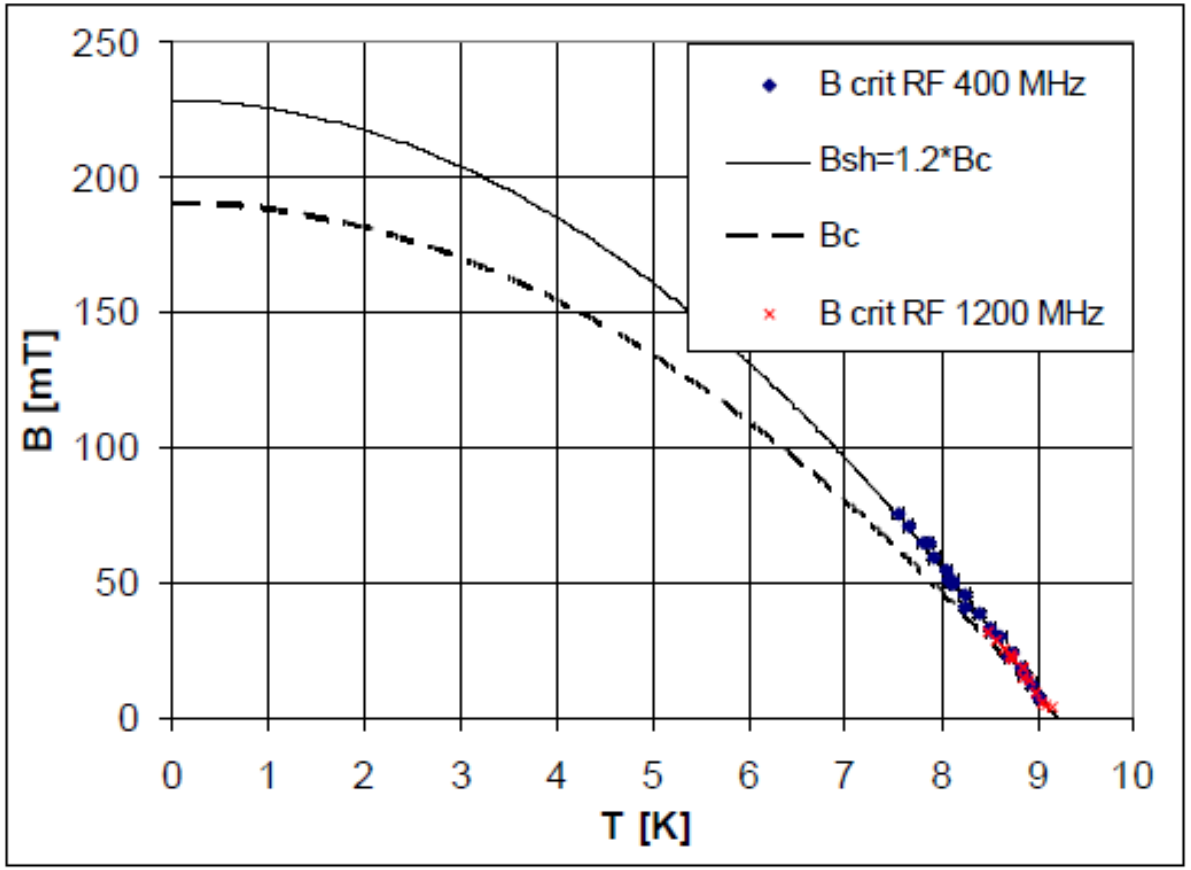

Courtesy: Tobias.Junginger@quasar-group.org

Thin Film Workshop
http://surfacetreatments.it/thinfilms/

Other deterministic parameters for cavity performance

Up till now we discussed the role of the RF frequency, lHe bath temperature, and sc material with its characteristic critical field and temperature. There are still other (less important) parameters that determine the performance of the cavity as well:

Influencing quantity	**Impact quantity**	**Physical explanation**	**Cure**
External static magnetic field B_{ext}	Residual surface resistance	Creation of vortices	Shielding of ambient magnetic field by Mu-metal / Cryoperm
Residual resistivity ratio *RRR*	BCS surface resistance	Mean free path dependence of R_{res}	Annealing steps during ingot production/after cavity manufacture
Ratio peak magnetic field to accelerating gradient B_p/E_a	Max. accelerating gradient	Critical magnetic field as ultimate gradient limitation	Optimization of cavity shape
Nb-H precipitate	Q-value / acc. gradient (Q-disease)	Lowering of T_c/B_c at precipitates of Nb-H	T-control during chemical polishing Degassing @ 700 °C Fast cool-down

Summary

Superconducting materials:

- are characterized by zero resistivity (in DC) and the Meissner effect;
- Show the (thermodynamic) phase transition into the superconding state below a critical temperature and below a critical field;
- have a non-zero surface resistance for RF which can be understood by the two-fluid model and the London theory
- are subdivided into type I and type II, depending on the value of the Ginzburg-Landau parameter κ;
- may be alloys or elements, for which they are of type I, except Nb, the technically most important one, which is type II and has the largest critical temperature and critical field;
- Seem to be ultimately limited for RF applications (accelerating gradient) by the super-heating field.

Basics of RF cavities

- Variety of RF cavities (examples)
- Cavity characteristics
  - Pillbox resonator
  - Field distribution
  - Pillbox resonator as accelerating cavity
  - Cavity characteristics (peak fields, stored energy, …)
  - Computer codes to determine the cavity parameters
  - Different mode families
- Transmission line
- Response of a sc cavity to RF (determination of Q_0, E_{acc}, …)
- Measuring setup ($Q(E_{acc})$ curve, …)
- Pass-band modes
- Typical example of storage ring cavity (LEP)
- Summary

Examples of RF cavities

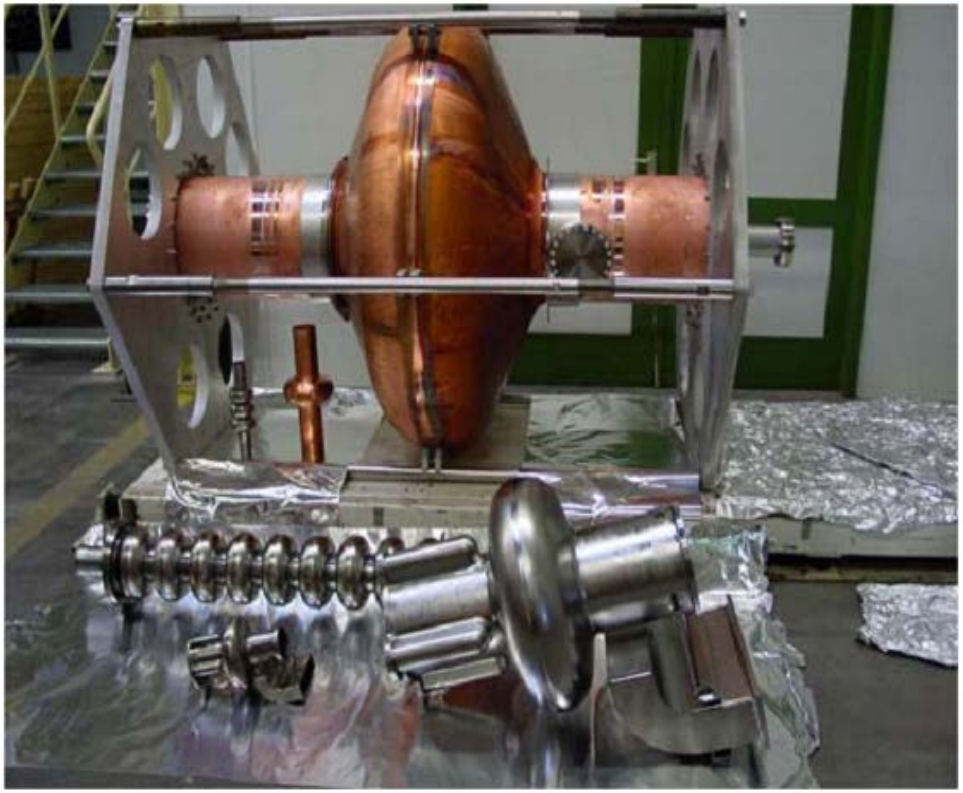

Fig. 1 A spectrum of superconducting cavities.

(from H. Padamsee, CERN-2004-008)

Pill box resonator

Source: The Feynman Lectures on Physics, Vol. II

Starting point: Capacitor

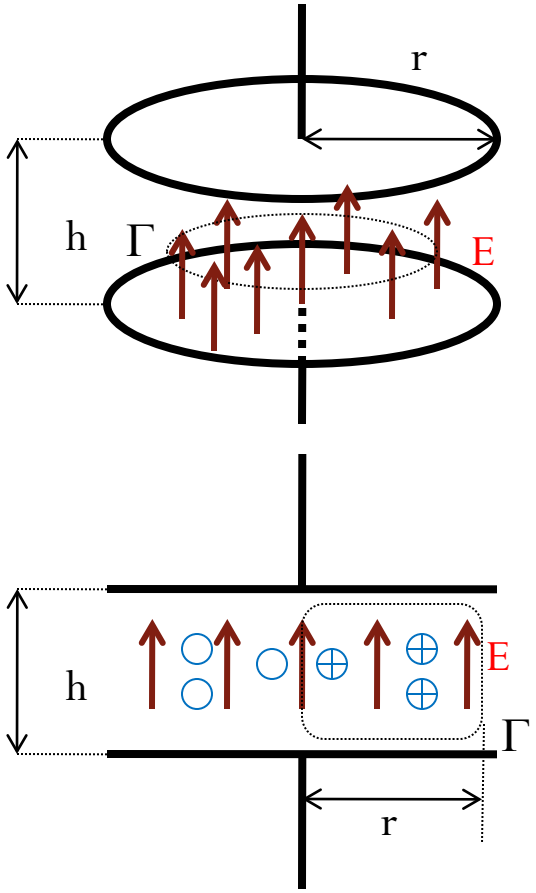

Assumption
E_0=constant

$$\vec{E} = \vec{E}_0 \cdot \mathrm{e}^{\mathrm{i}\omega t}$$

$$c^2 \oint_{\Gamma} \vec{B} \cdot d\vec{s} = \frac{\partial}{\partial t} \int_{\text{inside } \Gamma} \vec{E} \cdot \vec{n} da$$

$$c^2 B \cdot 2\pi r = \frac{\partial}{\partial t} E \cdot \pi r^2$$

$$B = \frac{\mathrm{i}\omega r}{2c^2} \cdot E_0 \mathrm{e}^{\mathrm{i}\omega t}$$

$$E = E_0 + E_1$$

E_1 is the first correction to E_0 due to the time varying field

$$\oint_{\Gamma} \vec{E} \cdot d\vec{s} = -\frac{\partial}{\partial t}(\text{flux of } B)$$

$$E_2(r) \cdot h = h \cdot \int B(r) dr = -h \cdot \frac{\omega^2 r^2}{4c^2} E_0 \mathrm{e}^{\mathrm{i}\omega t}$$

$$\Rightarrow E = E_1 + E_2 = \left(1 - \frac{\omega^2 r^2}{4c^2}\right) \cdot E_0 \mathrm{e}^{\mathrm{i}\omega t}$$

Field distribution 1/2

$$\Rightarrow E = \left(1 - \frac{1}{2^2}\left(\frac{\omega r}{c}\right)^2 + \frac{1}{2^2 \cdot 4^2}\left(\frac{\omega r}{c}\right)^4 - \frac{1}{2^2 \cdot 4^2 \cdot 6^2}\left(\frac{\omega r}{c}\right)^6\right) \cdot E_0 e^{i\omega t} =$$

$$= \left(1 - \frac{1}{(1!)^2}\left(\frac{\omega r}{2c}\right)^2 + \frac{1}{(2!)^2}\left(\frac{\omega r}{2c}\right)^4 - \frac{1}{(3!)^2}\left(\frac{\omega r}{2c}\right)^6 + \right) \cdot E_0 e^{i\omega t} =$$

$$= J_0\left(\frac{\omega r}{c}\right) \cdot E_0 e^{i\omega t}$$

Resonance-condition

$$\frac{\omega_0 \cdot R}{c} = 2.405$$

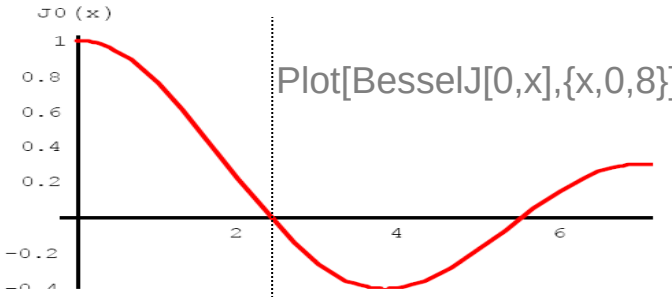

Plot[BesselJ[0,x],{x,0,8}]

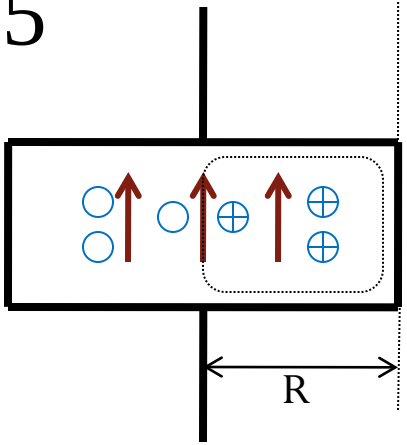

TM_{010} mode

Field distribution 2/2

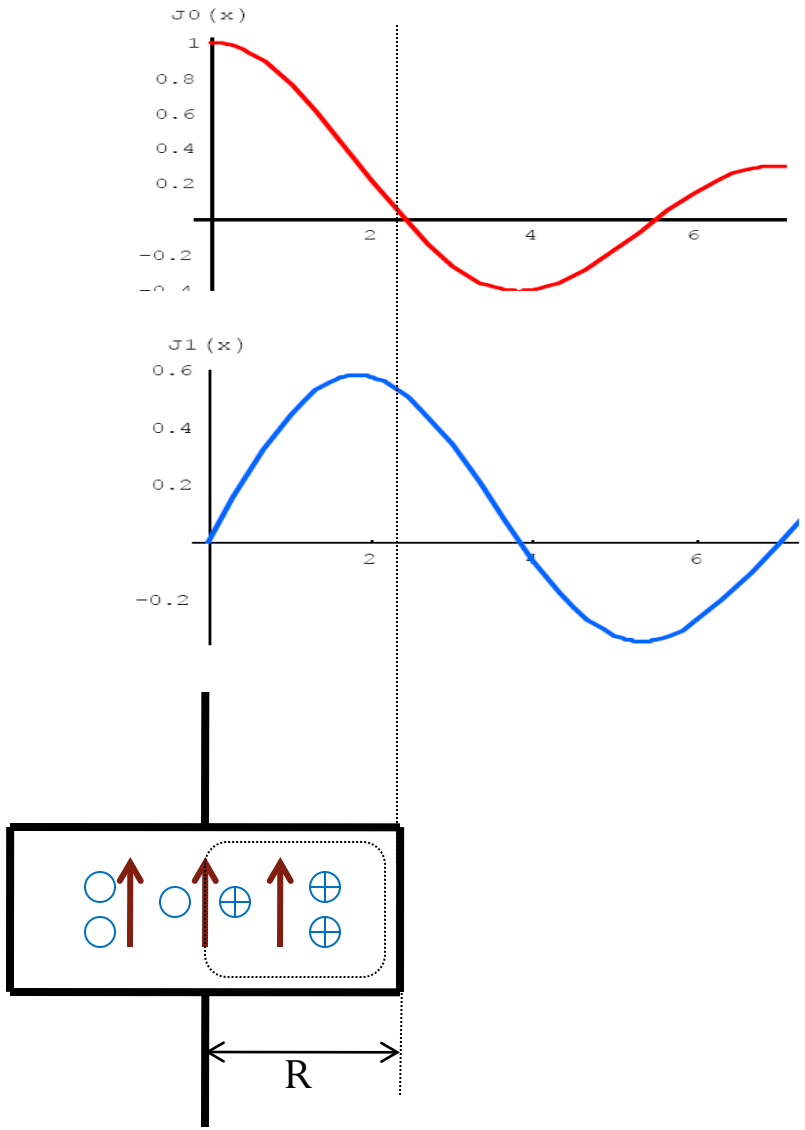

$$E = J_0\left(\frac{2.405 \cdot r}{R}\right) \cdot E_0 e^{i\omega_0 t}$$

$$c^2 \oint_{\Gamma} \vec{B} \cdot d\vec{s} = \frac{\partial}{\partial t} \int_{\text{inside } \Gamma} \vec{E} \cdot \vec{n} da$$

$$c^2 B_\varphi(r) \cdot 2\pi r = i\omega \int_0^{2\pi} d\varphi \int_{\text{inside } \Gamma} E(r) \cdot r dr$$

$$\Rightarrow B_\varphi(r) = \frac{i}{c} J_1\left(\frac{2.405 \cdot r}{R}\right) \cdot E_0 e^{i\omega_0 t}$$

Pill box resonator as accelerating cavity

How to accelerate a particle beam with a pillbox resonator?

The unavoidable beam tube opening is considered to be small compared to *l*

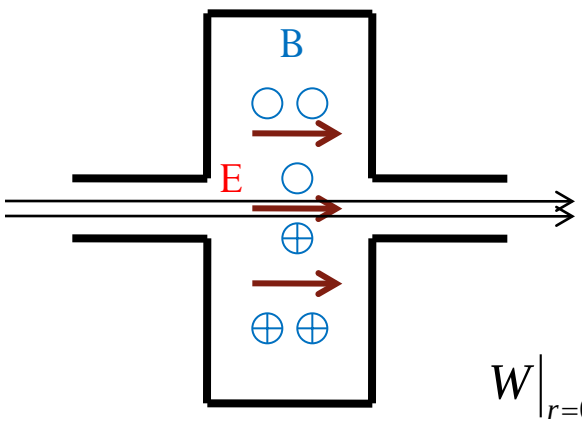

$$E(r,t) = J_0\left(\frac{2.405 \cdot r}{R}\right) \cdot E_0 \sin(\omega_0 \cdot t)$$

$$t(z) = z/(\beta \cdot c)$$

$$W\big|_{r=0} = e\int_0^h E(r=0,t(z))dz = eE_0 \cdot \int_0^h \sin(\omega_0 \cdot z/(\beta \cdot c))dz =$$

$$h = \beta \cdot \frac{\lambda}{2}$$

$$V_a = \frac{W}{e} = \frac{E_a \cdot h}{e} = E_0 \cdot \frac{2}{\pi} \cdot h \Rightarrow E_a = \frac{2E_0}{\pi}$$

Cavity characteristics 1/6

The **peak surface electric and magnetic fields** constitute the ultimate limit for the accelerating gradient => minimize the ratio E_p/E_a and B_p/E_a.

Remember:

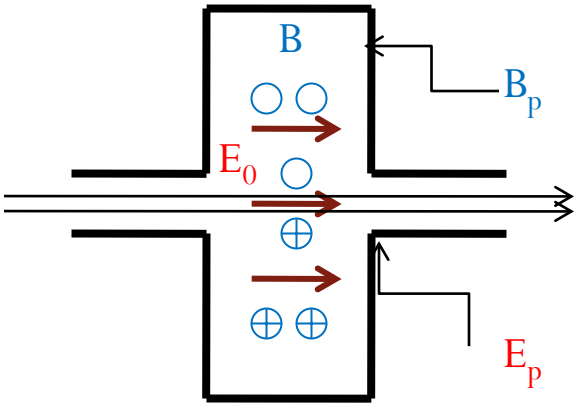

$$E = J_0\left(\frac{2.405\cdot r}{R}\right)\cdot E_0 e^{i\omega_0 t}$$

$$B_\varphi(r) = \frac{i}{c} J_1\left(\frac{2.405\cdot r}{R}\right)\cdot E_0 e^{i\omega_0 t}$$

$$E_a = \frac{2E_0}{\pi}$$

$$\frac{B_p}{E_a} = \underset{r\in[0,R]}{Max}\frac{\frac{1}{c}J_1\left(\frac{2.405\cdot r}{R}\right)\cdot E_0}{\frac{2E_0}{\pi}} = \frac{0.581865\cdot\pi}{2\cdot c} \approx 3.07\left[\frac{\text{mT}}{\text{MV/m}}\right]$$

$$\frac{E_p}{E_a} = \underset{r\in[0,R]}{Max}\frac{J_0\left(\frac{2.405\cdot r}{R}\right)\cdot E_0}{\frac{2E_0}{\pi}} = \frac{\pi}{2} \approx 1.57$$

Cavity characteristics 2/6

Stored energy U

$$U = \frac{\varepsilon_0}{2}\int_0^{2\pi} d\varphi \int_0^{h} dz \int_0^{R} r dr \cdot |E(r)|^2 =$$

$$= \frac{\varepsilon_0}{2}\int_0^{2\pi} d\varphi \int_0^{h} dz \int_0^{R} r dr \left| J_0\left(\frac{2.405 \cdot r}{R}\right)\right|^2 \cdot |E_0|^2 =$$

$$= \frac{\varepsilon_0}{2} \cdot \underbrace{\pi R^2 h}_{V} \cdot \left| \underbrace{J_1(2.405)}_{0.581865} \right|^2 |E_0|^2$$

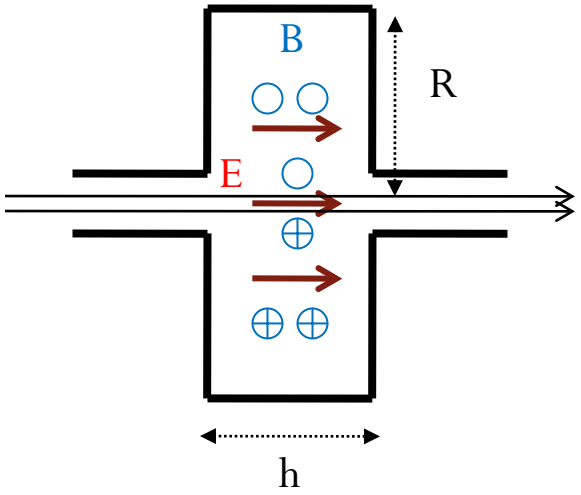

Cavity characteristics 3/6

Power loss

$$P = \frac{R_s}{2\mu_0^2}\int_0^{2\pi} d\varphi \cdot \left(\int_0^h dz \left|B_\varphi(R)\right|^2 + 2 \cdot \int_0^R r dr \left|B_\varphi(r)\right|^2 \right) =$$

$$= \frac{R_s}{2\mu_0^2}\frac{1}{c^2}\left|E_0\right|^2 \int_0^{2\pi} d\varphi \cdot \left(R\int_0^h dz \left|J_1(2.405)\right|^2 + 2 \cdot \underbrace{\int_0^R r dr \left| J_1\left(\frac{2.405 \cdot r}{R}\right)\right|^2}_{\frac{1}{2}R^2\left|J_1(2.405)\right|^2} \right) =$$

$$= R_s \frac{1}{\eta^2}\left|E_0\right|^2 \cdot \pi R \cdot (h+R) \cdot \left| \underbrace{J_1(2.405)}_{0.581865} \right|^2 ; \qquad \eta = \sqrt{\frac{\mu_0}{\varepsilon_0}}$$

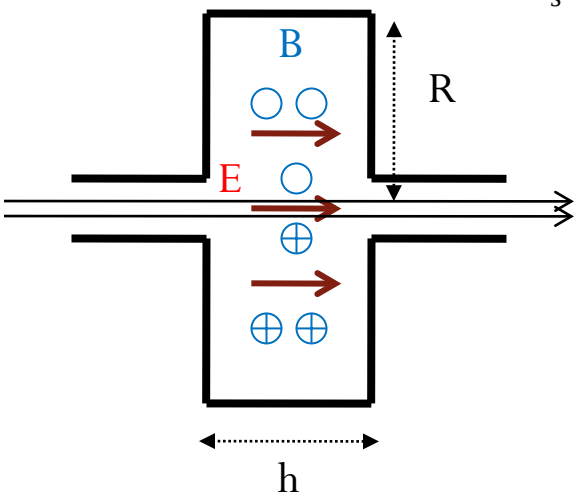

Cavity characteristics 4/6

The **Q-factor** measures the dissipation of the stored energy to the cavity wall consequent to the unavoidable surface currents associated with that stored energy.

$$Q = \frac{\text{Stored energy } U}{\text{Energy lost during 1 RF period}} = \frac{\text{Stored energy } U}{\Delta U/(2\pi)} =$$

$$= 2\pi \cdot \frac{\text{Stored energy } U}{\text{Dissipated power } P \cdot \underbrace{T}_{f^{-1}}} = \underbrace{2\pi f}_{\omega} \cdot \frac{\text{Stored energy } U}{P} = \omega \cdot \frac{U}{P}$$

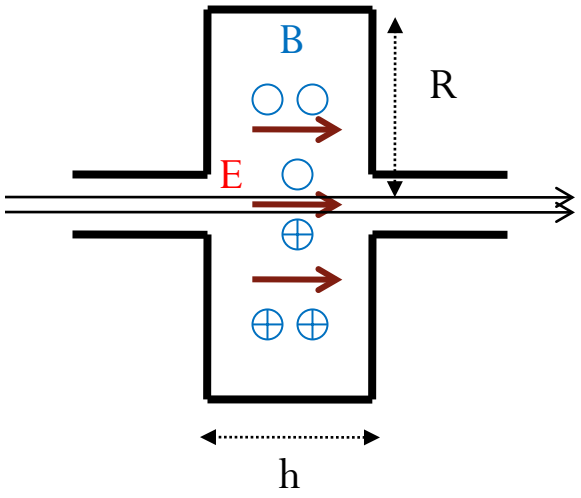

$$Q = \omega \cdot \frac{\varepsilon_0 \cdot \eta^2}{2R_s \cdot \left(\frac{1}{R} + \frac{1}{h}\right)} =$$

$$= \frac{1}{R_s} \cdot \underbrace{\eta \cdot \frac{2.405}{2\left(1 + \frac{R}{h}\right)}}_{=G\ (\text{Geometry-factor})} = \frac{G}{R_s}$$

$$\frac{\omega_0 \cdot R}{c} = 2.405$$

$$\eta = \sqrt{\frac{\mu_0}{\varepsilon_0}}$$

$$G \approx 260\,\Omega$$

Cavity characteristics 5/6

The **shunt impedance *R*** measures the acceleration action of the beam of charged particles in terms of the unavoidable dissipation of energy in the cavity wall.

$$R = \frac{V_a^2}{2 \cdot P} = \frac{\left(E_0 \cdot \frac{2}{\pi} \cdot h \right)^2}{2 \cdot R_s \frac{1}{\eta^2} \left| E_0 \right|^2 \cdot \pi R \cdot (h + R) \cdot \left| \underbrace{J_1(2.405)}_{0.581865} \right|^2} =$$

$$= \frac{2\eta^2}{R_s \cdot \pi^3 \frac{R}{h} \cdot \left(1 + \frac{R}{h} \right) \cdot \left| \underbrace{J_1(2.405)}_{0.581865} \right|^2}$$

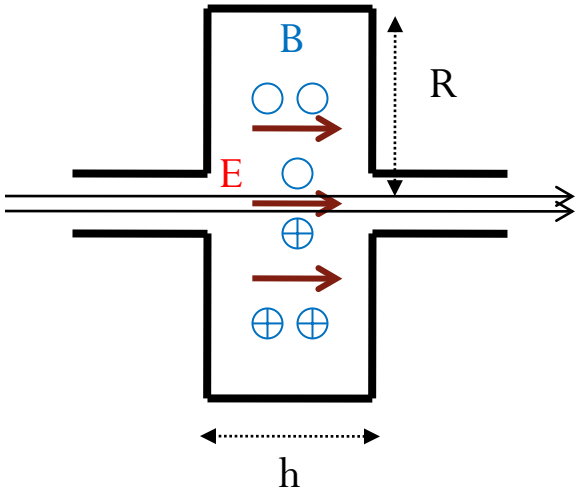

Cavity characteristics 6/6

The quantity R/Q measures the interaction of the cavity with the beam.

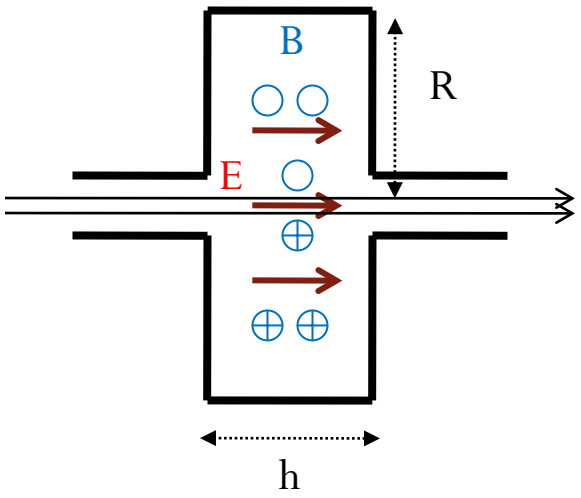

$$\frac{R}{Q} = \frac{V_a^2}{\underbrace{2 \cdot P}_{R}} \cdot \frac{P}{\underbrace{\omega \cdot U}_{1/Q}} = \frac{V_a^2}{2 \cdot \omega \cdot U} =$$

$$= \frac{4h}{\omega \cdot \varepsilon_0 \cdot \pi^3 R^2 \cdot \left| \underbrace{J_1(2.405)}_{0.581865} \right|^2} =$$

$$= \frac{4}{\pi^3} \cdot \frac{h}{R} \cdot \eta \cdot \frac{2.405}{\left| \underbrace{J_1(2.405)}_{0.581865} \right|^2}$$

$$\frac{h}{R} = \frac{\lambda}{2 \cdot 2.405} \cdot \frac{\omega}{c} = \frac{\lambda}{2 \cdot 2.405} \cdot \frac{2\pi f}{c} = \frac{\pi}{2.405} = 1.31$$

$$\eta = 377\,\Omega$$

$$\Rightarrow \frac{R}{Q} \approx 450\,\Omega$$

Cavity characteristics - Summary

Symbol	Name	Definition	Pillbox cavity [0.35 GHz, 4.2 K, Nb]	Accelerating cavity [0.35 GHz, 4.2 K, Nb]
E_p/E_a	Peak normalized surface electric field	n/a	1.6	2
B_p/E_a [mT/(MV/m)]	Peak normalized surface magnetic field	n/a	3.1	4
R_s [nΩ]	Surface resistance	E_x/H_y	40	40
h [m]	Cavity length	$h=\lambda/2$	0.43	0.43
E_a [MV/m]	Accelerating gradient	(1/e) ·Energy gain/length	10	10
V [MV]	Accelerating voltage	$V=E_a \cdot h$	4.3	4.3
G [Ω]	Geometry factor	$G=R_s \cdot Q$	260	275
Q [10^9]	Quality factor	$Q=\omega U/P$	6.5	6.9
R/Q [Ω]	(R/Q) factor	$(R/Q)=V^2/(2\omega U)$	450	280
R [MΩ]	Shunt impedance	$R=V^2/(2P)$	$3 \cdot 10^6$	$2 \cdot 10^6$
U [J]	Stored energy	$U=V^2/[2\omega(R/Q)]$	9	15
P [W]	Dissipated power	$P=\omega U/Q$	3	5
h/R	Ratio cavity length to radius	n/a	1.3	0.5

Computer codes for RF cavities

Computer codes to determine the cavity parameters

For real structures with contoured shapes, beam apertures and beam pipes, it is necessary to use field computation codes, such MAFIA and Microwave Studio. Figure 10 shows the electric and magnetic fields computed by Microwave Studio for the accelerating mode of a pillbox cavity with a beam hole, and for a round wall cavity. Such codes are also necessary for computing the fields in the higher order modes of a cavity that can have an adverse effect on beam quality or cause instabilities. Figure 11 shows the electric and magnetic fields of the first monopole HOM. Beam induced voltages are also proportional to the R/Q of HOMs.

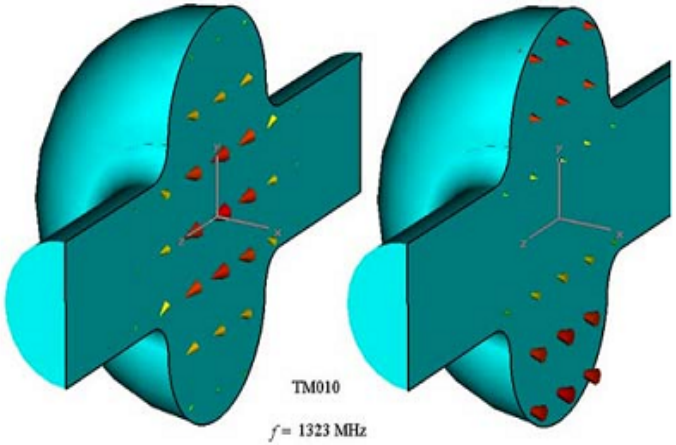

Fig.10 (Left) Electric and (Right) Magnetic fields for a round cavity with beam holes.

Different mode families 1/2

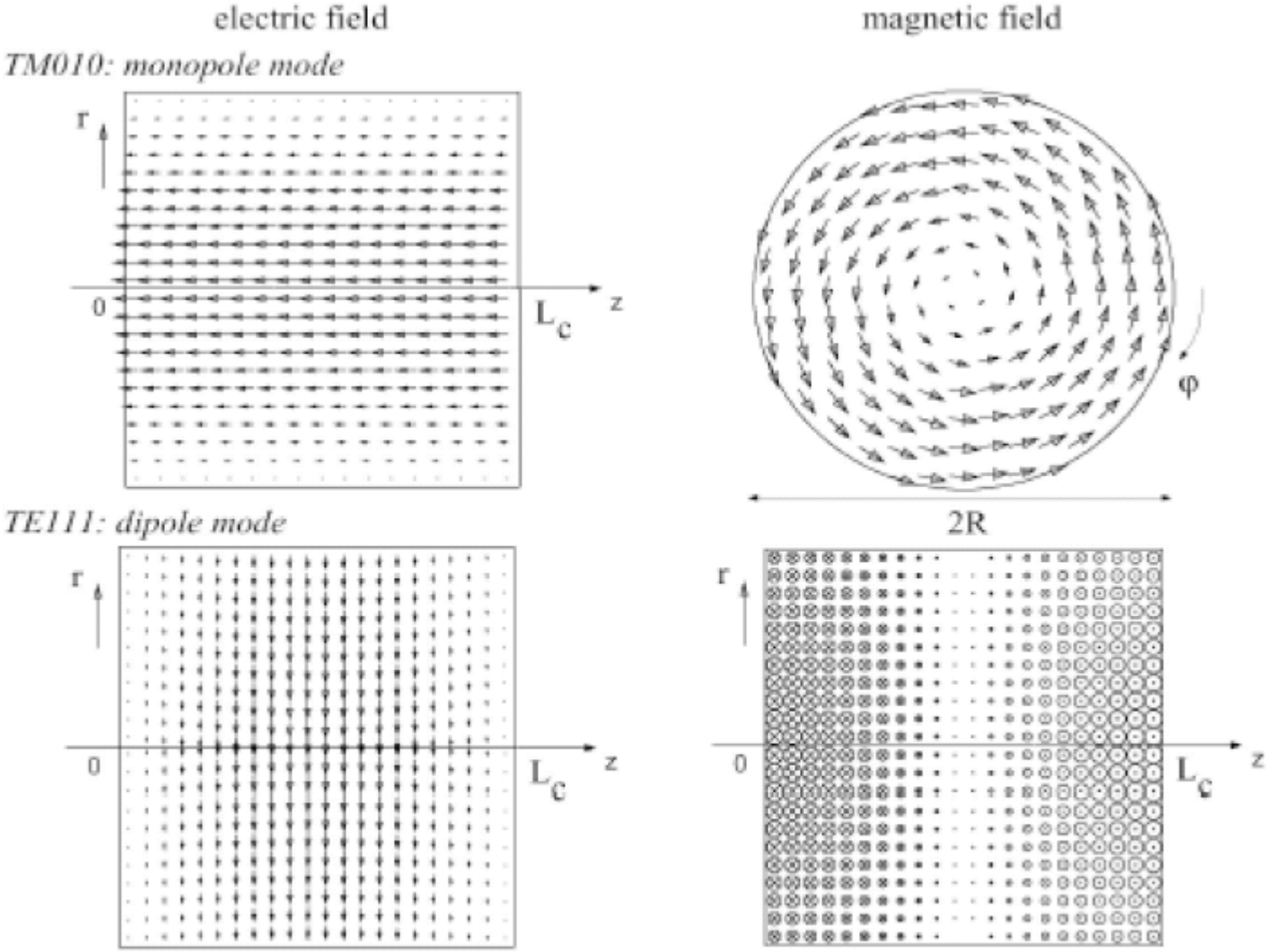

Lilje&Schmueser

Different mode families 2/2

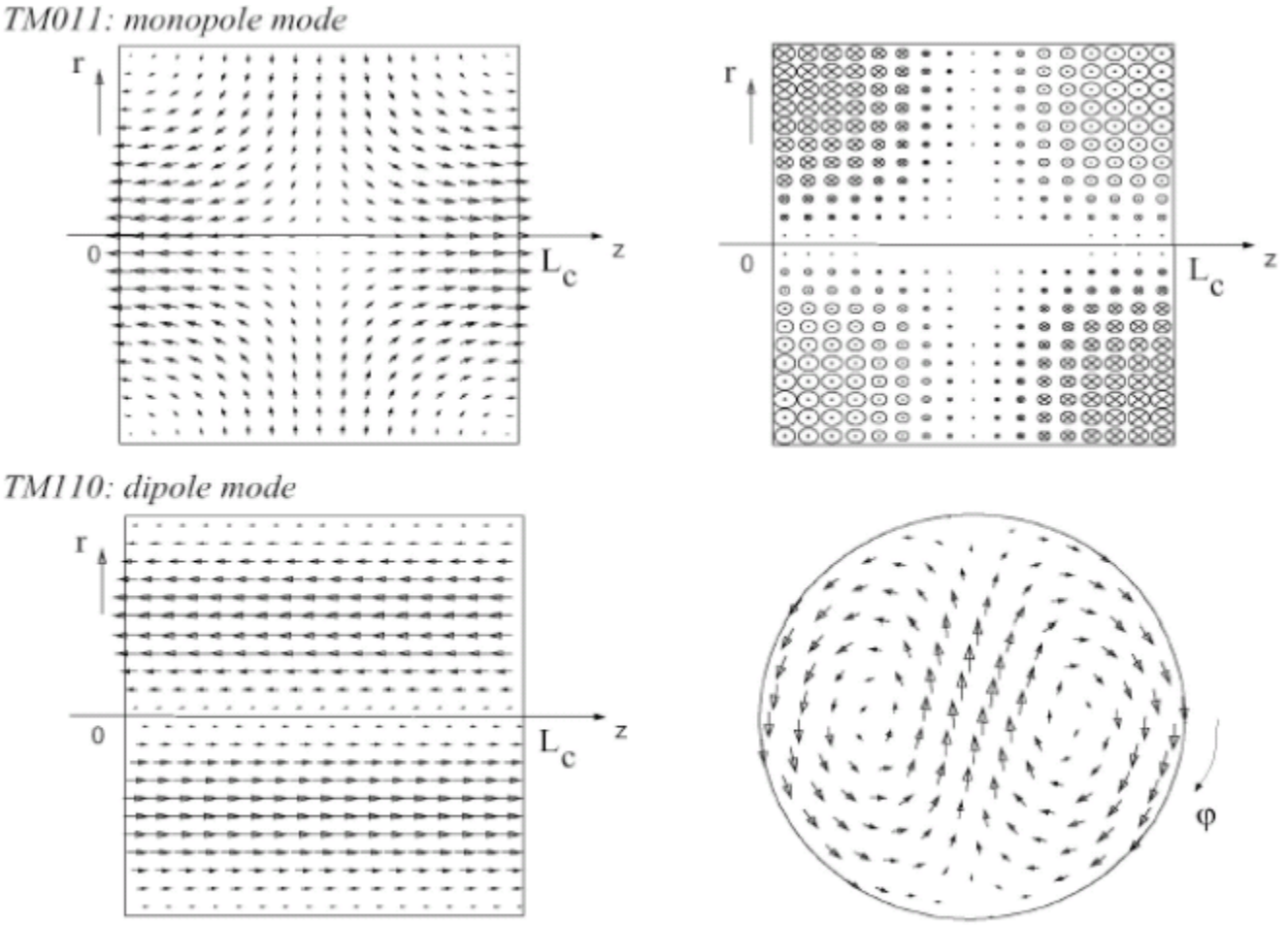

Figure 1: Electric and magnetic field in a pillbox cavity for several resonant modes (Courtesy of M. Liepe).

Lilje&Schmueser

Cavity characteristics – Summary table

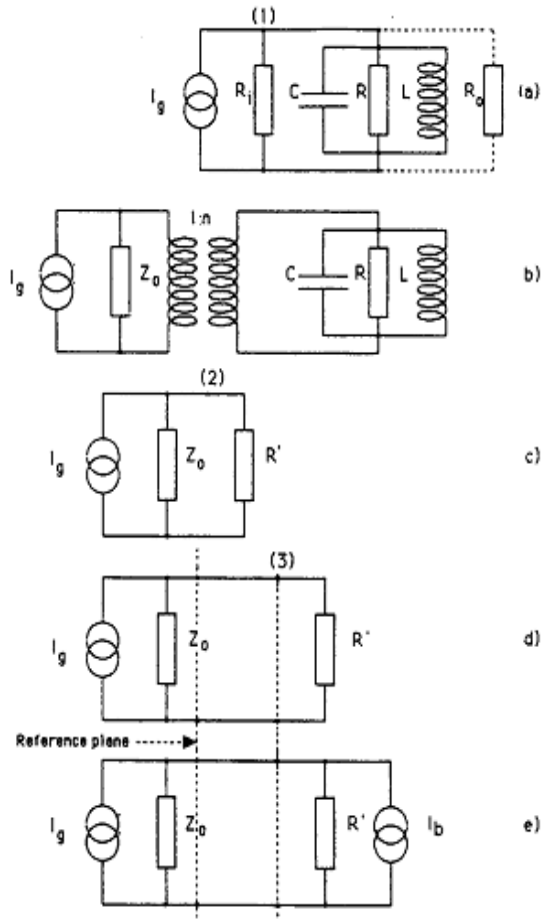

Fig. 8 Lumped element equivalent circuit model of an accelerating cavity resonator

Table: Equivalence of cavity and lumped-element circuit parameters

Cavity	Lumped-element circuit
Accelerating voltage V	Peak voltage V
Resonant frequency ω_0	$\omega_0 = 1/\sqrt{(LC)}$
Stored energy U	$U = (1/2)CV^2$
Dissipated power P_c	$P_c = (1/2)\ V^2/R$
Radiated power P_{rad}	$P_{rad} = (1/2)\ V^2/R_i$
Shunt impedance $R = V^2/(2 \cdot P_c)$	R
Unloaded Q - value $Q_0 = \omega_0 \cdot U/P_c$	$Q_0 = \omega_0 \cdot RC$
External Q - value $Q_{ext} = \omega_0 \cdot U/P_{rad}$	$Q_{ext} = \omega_0 \cdot R_i C = R_i/(R/Q)$
(R/Q) value $R/Q = V^2/(2\ \omega_0 \cdot U)$	$R/Q = \sqrt{(L/C)} = 1/(\omega_0 \cdot C)$
Coupling factor $\beta = Q_0/Q_{ext}$	$\beta = R/R_i$
Loaded Q - value $Q_L = Q_0/(1+\beta)$ (because $Q_L^{-1} = Q_0^{-1} + Q_{ext}^{-1}$)	$Q_L = \omega_0 \cdot RC/(1+\beta)$
Turns ratio $n = \sqrt{[(R/Q) \cdot Q_{ext}/Z_0]}$	$n = \sqrt{(R_i/Z_0)}$
Wave impedance $Z_0 = 50\ \Omega$	

From W. Weingarten, CERN-1992-03

Transmission line 1/2

Introduction of the notion of reflection and transmission factors.

$$Z = E_y / H_z$$

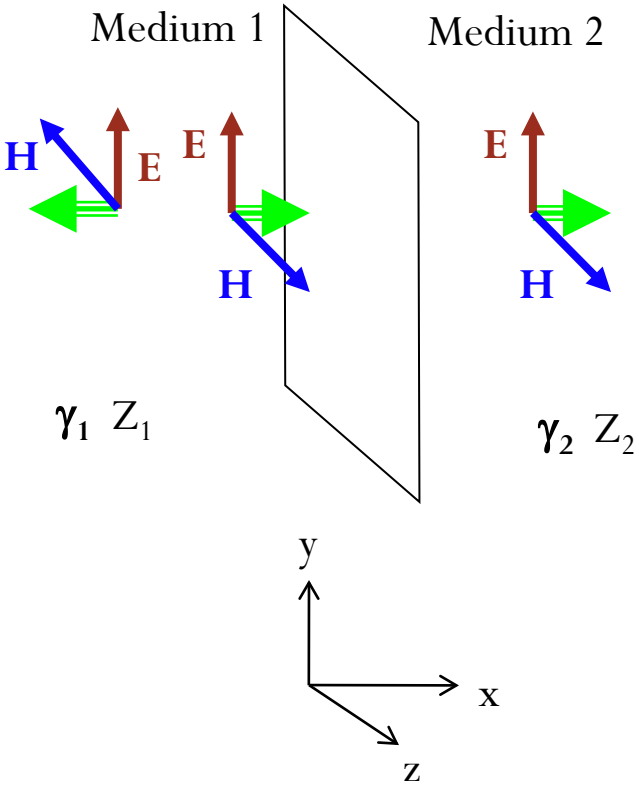

$$E_{yi} = \hat{E} e^{-\gamma_1 x} e^{i\omega t}$$

$$H_{zi} = \frac{\hat{E}}{Z_1} e^{-\gamma_1 x} e^{i\omega t}$$

$$E_{yr} = \rho \hat{E} e^{\gamma_1 x} e^{i\omega t}$$

$$H_{zr} = -\rho \frac{\hat{E}}{Z_1} e^{\gamma_1 x} e^{i\omega t}$$

$$E_{yt} = \tau \hat{E} e^{-\gamma_2 x} e^{i\omega t}$$

$$H_{zt} = \tau \frac{\hat{E}}{Z_2} e^{-\gamma_2 x} e^{i\omega t}$$

Transmission line 2/2

From continuity at the interface:

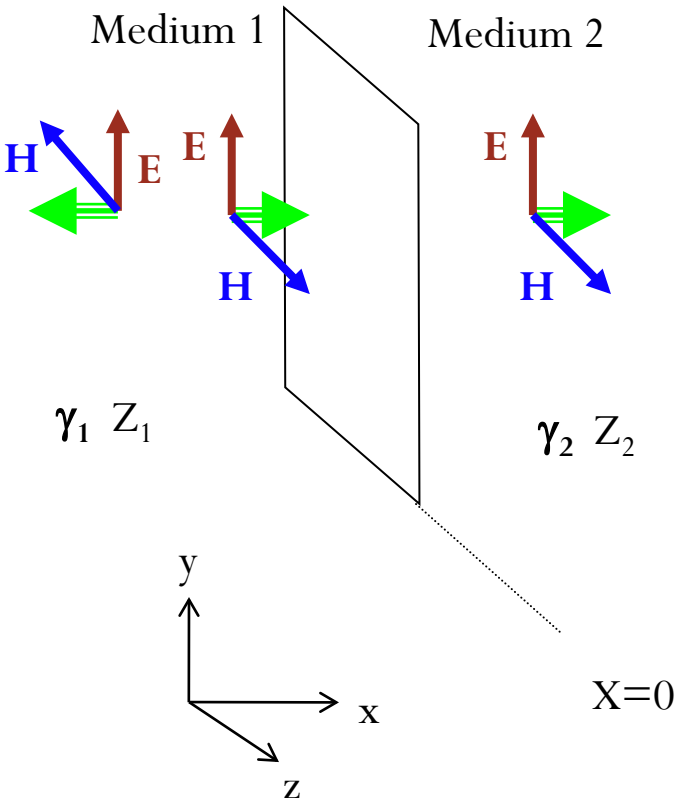

$$\left.\begin{aligned} E_{yi} + E_{yr} &= E_{yt} \\ H_{zi} + H_{zr} &= H_{zt} \end{aligned}\right\} x = 0$$

$$1 + \rho = \tau$$

$$\frac{1}{Z_1} - \rho\frac{1}{Z_1} = \tau\frac{1}{Z_2}$$

$$\frac{Z_2}{Z_1}(1-\rho) = \tau$$

$$1 + \rho = \frac{Z_2}{Z_1}(1-\rho)$$

$$\rho = \frac{Z_2 - Z_1}{Z_2 + Z_1}$$

$$\tau = \frac{2Z_2}{Z_2 + Z_1}$$

Response of a cavity to RF 1/5

- Apply transmission line theory (to a one-port impedance):

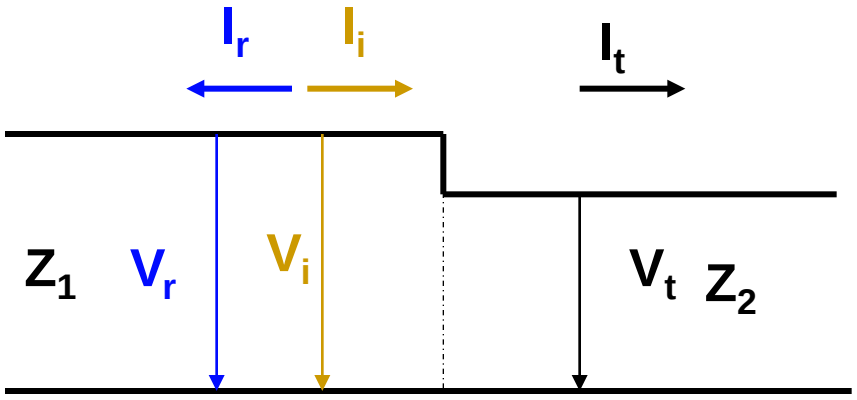

$$V_t = V_i + V_r$$

$$I_t = I_i - I_r$$

$$V_t = \tau \cdot V_i \qquad V_r = \rho \cdot V_i$$

$$V_r = Z_1 \cdot I_i$$

$$V_t = Z_2 \cdot I_t$$

Reflexion factor ρ Transmission factor τ

$$\Rightarrow \rho = \frac{Z_2 - Z_1}{Z_2 + Z_1} \qquad \Rightarrow \tau = \frac{2 \cdot Z_2}{Z_2 + Z_1}$$

$$\tau - \rho = \frac{2 \cdot Z_2 - (Z_2 - Z_1)}{Z_1 + Z_2} = 1$$

Response of a cavity to RF 2/5

- Reflexion factor ρ depends on position, the coupling factor β does not:

$$\beta = \frac{Z_2}{Z_1}$$

$$\beta = \begin{cases} \frac{1-|\rho|}{1+|\rho|}, \beta \le 1 \\ \frac{1+|\rho|}{1-|\rho|}, \beta \ge 1 \end{cases}$$

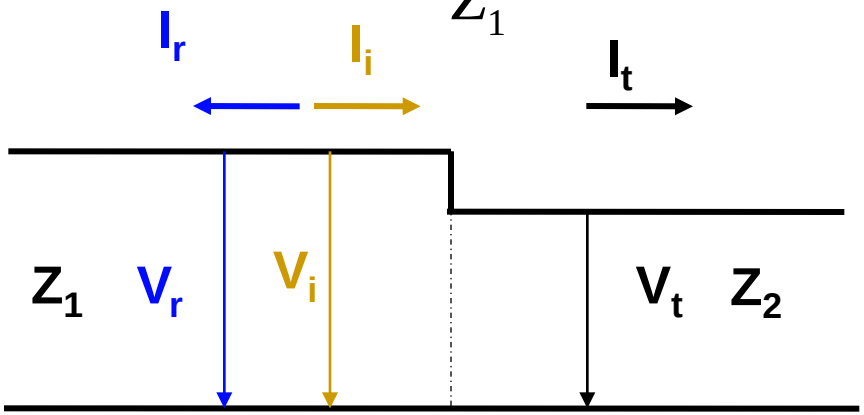

$$|\rho| = \left|\frac{Z_2 - Z_1}{Z_2 + Z_1}\right| = \left|\frac{Z_2/Z_1 - 1}{Z_2/Z_1 + 1}\right| = \begin{cases} \frac{\beta-1}{\beta+1}, \text{if } \beta \ge 1 \\ \frac{1-\beta}{1+\beta}, \text{if } \beta \le 1 \end{cases}$$

$$|\tau| = |1+\rho| \underset{\rho \ge 0}{=} 1+|\rho| = 1+\frac{\beta-1}{\beta+1} = \frac{2\beta}{1+\beta} \qquad |\tau| = |1+\rho| \underset{\rho \le 0}{=} 1-|\rho| = 1-\frac{1-\beta}{1+\beta} = \frac{2\beta}{1+\beta}$$

Response of a cavity to RF 3/5

- Determination of Q_0 and accelerating voltage/gradient

$$V_t = \tau \cdot V_i = \frac{2\beta}{1+\beta} V_i \Rightarrow V_t^2 = \frac{4\beta^2}{(1+\beta)^2} V_i^2 = \frac{8\beta^2}{(1+\beta)^2} \cdot \underbrace{Z_1}_{(R/Q)\cdot Q_0/\beta} \cdot \underbrace{\frac{V_i^2}{2Z_1}}_{P_i} \qquad 1)$$

$$\Rightarrow V_t = \sqrt{\frac{8\beta}{(1+\beta)^2} \cdot (R/Q) \cdot Q_0 \cdot P_i}$$

$$\beta = \begin{cases} \frac{1-|\rho|}{1+|\rho|}, \beta \le 1 \\ \frac{1+|\rho|}{1-|\rho|}, \beta \ge 1 \end{cases}$$

$$\frac{1}{Q_L} = \frac{1}{Q_0} + \frac{1}{Q_{ext}} = \frac{1+\frac{Q_0}{Q_{ext}}}{Q_0} \Rightarrow Q_0 = \left(1 + \underbrace{\frac{Q_0}{Q_{ext}}}_{=\beta}\right) \cdot Q_L = (1+\beta) \cdot \underbrace{Q_L}_{\omega\tau}$$

$$E_{acc} = V_t / L$$

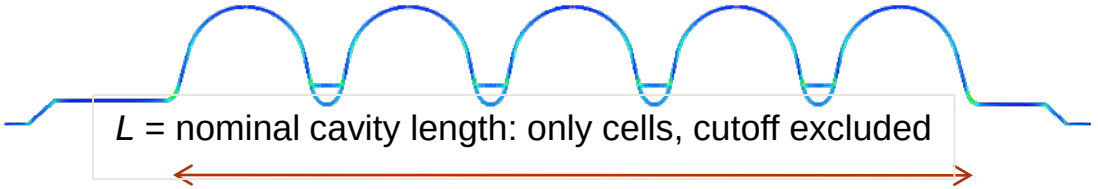

1) Remember

$$Z_1 = \underbrace{\frac{Z_1}{Z_2}}_{1/\beta} \cdot Z_2 = \frac{Z_2}{\beta} = \frac{R}{\beta} = \frac{1}{\beta} \cdot \underbrace{\frac{R}{V_c^2/2}}_{P_c} \cdot \omega U \cdot \frac{V_c^2}{2\omega U} = \frac{1}{\beta} \cdot \underbrace{\frac{\omega U}{P_c}}_{Q_0} \cdot \underbrace{\frac{2\omega U}{R/Q}}_{} \cdot \frac{V_c^2}{} = \frac{(R/Q)\cdot Q_0}{\beta}$$

Response of a cavity to RF 4/5

- The response of a **two port cavity** is equivalent to that of a one-port cavity

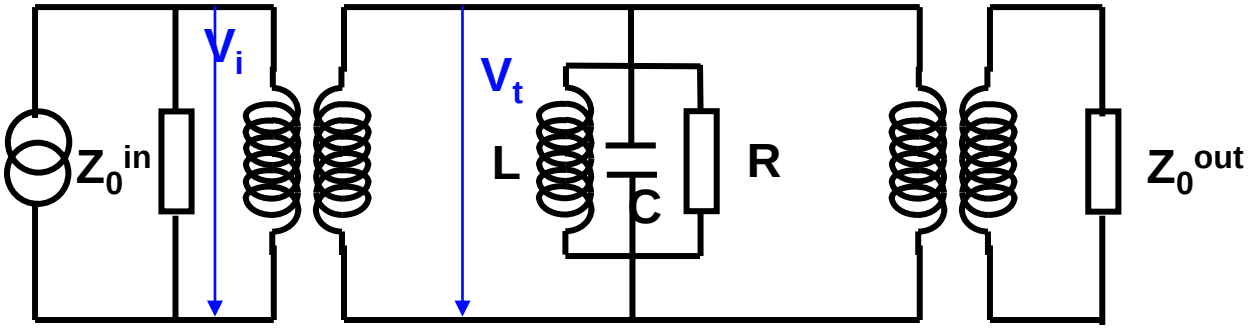

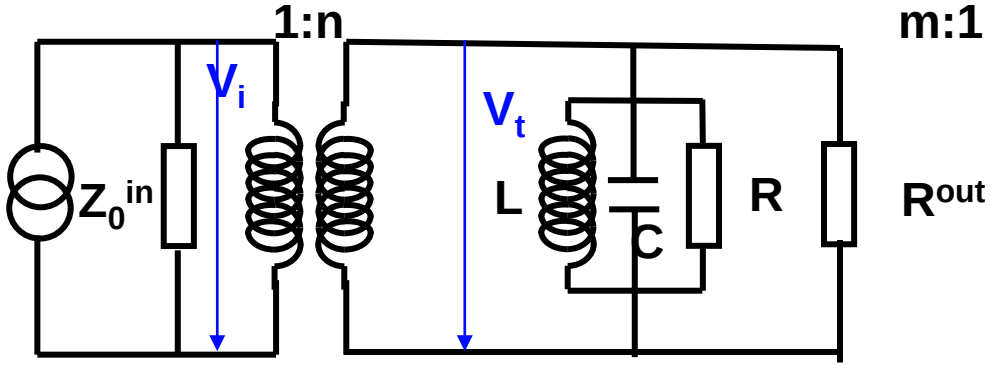

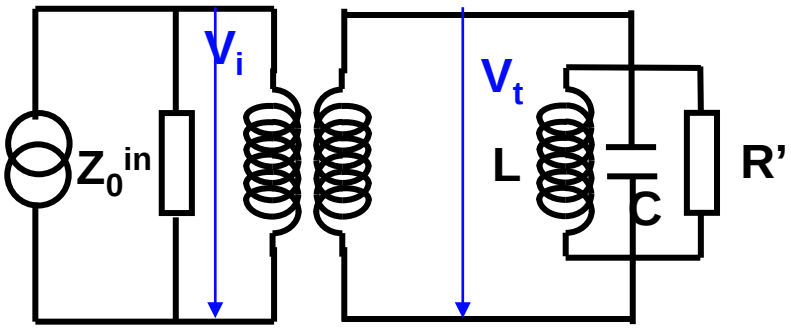

$$R^{out} = m^2 Z_0^{out}$$

$$m^2 = \frac{(R/Q)\cdot Q_{ext}^{out}}{Z_0^{out}}$$

$$\frac{1}{R'} = \frac{1}{R} + \frac{1}{R^{out}}$$

Response of a cavity to RF 5/5

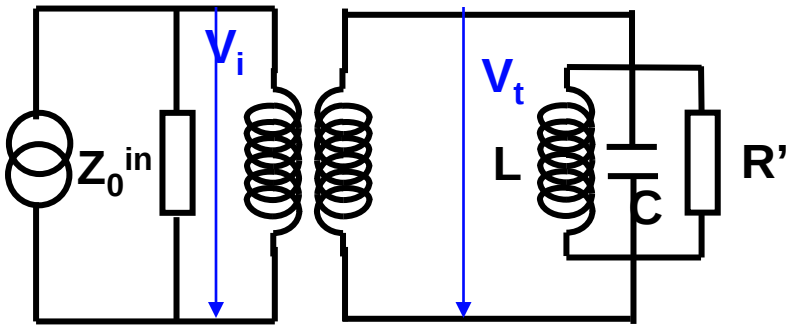

$$V_t = \tau \cdot V_i = \frac{2\beta'}{1+\beta'} V_i \Rightarrow V_t^2 = \frac{4\beta'^2}{(1+\beta')^2} V_i^2 = \frac{8\beta'^2}{(1+\beta')^2} \cdot \underbrace{Z_0^{in}}_{(R/Q)\cdot Q_0'/\beta'} \cdot \underbrace{\frac{V_i^2}{2Z_0^{in}}}_{P_i}$$

$$\Rightarrow V_t = \sqrt{\frac{8\beta'}{(1+\beta')^2} \cdot (R/Q) \cdot Q_0' \cdot P_i}$$

$$Q_0' = (1+\beta') \cdot \underbrace{Q_L}_{\omega\tau} \qquad E_{acc} = V_t / L \qquad \beta' = \begin{cases} \frac{1-|\rho|}{1+|\rho|}, \beta' \le 1 \\ \frac{1+|\rho|}{1-|\rho|}, \beta' \ge 1 \end{cases}$$

$$\frac{1}{Q_0} = \frac{1}{Q_0'} - \frac{1}{Q_{ext}^{out}} \qquad Q_{ext}^{out} = \frac{\omega U}{P_{out}} = \frac{V^2}{2 \cdot (R/Q) \cdot P_{out}}$$

Transient Response 1/2

1. Apply Kirchhoff's current law at node (1)

$$\frac{V}{R_i}+\frac{1}{L}\int V(t)+C\frac{dV}{dt}+\frac{V}{R}=I_{g0}\cdot\cos\omega t$$

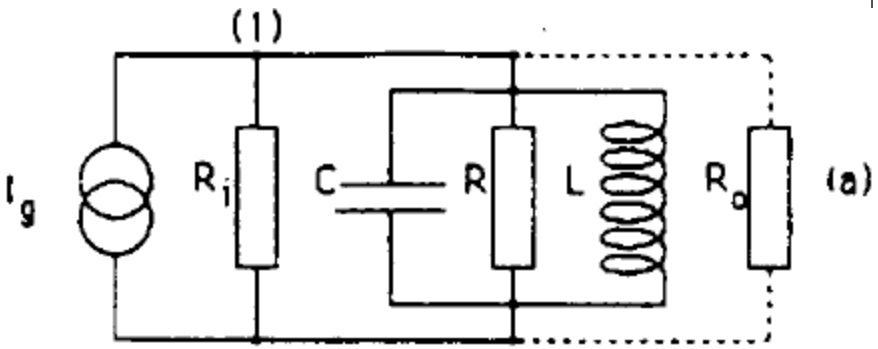

2. Differentiate and transform lumped circuit elements into cavity parameters by using preceding "Table 7"

$$\frac{d^2V}{dt^2}+\frac{\omega_0}{Q_L}\frac{dV}{dt}+\omega_0^2V=-I_{g0}\cdot\left(\frac{R}{Q}\right)\cdot\omega\cdot\omega_0\cdot\sin\omega t$$

3. Find the general solution of the homogeneous differential equation

$$V(t)=\mathrm{e}^{-\frac{\omega_0 t}{2Q_L}}\cdot\left(c_1\cdot\mathrm{e}^{\mathrm{i}\sqrt{1-1/(2Q_L)^2}\cdot\omega_0 t}+c_2\cdot\mathrm{e}^{-\mathrm{i}\sqrt{1-1/(2Q_L)^2}\cdot\omega_0 t}\right)$$

4. Find the solution of the inhomogeneous differential equation

$$V(t)=V_0\cdot\cos\omega_0 t\cdot\left\{1-\mathrm{e}^{-\frac{\omega_0 t}{2Q_L}}\right\}$$

Transient response 2/2

- Determination of Q_0 and accelerating voltage/gradient (2)
- Oscilloscope signal for voltage measurement

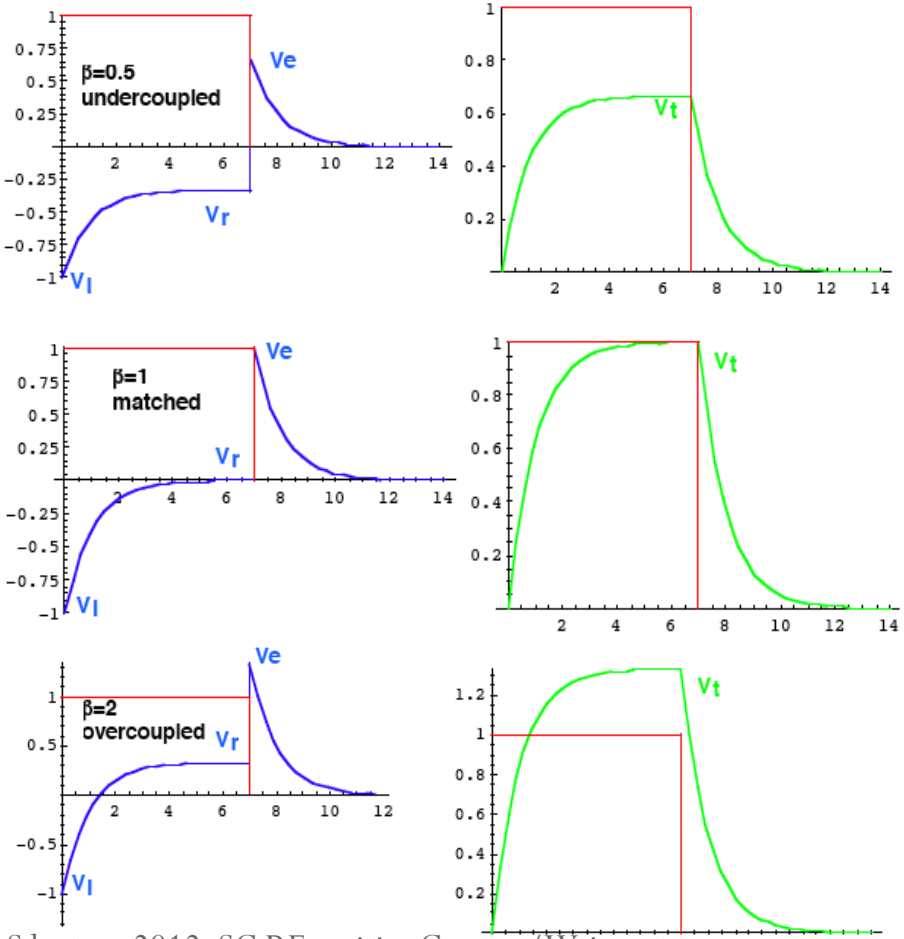

$$V_t = V_i + V_r$$

Remember: $V_e = V_i + V_r$

$$|\rho| = \left|\frac{V_r}{V_i}\right| \Rightarrow 1^{\text{st}}\text{ method:}$$

$$\beta = \frac{1-\left|\frac{V_r}{V_i}\right|}{1+\left|\frac{V_r}{V_i}\right|} = \begin{cases} \frac{|V_i|-|V_r|}{|V_i|+|V_r|}; \beta \le 1 \\ \frac{|V_i|+|V_r|}{|V_i|-|V_r|}; \beta \ge 1 \end{cases}$$

$$2^{\text{nd}}\text{ method: } \beta = \frac{1-\left|\frac{V_r}{V_i}\right|}{1+\left|\frac{V_r}{V_i}\right|} = \frac{1-\left|\frac{V_i - V_e}{V_i}\right|}{1+\left|\frac{V_i - V_e}{V_i}\right|} =$$

$$= \frac{|V_e|}{2\cdot|V_i| - |V_e|} = \frac{1}{2\cdot\left|\frac{V_i}{V_e}\right| - 1}$$

Measuring setup

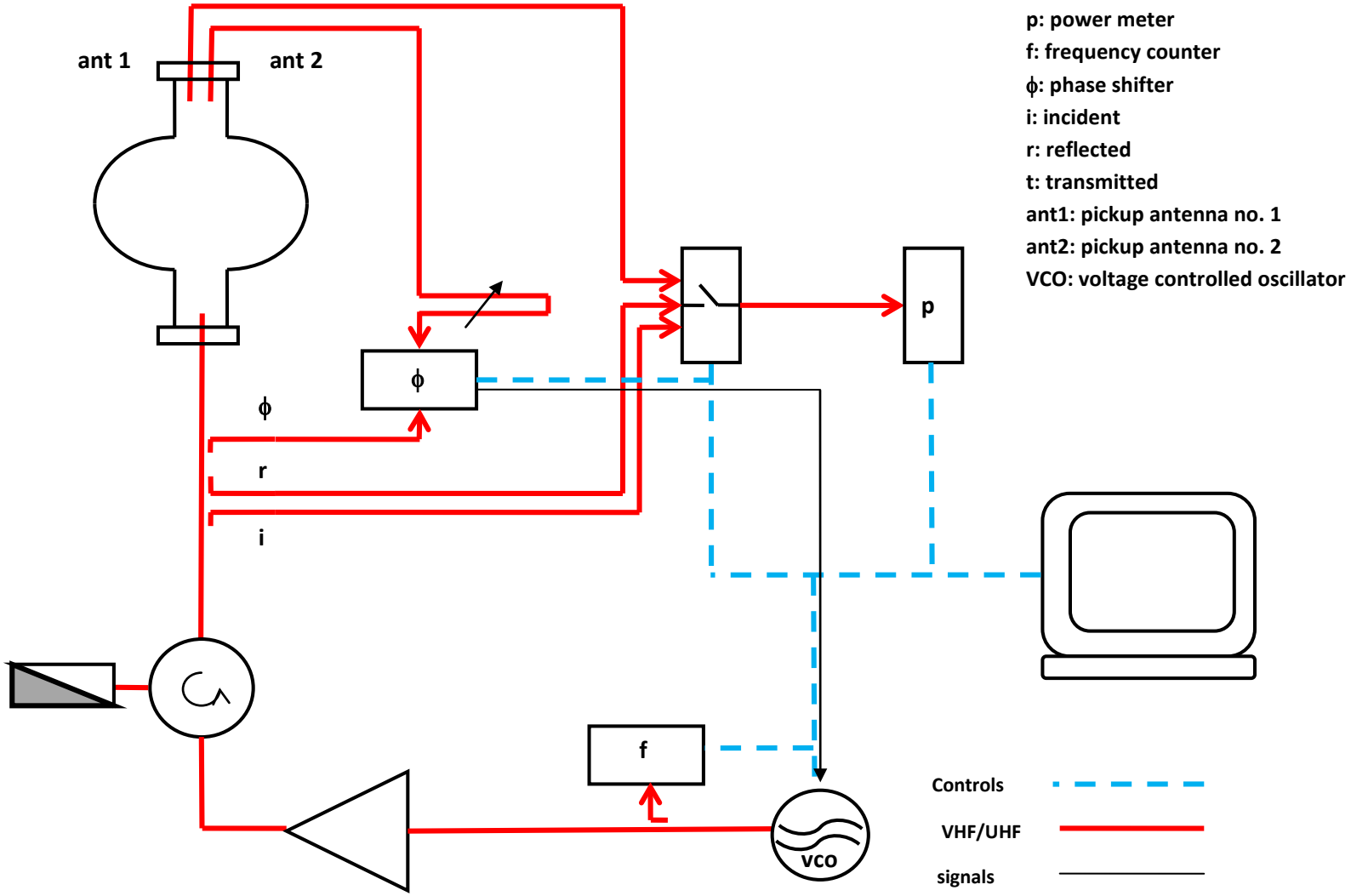

$Q(E_{acc})$ curve

Electropolishing and in-situ Baking of 1.3 GHz Niobium Cavities

L. Lilje[+], D. Reschke, K. Twarowski, DESY, Notkestraße 85, 22607 Hamburg
P. Schmüser, Universität Hamburg
D. Bloess, E. Haebel, E. Chiaveri, J.-M. Tessier, H. Preis, H.Wenninger, CERN, Geneva
H. Safa, J.-P. Charrier, CEA, Saclay

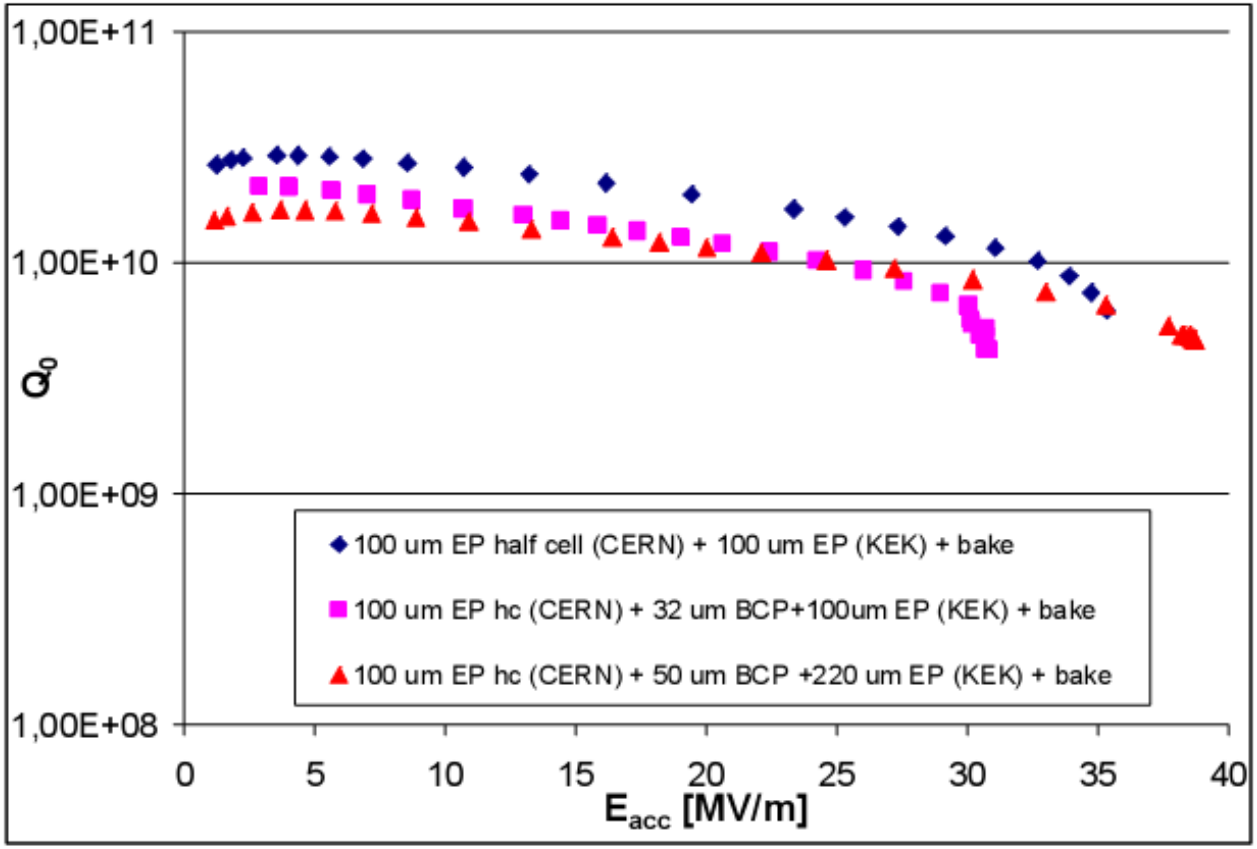

Figure 6: The cavities after bakeout show no Q-drop. One cavitiy is limited at 30 MV/m due to strong field emission and available RF power.

Passband modes

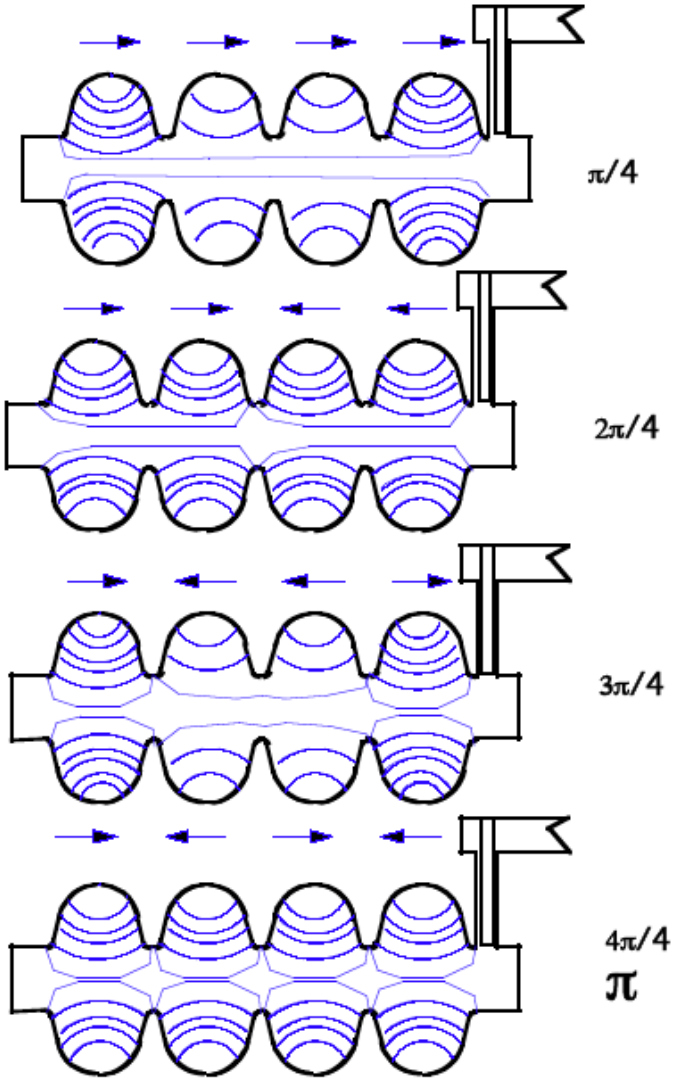

Typical storage ring cavity (LEP)

Summary

- The pillbox resonator (TM_{010} mode) allows – as a paradigm - the analytical description of typical accelerator parameters, such as peak surface fields (E and H), power loss and Q-value, shunt impedance, geometrical shunt impedance, geometry factor, etc.
- « Real » accelerator cavities are designed by making use of computer codes such as Microwave Studio, MAFIA, SUPERFISH, etc.
- The response of a cavity to an RF pulse is well described by lumped circuit networks, in particular by the transmission and reflection of an electromagnetic wave at a discontinuity in the line.
- An algorithm is presented to determine the coupling factor β (or the reflection factor ρ), and finally the unloaded Q-value Q_0, the accelerating voltage V (accelerating gradient E_a) and the surface resistance R_s.

Interaction of cavity with beam

- Descriptive introduction
- Analytical introduction
- Transfer of RF power from the cavity to the beam
  - The fundamental mode power coupler
- Transfer of RF power from the beam to the cavity
  - Higher order modes and their damping
- The frequency tuner
- Summary

Descriptive Introduction

THE SUPRACONDUCTIVITY

THE USE OF SUPRACONDUCTIVITY TO INCREASE
PERFORMANCES AND CONSIDERABLY REDUCE
ELECTRICITY CONSUMPTION

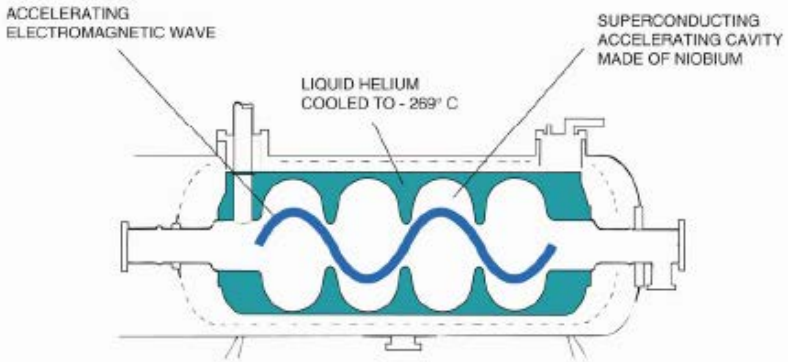

Particle passing through cavity

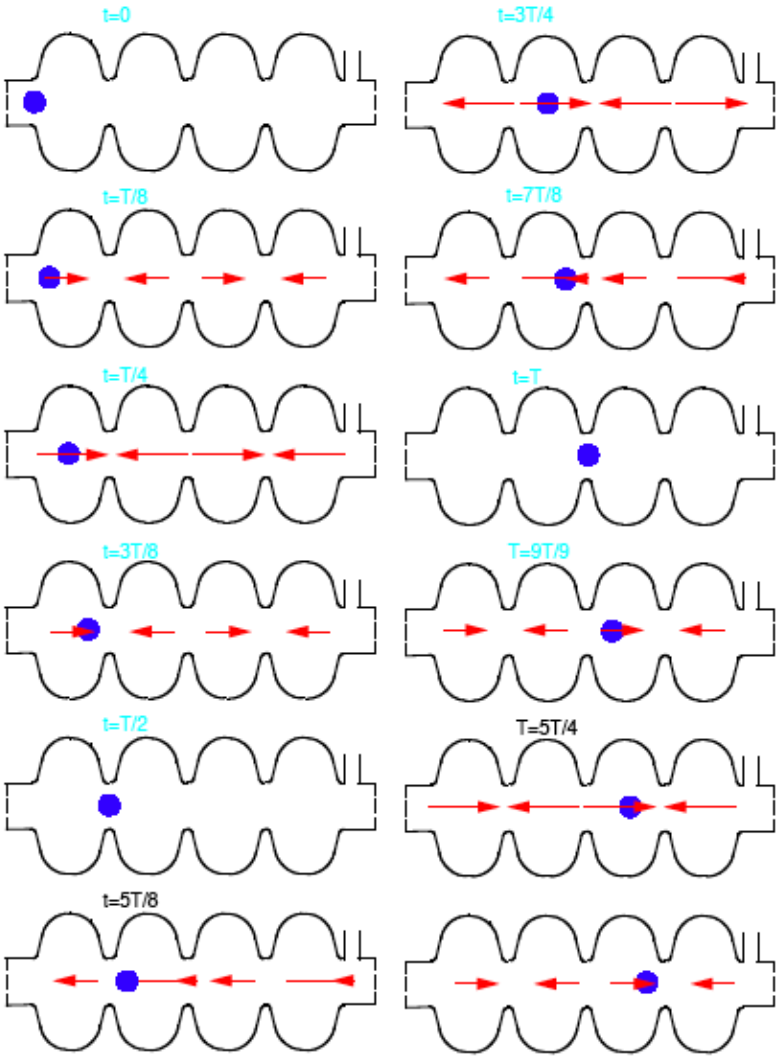

Analytical Introduction

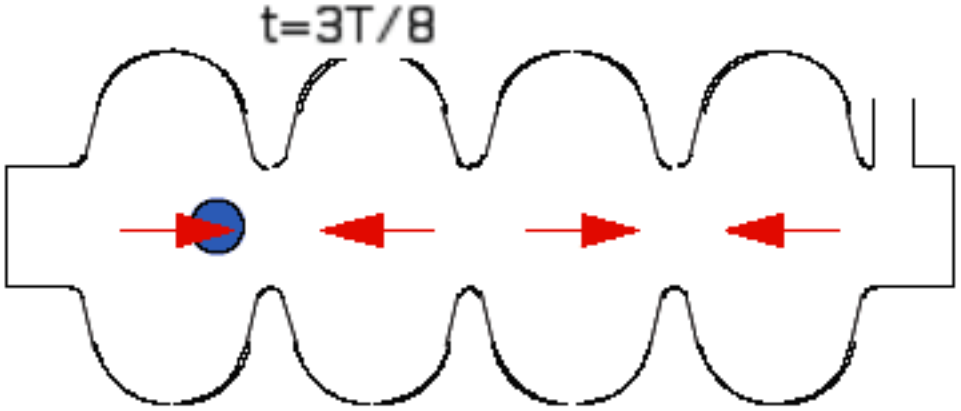

$$V = E(z_1,t_1)\Delta z_1 + E(z_2,t_2)\Delta z_2 + \ldots\ldots$$

$$\Rightarrow V = \int_{-\infty}^{+\infty} E(z,\ t\ (z)\ )\ dz$$

$$E(z,t) = E(z) * \cos(\omega t + \varphi)$$

$$t = z/v$$

$$V(\varphi) = \int_{-\infty}^{+\infty} E(z) * \cos(z\omega/v + \varphi)\ dz$$

Transfer of RF power from the cavity to the beam 1/3

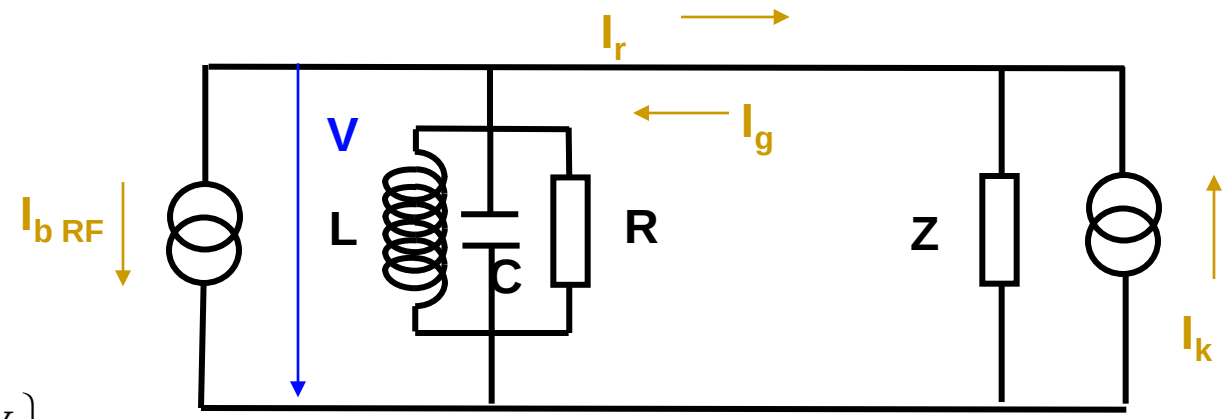

$$\left.\begin{aligned} I_r - I_g + I_k &= \frac{V}{Z} \\ I_k &= 2I_g \end{aligned}\right\} \Rightarrow I_r + I_g = \frac{V}{Z}$$

A circulator guarantees that under no circumstances there is no reflected wave impinging to the RF generator

$$I_{LCR} = I_g - I_r - I_{b,RF} = 2I_g - I_{b,RF} - \frac{V}{Z}$$

$$I_{LCR} = V\left(\frac{1}{i\omega L} + i\omega C + \frac{1}{R}\right)$$

$$\omega_0 = \frac{1}{\sqrt{LC}}$$

With $\omega_0^2 - \omega^2 \approx 2\omega_0\Delta\omega$ and $\Delta\omega \prec \omega$

$$\Rightarrow V\left(-\frac{2\Delta\omega}{\omega} + \frac{1}{i\omega C}\left(\frac{1}{R} + \frac{1}{Z}\right)\right) = \frac{2I_g - I_{b,RF}}{i\omega C}$$

Transfer of RF power from the cavity to the beam 2/3

Re-write preceding equation

$$V\left(-\frac{2\Delta\omega}{\omega}+\frac{1}{i\omega C}\left(\frac{1}{R}+\frac{1}{Z}\right)\right)=\frac{2I_g-I_{b,RF}}{i\omega C}$$

in cavity parameters

$$V\left(\frac{1}{2(R/Q)}\left(\frac{1}{Q_{ext}}+\frac{1}{Q_0}\right)-i\frac{\Delta\omega}{\omega(R/Q)}\right)=I_g-\frac{1}{2}I_{b.RF}$$

Transfer of RF power from the cavity to the beam 3/3

$$V\left(\frac{1}{2(R/Q)}\left(\frac{1}{Q_{ext}}+\frac{1}{Q_0}\right)-i\frac{\Delta\omega}{\omega(R/Q)}\right)=I_g-\frac{1}{2}I_{bRF}$$

- Minimize reflected power

$$\Rightarrow I_g=\frac{V}{2(R/Q)}\left(\frac{1}{Q_{ext}}+\frac{1}{Q_0}\right)+I_{DC}\cos\Phi-i\left(I_{DC}\sin\Phi+\frac{V\Delta\omega}{\omega(R/Q)}\right)$$

$$\frac{1}{Q_0}\prec\frac{1}{Q_{ext}}\ \text{for sc cavities}$$

$$I_r=\frac{V}{Q_{ext}\cdot(R/Q)}-I_g=\frac{V}{2\cdot(R/Q)}\left(\frac{1}{Q_{ext}}-\frac{1}{Q_0}\right)-I_{DC}\cos\Phi-i\left(I_{DC}\sin\Phi+\frac{V\Delta\omega}{\omega(R/Q)}\right)$$

Actions: 1) compensate « reactive beam loading » to zero by detuning $\Delta\omega$

$$\Delta\omega=-\omega\frac{(R/Q)\cdot I_{DC}}{V}\sin\Phi$$

2) define optimum Q_{ext} for nominal beam current for $I_r = 0$

$$Q_{ext,opt}=\frac{V}{2\cdot(R/Q)I_{DC}\cos\Phi}$$

RF power $$P_{g,r}=\frac{1}{2}Z\left|I_{g,r}\right|^2=\frac{1}{2}(R/Q)\cdot Q_{ext}\cdot\left|I_{g,r}\right|^2$$

Check: $$P_{beam,r}=P_{g,r}-P_{r,r}=V\cdot I_{DC}\cdot\cos\Phi$$

The fundamental mode power coupler

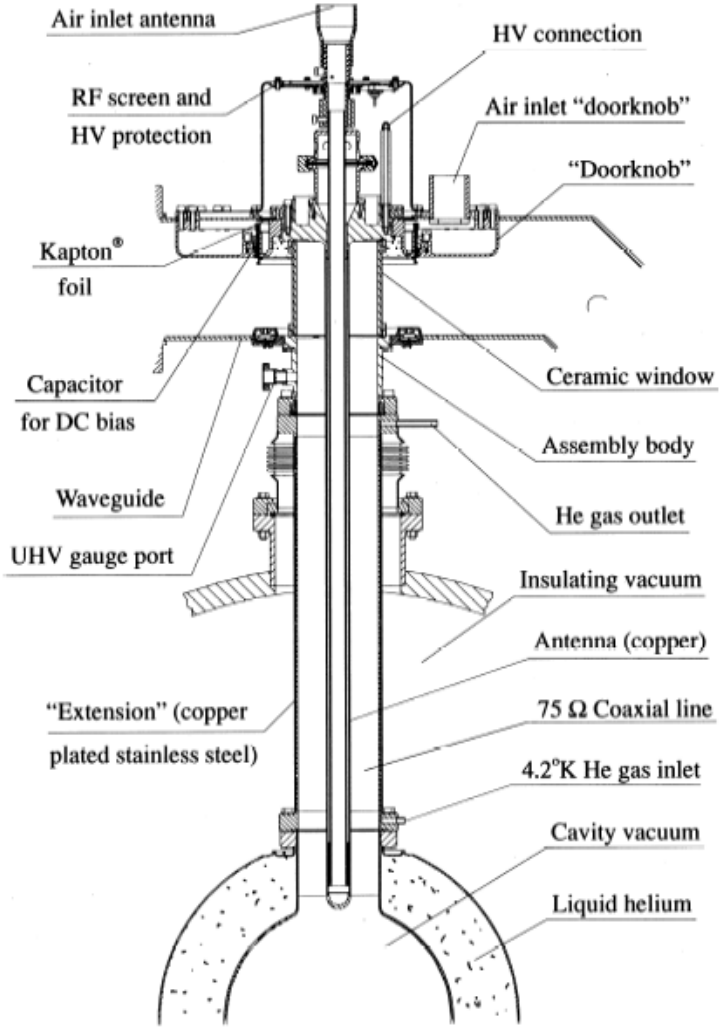

LEP solution of the power coupler

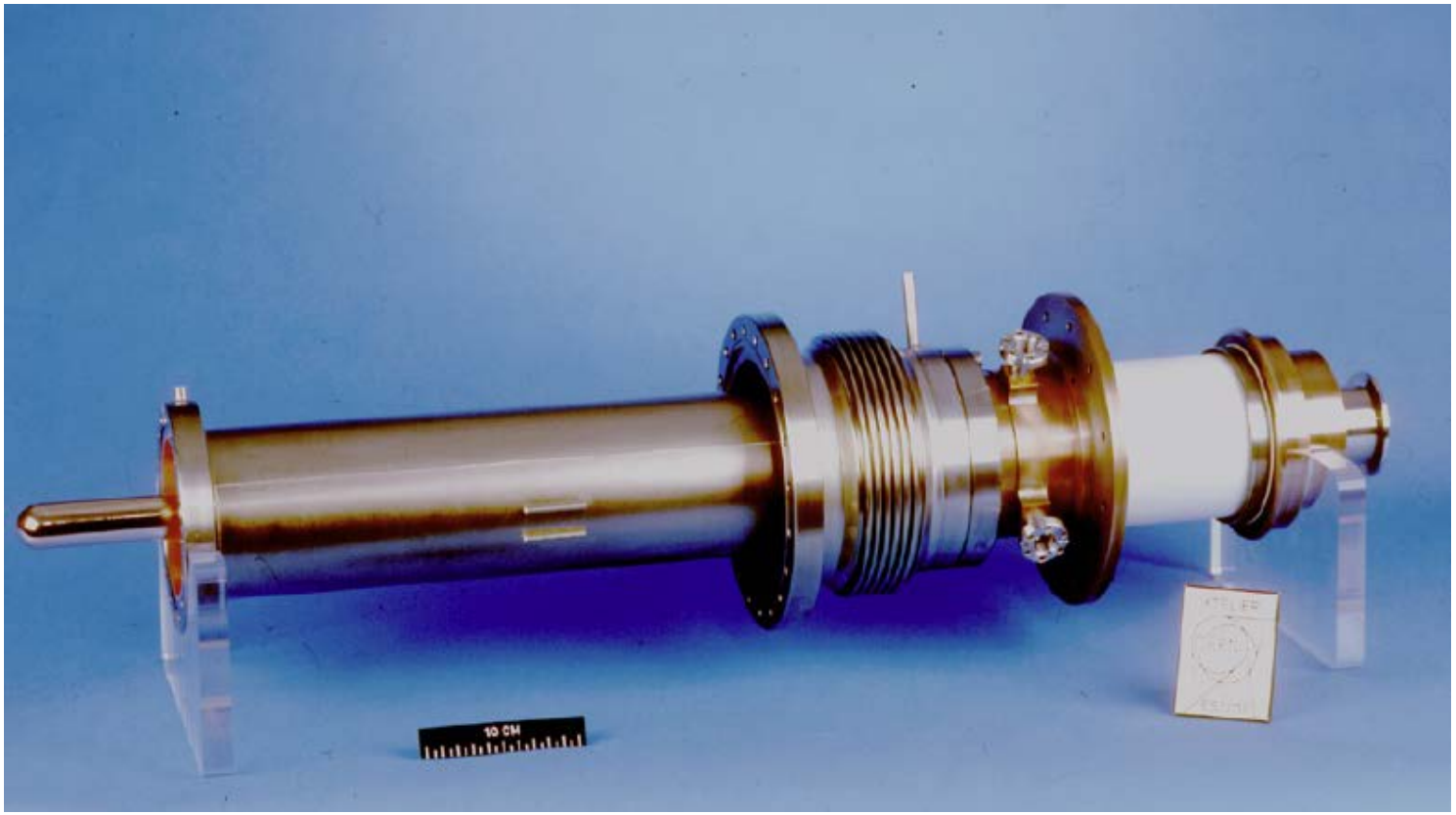

Transfer of RF power from the beam to the cavity

- Need for Higher Order Mode (HOM) coupler

  Imagine worst case

  1. the cavity resonant frequency is « tuned » to a spectral line of the beam
  2. Generator switched off, I_g=0.

$$V\left(\frac{1}{2(R/Q)}\left(\frac{1}{Q_{ext}}+\frac{1}{Q_0}\right)-i\frac{\Delta\omega}{\omega(R/Q)}\right)=I_g-\frac{1}{2}I_{b.RF} \qquad \Rightarrow \Delta\omega=0;\Phi=0$$

$$\Rightarrow V=-I_{b.RF}\cdot(R/Q)\cdot Q_{ext}=-2\cdot I_{DC}\cdot(R/Q)\cdot Q_{ext}$$

This means that the beam is decelerated.
Remedy: keep Qext as low as possible.

Output power (reflected):

$$P_r=\frac{V^2}{2\cdot Z}=\frac{V^2}{2\cdot(R/Q)\cdot Q_{ext}}=2\cdot(R/Q)\cdot Q_{ext}\cdot I_{DC}^2$$

1st example (LEP); RF Generator trip.
We obtain for the **accelerating mode** $R/Q=232\,\Omega;\ Q_{ext}=2\cdot10^6;\ I_{DC}=6\,\text{mA};\ P_r=33\,\text{kW}$

2nd example;
We obtain for the **higher order mode** with (R/Q) = 10 Ω, Qext = 20000

$$V=-2.4\,\text{kV}\Rightarrow P_r=14.4\,\text{W}$$

Higher order modes

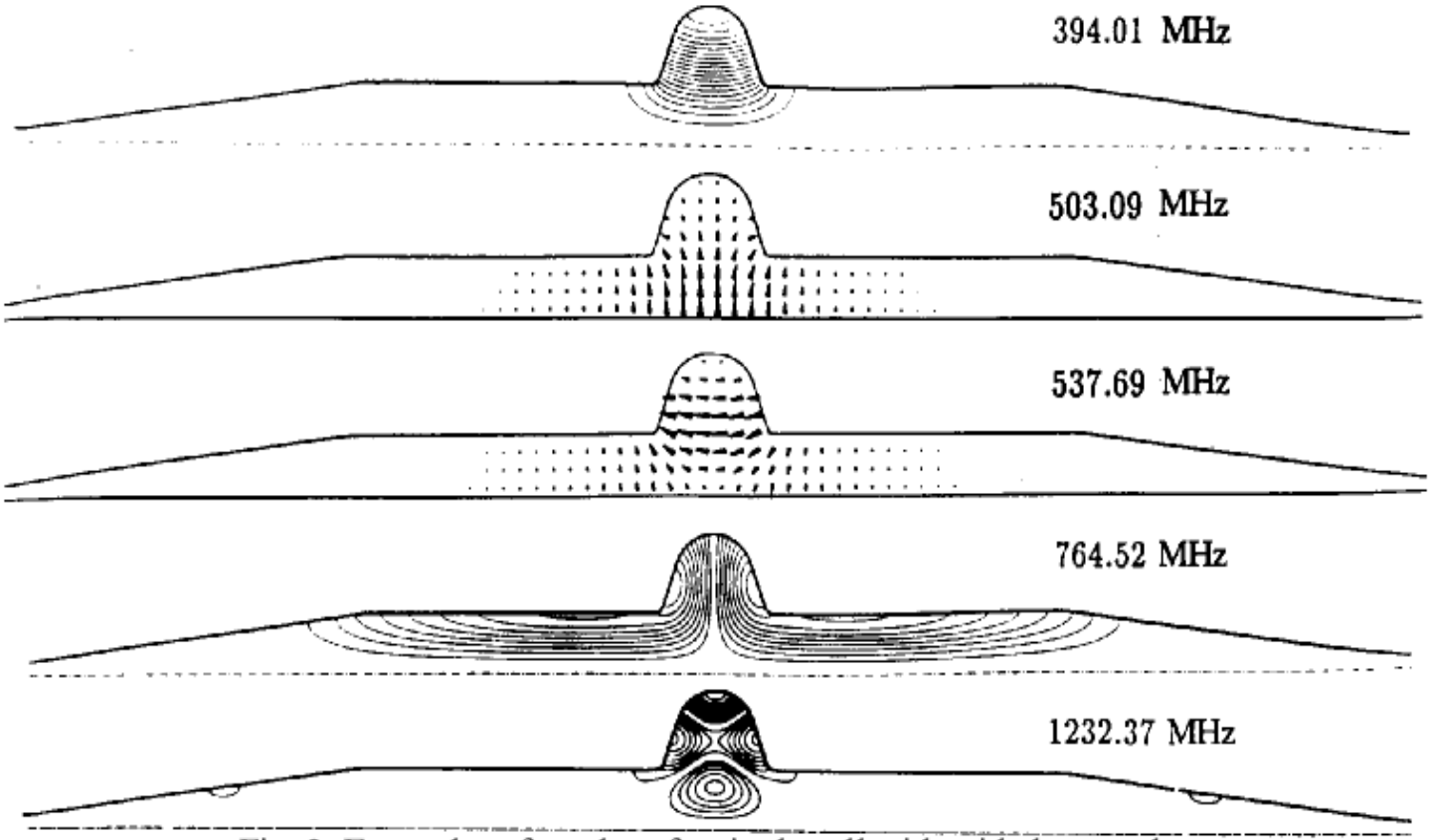

Fig. 3 Examples of modes of a single cell with wide beam tubes

A typical HOM spectrum

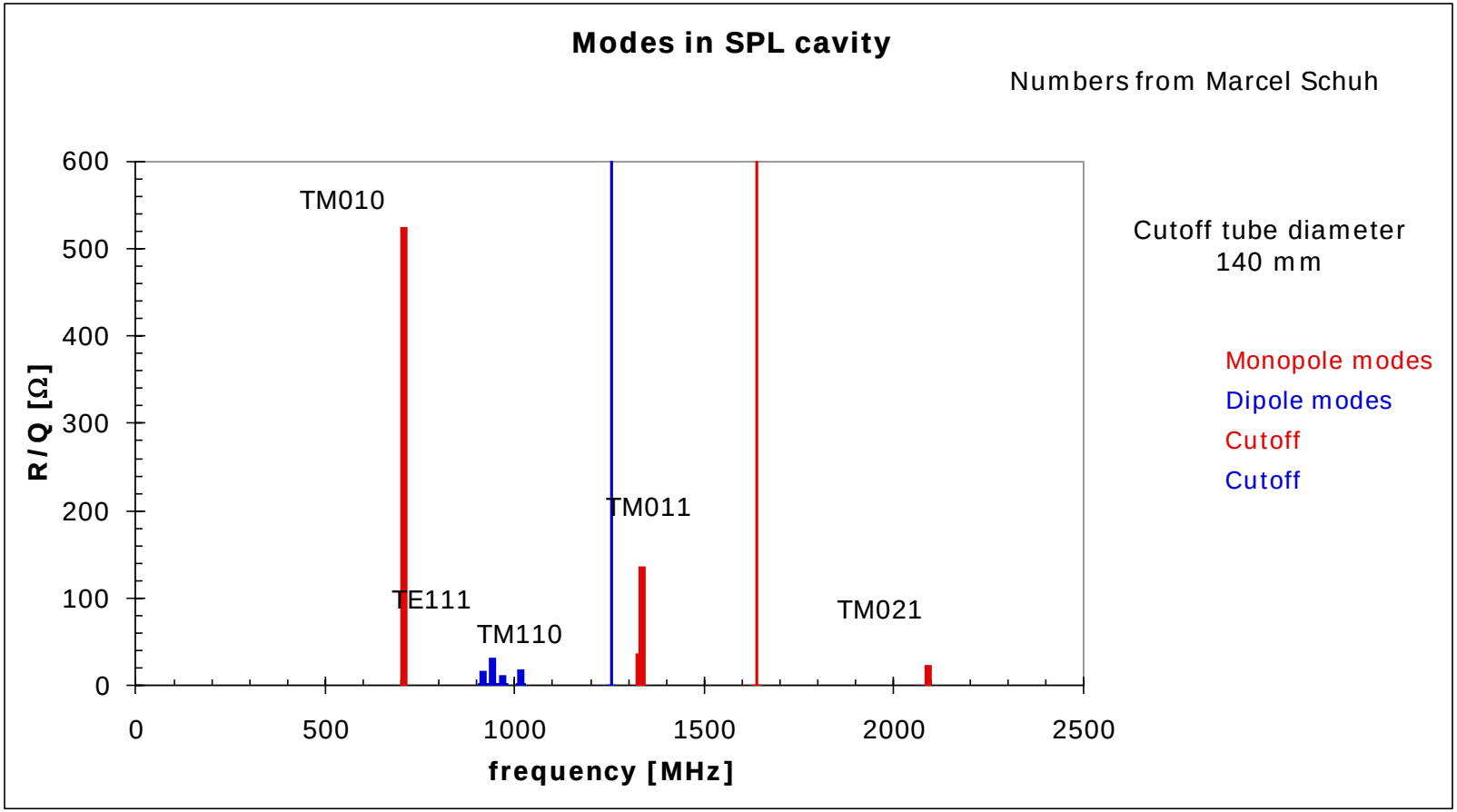

How to deconfine HOMs[1] 1/2

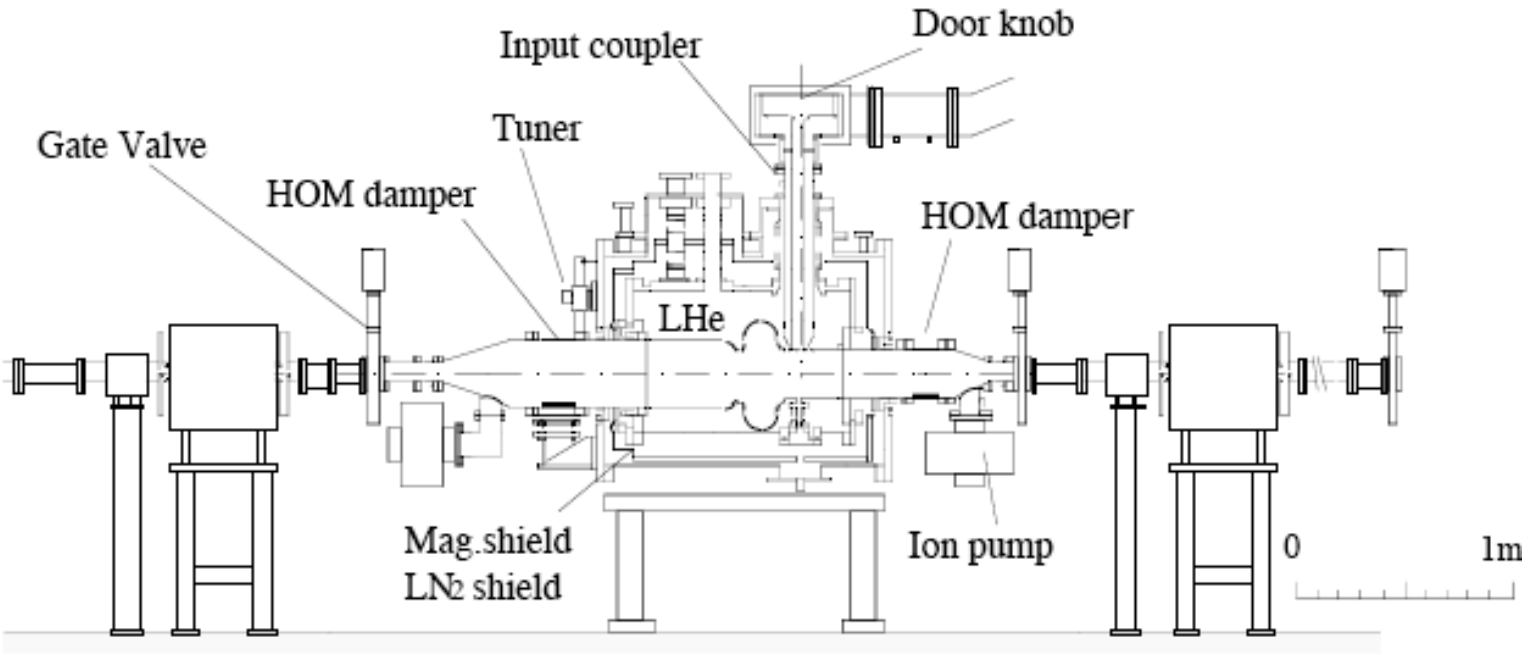

Figure: 1 A sketch of the prototype module in TRISTAN Accumulation Ring.

Open beam tube

OK for single cell cavity, but high cryo-load by thermal radiation

[1]http://www.lns.cornell.edu/Events/HOM10/Agenda.html

How to deconfine HOMs 2/2

Open beam tube:

Use ridge-shaped beam tubes (Cornell)

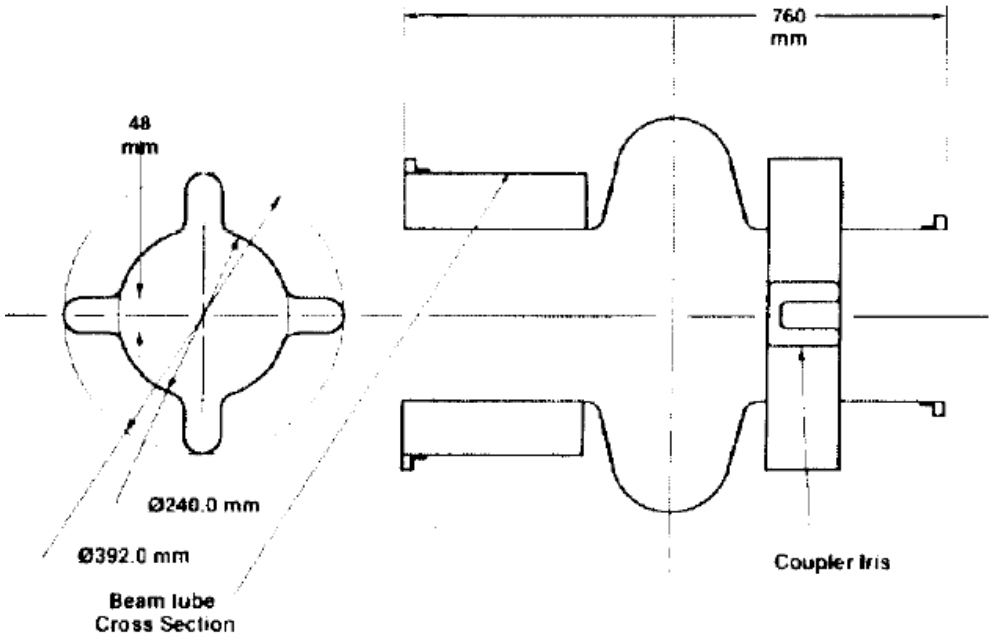

Fig. 3 Fluted beam pipe and input coupler geometries

Damping HOMs 1/2: Beam tube loads

Ferrites

- low power handling capacity if cold
- higher power handling capacity if warm
- mechanical and vacuum design not easy

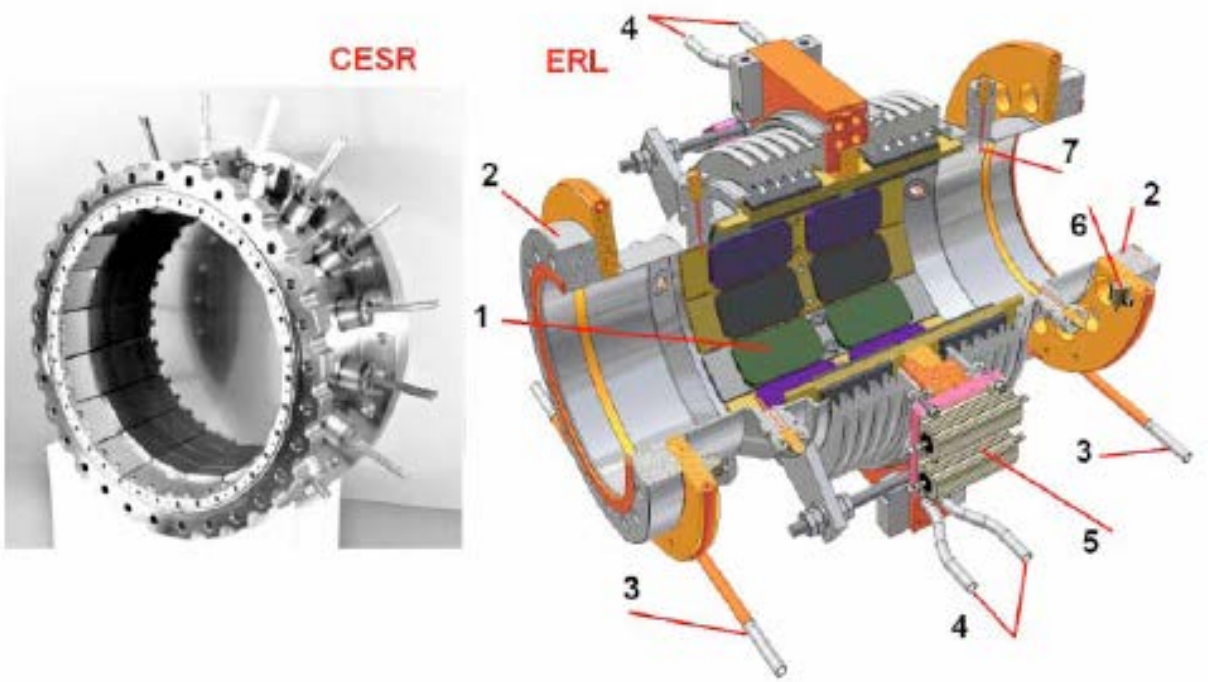

Figure 1: CESR and ERL HOM loads. 1 – absorber plates, 2 – flange to cavity, 3 – 5 K He cooling loop, 4 – 80 K cooling loop, 5 – 80 K heater, 6 – 5 K heaters, 7 – HOM pickup.

Damping HOMs 2/2: Resonant coaxial transmission line dampers

- Compensate internal impedances: The HOM coupler becomes a resonator coupled to the cavity resonator. It may have two eigenfrequencies.

  Obtainable Q_{ext}: 50
- Pros:
  - Couplers with several resonances possible (HERA, LEP, LHC, ILC are of this type)
  - Demountability
  - Fundamental mode rejection:
    - LEP: Fundamental mode E-field rejected by stop-filter in front of HOM coupler
    - Fundamental mode H-field rejected by loop plane perpendicular to cavity axis
    - Risk of detuning of notch filter
- BUT: High currents request for superconducting material prepared under ultra-clean conditions (like the cavity) and lHe cooling
- Prone to electron emission from inside cavity

Resonant coaxial transmission line dampers: Technical solution 1/3

LHC HOM coupler

Resonant coaxial transmission line dampers: Technical solution 2/3

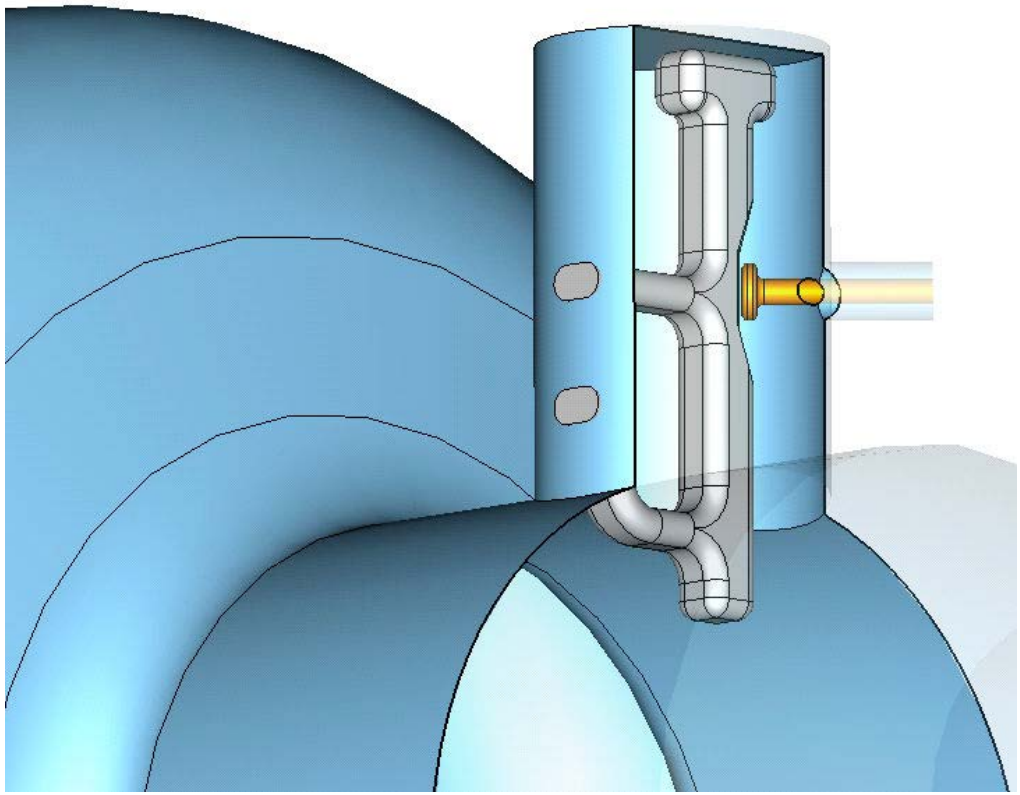

SNS HOM coupler

Resonant coaxial transmission line dampers : Technical solution 3/3

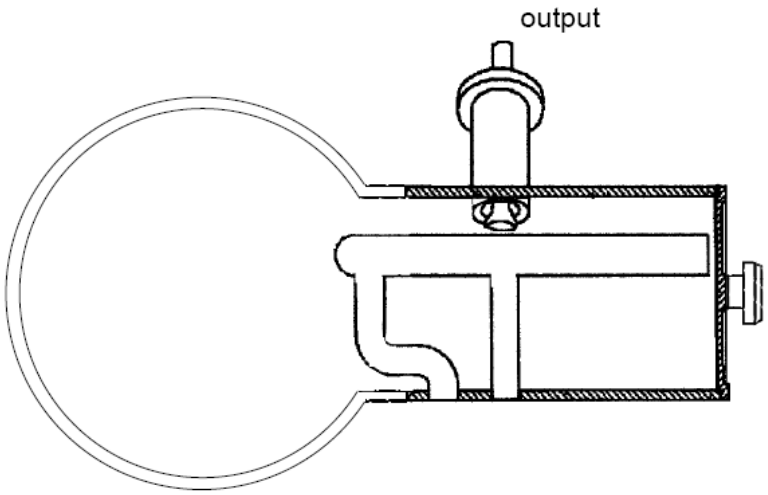

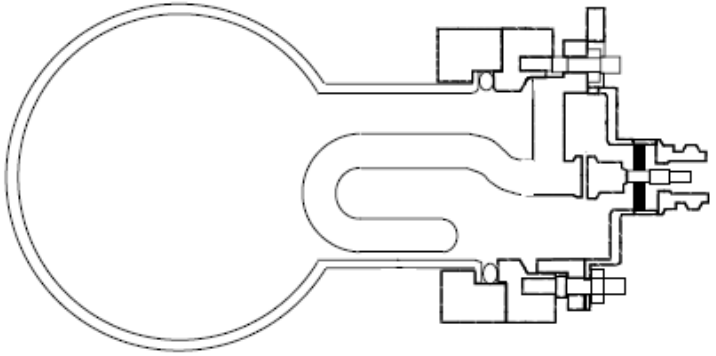

TESLA HOM coupler

The frequency tuner

The frequency of the cavity must be tuned to the harmonic spectral line of the bunched beam => need to develop a frequency tuner. Slater's theorem states that

$$\frac{\Delta f}{f} = \frac{1}{4U}\int_{\Delta V}\left(\varepsilon_0 E^2 - \mu_0 H^2\right)dV$$

$$U = \frac{1}{4}\int_{V}\left(\varepsilon_0 E^2 + \mu_0 H^2\right)dV$$

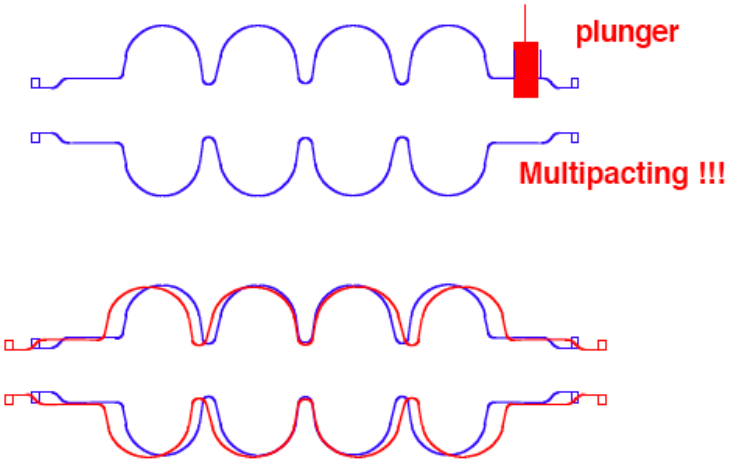

Mechanical oscillations

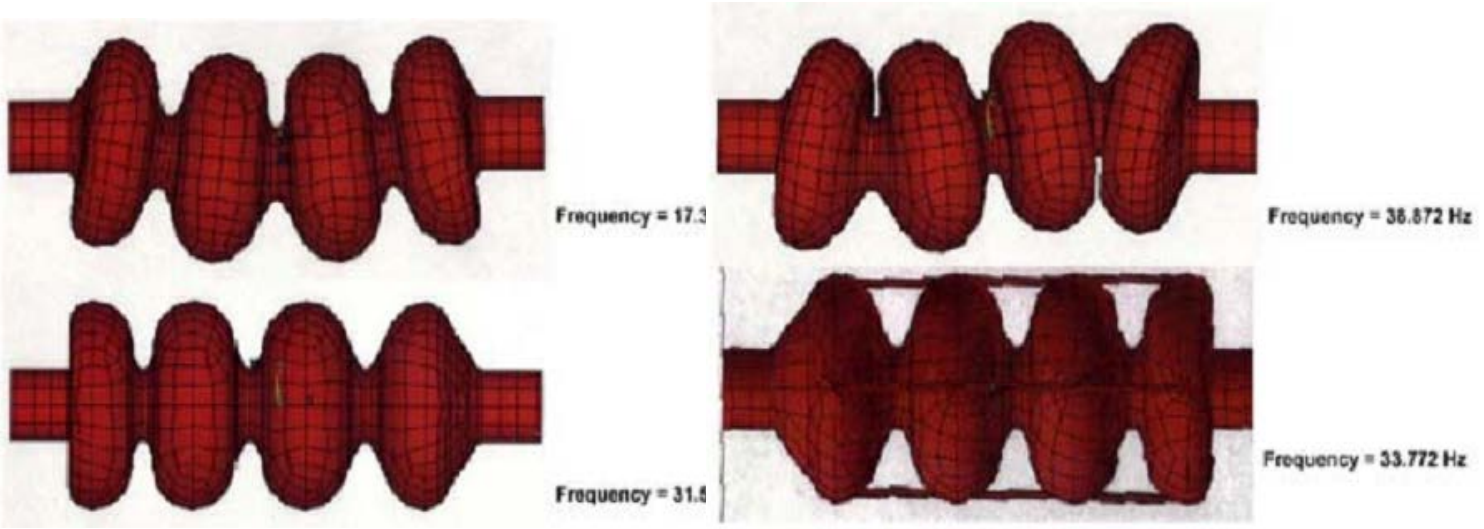

Fig. 20 Mechanical resonant modes of a 4-cell, 200 MHz cavity with 8 mm wall thickness. The low resonant frequencies spell trouble in the form of microphonics. Reducing the number of cells or stiffening is essential.

The LEP solution

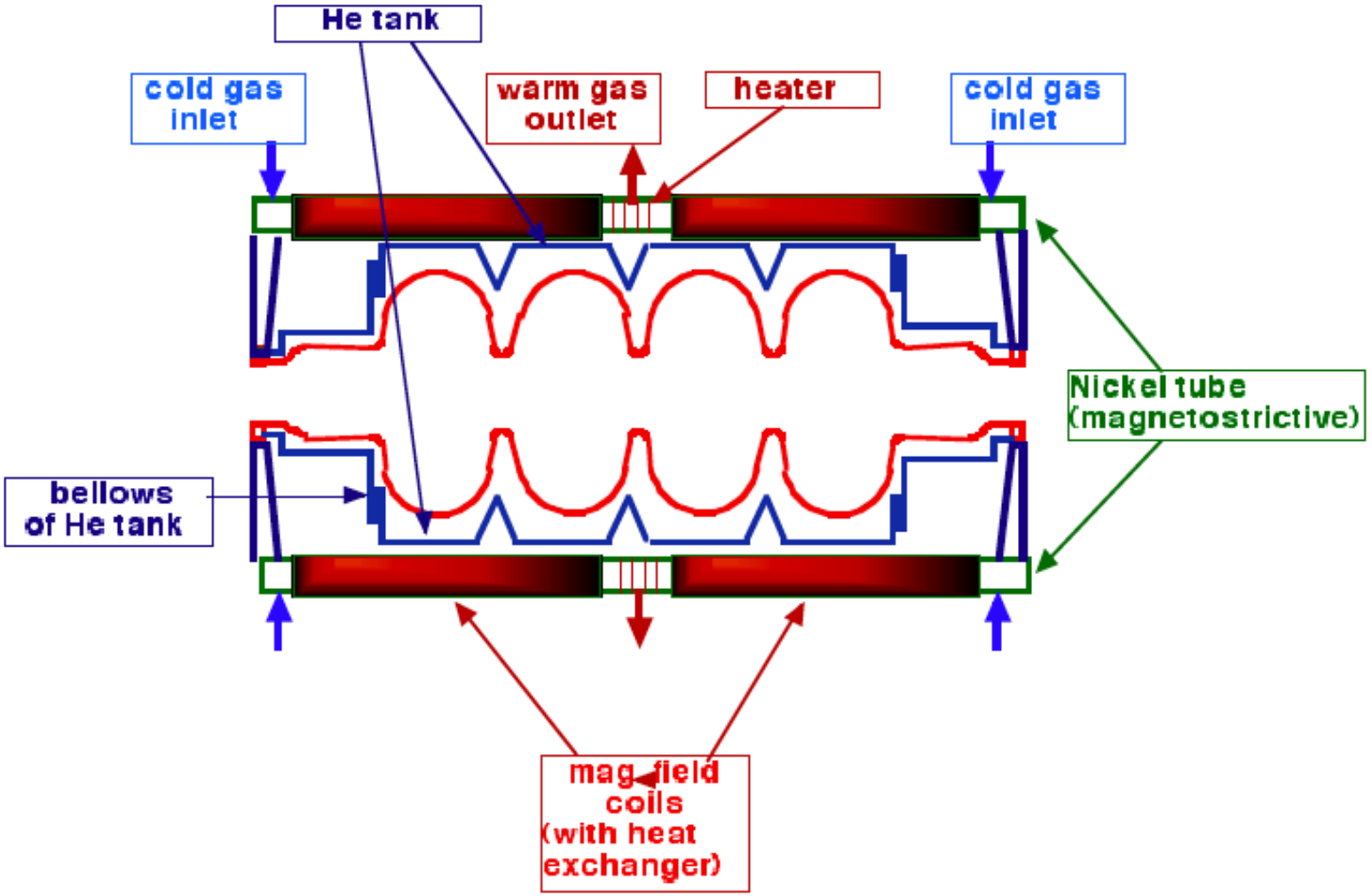

Integration into LEP cryostat 1/2

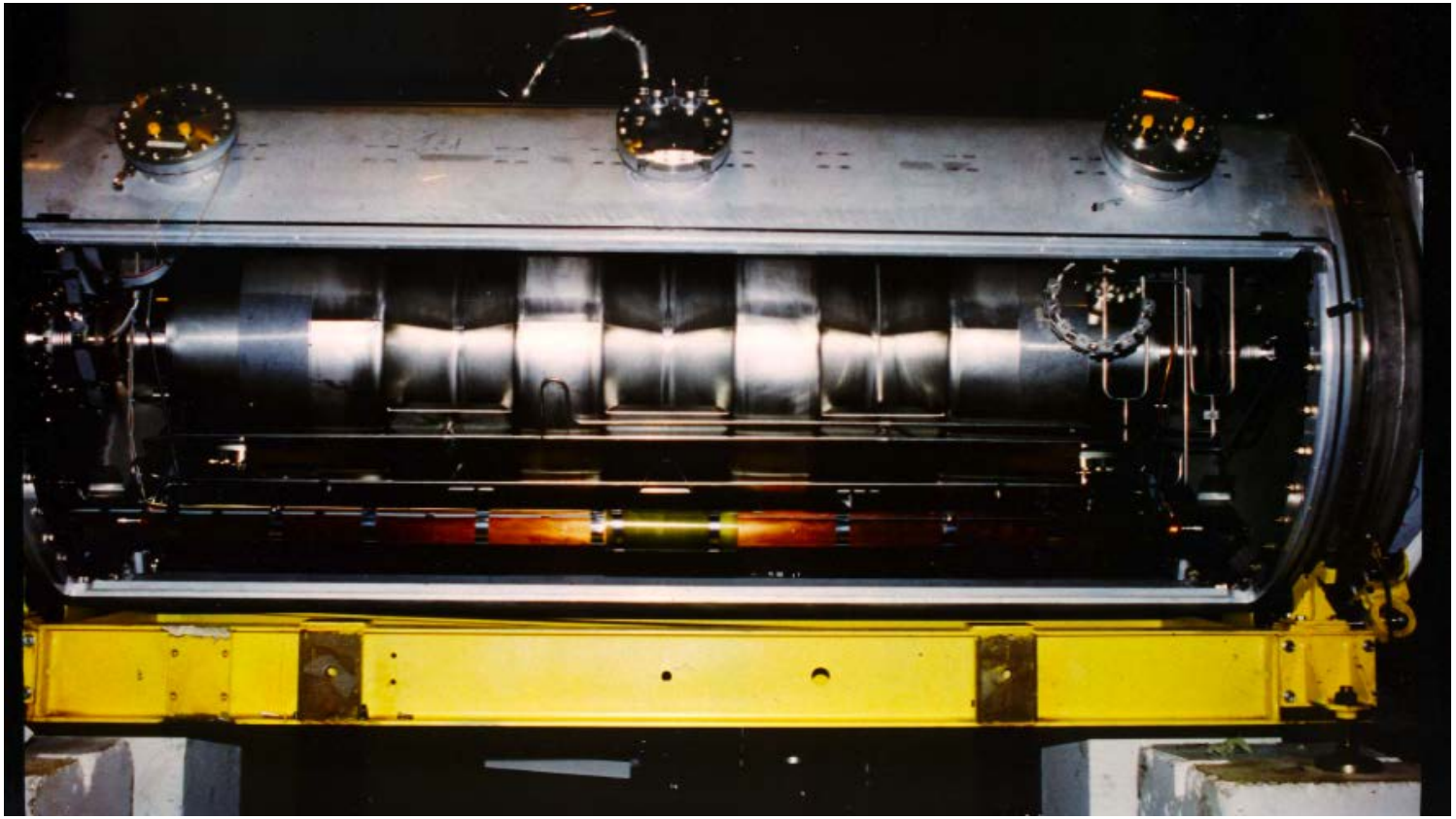

Integration into LEP cryostat 2/2

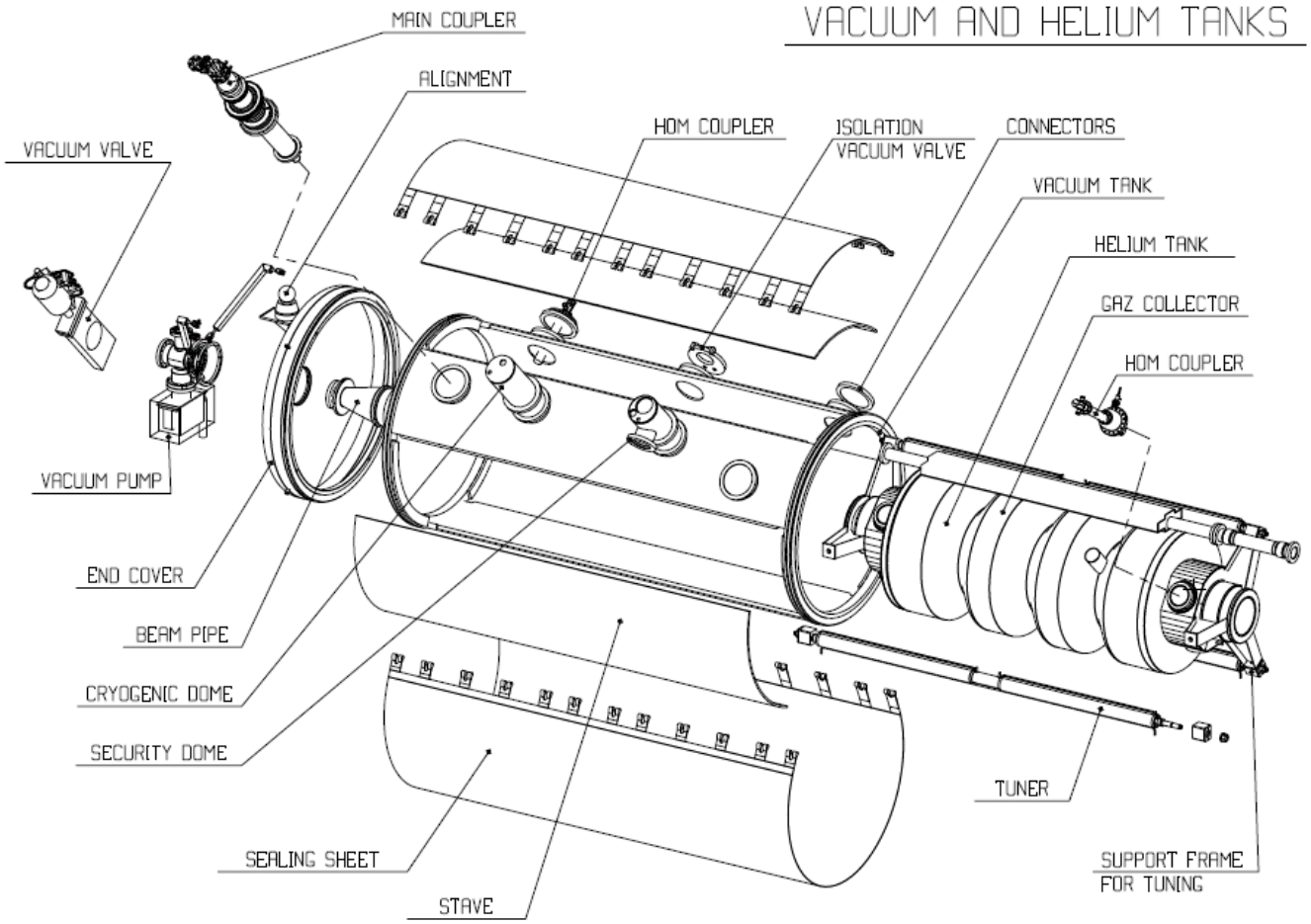

Comments:

The LEP cryostat could reliably be operated under CW conditions with beam and in pulsed conditions without beam in the present LHC tunnel environment (1.4 % slope).

It is worth noting that the lHe tank, the gas openings, and gHe collector were relatively small.

Pulsed operation: The thermal diffusivity $\kappa = \lambda/(c \cdot \rho)$ is such that it takes ~1 ms before the temperature pulse arrives at the niobium helium interface => advantage compared to CW operation.

This cryostat was tested under pulsed conditions with beam in the CERN SPS.

Summary

- A lumped network circuit diagram allows an analytical description of the interaction of the RF cavity with the beam
- The cavity is designed to minimize the reflected RF power (which would be wasted anyhow in a load) by eliminating the « reactive beam loading » through tuning the frequency of the cavity and by matching the external Q to the nominal beam current.
- The beam consists of bunches passing the cavity in fractions of milliseconds[1] that may excite higher order modes (HOMs) of the cavity to high voltages, if not sufficiently damped by HOM couplers.
- Frequency tuners are in addition needed to damp frequency shifts from mechanical resonances excited by external noise sources (microphonics) or the interaction of the electromagnetic pressure with the cavity wall (Lorentz force detuning).

[1] for large storage rings such as LEP

Technological issues

- What are the technological issues at stake for the design of an accelerating system with emphasis on the superconducting option?
  - Circular vs. linear
  - Superconducting vs. normal conducting
  - Operating frequency and temperature, if sc
- Anomalous losses
- Diagnostics (Temperature mapping)
- Electron field emission
- Electron Multipacting (dust free assembly)
- Heat removal (Quench - the role of large thermal conductivity, Coating a copper cavity with a thin niobium film)
- Quality assurance and stochastic parameters
- Cryostat
- Cryomodules
- Magnetic shielding
- Summary

Circular vs. linear

Circular vs linear: With P as beam power to be replaced by the acceleration system, E the beam energy, ρ the radius, L_{RF} the length of the RF system, g the accelerating gradient, for a circular accelerator (if limited by synchrotron radiation)

$$\underbrace{g \cdot L_{RF}}_{V_a} \cdot I = V_a \cdot I = P = \text{const} \cdot \frac{(E/m)^4}{\rho^2} \quad \Rightarrow \rho \propto \frac{E^2}{\sqrt{g}}$$

whereas for a linear accelerator

$$E \propto L_{RF} \cdot g \Rightarrow L_{RF} = \frac{E}{g}$$

With assumption that the costs are proportional to the linear dimensions (L_{RF} or ρ), for very high energies the linear accelerator is less costly than a circular accelerator.

SC vs. NC 1/4 under CW operation

Superconducting vs normal conducting:

A figure of merit is the mains to beam power conversion eficiency

With P_b as beam power and P_c dissipated power in the RF system, the efficiency is defined as

$$\eta = \frac{P_b}{P_b + P_c} = \frac{1}{1 + \frac{P_c}{P_b}}$$

With the accelerating voltage V the shunt impedance R is defined as

$$R = \frac{V^2}{2 \cdot P_c}$$

The beam power P_b is simply the product of beam current I_b and accelerating voltage V**:**

$$P_b = V \cdot I_b$$

which leads to

$$\eta = \frac{1}{1 + \frac{V}{2 \cdot R \cdot I_b}}$$

SC vs. NC 2/4

- Carnot efficiency

However:

The dissipated power must be removed at a very low temperature (4.2 – 4.5 K).
Hence we have to take into account the cryogenic efficiency η_{cr}

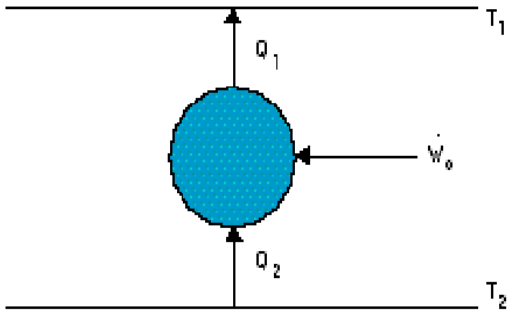

Schematic power flow in a refrigerator

According to the first law of thermodynamics, the power

$$\dot{W}_c = Q_1 - Q_2 = Q_2(Q_1/Q_2 - 1) = Q_2(T_1/T_2 - 1) \qquad (2)$$

has to flow into the compressor. The Carnot efficiency η_c for a refrigerator is defined as

$$\eta_c = Q_2 / \dot{W}_c = T_2 / (T_1 - T_2). \qquad (3)$$

For $T_1 = 300$ K and $T_2 = 4.2$ K, $\eta_c = 1/70$. The 'thermodynamic efficiency'

$$\eta_{td} = \dot{W}_c / \dot{W} \qquad (4)$$

SC vs. NC 3/4

is the ratio of the power $\dot{W}_c$ needed to operate the compressor in the ideal case to the 'real' power $\dot{W}$. The total cryogenic efficiency is

$$\eta_{cr} = Q_2 / \dot{W} = \left(Q_2 / \dot{W}_c\right)\left(\dot{W}_c / \dot{W}\right) = \eta_c \eta_{td} \,. \tag{5}$$

With $\eta_{td} \approx 0.3$ for large units the total cryogenic efficiency is $\eta_{cr} = 4.5 \times 10^{-3}$. Unavoidably, in an sc accelerator some power P_{cr} flows into the liquid He, even in the absence of RF (standby heat load of cryostat). The efficiency η for a sc accelerator of RF-to-beam power conversion is then

$$\eta = \left[1 + \left(P_c + P_{cr}\right) / \left(P_b \eta_{cr}\right)\right]^{-1} \,. \tag{6}$$

As an example, for the sc cavity and cryostat for LEP with P_c = 50 W, P_b = 50 kW and P_{cr} = 25 W, we obtain a total efficiency of η = 0.75, which is larger by a factor of 5 than for a conventional RF system (Table 1).

SC vs. NC 4/4

- Comparison Table

	nc	sc	
Beam current	6	6	mA
Accelerating voltage	3	8.5	MV
Field gradient	1.4	5	MV/m
Shunt impedance R	43	3150 [1])	MΩ
P_c	105000	52 @ 4.2 K	W
P_b	18000	51000	W
P_{cr}	0	25	W
η_{cr}	100	0.45	%
η_{RF}	15	75	%

[1]) including the total cryogenic efficiency η_{cr}

Operating Frequency and temperature

The figure of merit is the shunt impedance R, or the shunt impedance r per length, which should be maximized:

$$\frac{R}{L} = r = \frac{V^2}{2P_c L} = \frac{E_a^2 L^2}{2\omega U L}\frac{\omega U}{P_c}$$
$$= \frac{E_a^2}{2\omega U/L}\frac{\omega U}{P_c} = \frac{r}{Q}Q = \frac{r}{Q}\frac{G}{R_s}$$
$$= \frac{r}{Q}\frac{G}{R_s^{BCS} + R_{s0}}$$

where we have made use of the definition of $r/Q = E_a^2/(2\omega U/L)$, $Q = \omega U/P_c$, $V = E_a L$, $R_s Q = G$, the geometry factor. U is the stored energy, E_a the accelerating gradient, R_s^{BCS} the BCS part of the surface resistance, and R_{s0} its residual part (cf. sections 4.1 and 6.1). Now we shall look at the dependence on the frequency f of the different factors. From Fig. 8 (see below) we learn that for niobium the condition $R_s^{BCS} \gg R_{s0}$ is valid for frequencies larger than 3 GHz, and the condition $R_s^{BCS} \ll R_{s0}$ is valid for frequencies smaller than 300 MHz:

$$\underbrace{(r/Q)}_{\propto f}\frac{G}{\underbrace{R_s^{BCS}}_{\propto f^2} + R_{res}} \propto \begin{cases} f^{-1}, R_s^{BCS} \gg R_{res}, f > 3\ \text{GHz} \\ f, R_s^{BCS} \ll R_{res}, f < 300\ \text{MHz} \end{cases} \quad (8)$$

To maximize r, we are forced to prefer lower frequencies for $f \geq 3$ GHz, and higher frequencies for $f < 300$ MHz. Therefore, neither very low nor very high frequencies are useful, and $\beta = 1$ accelerating structures are operated between 300 MHz and 3 GHz, approximately.

Anomalous losses

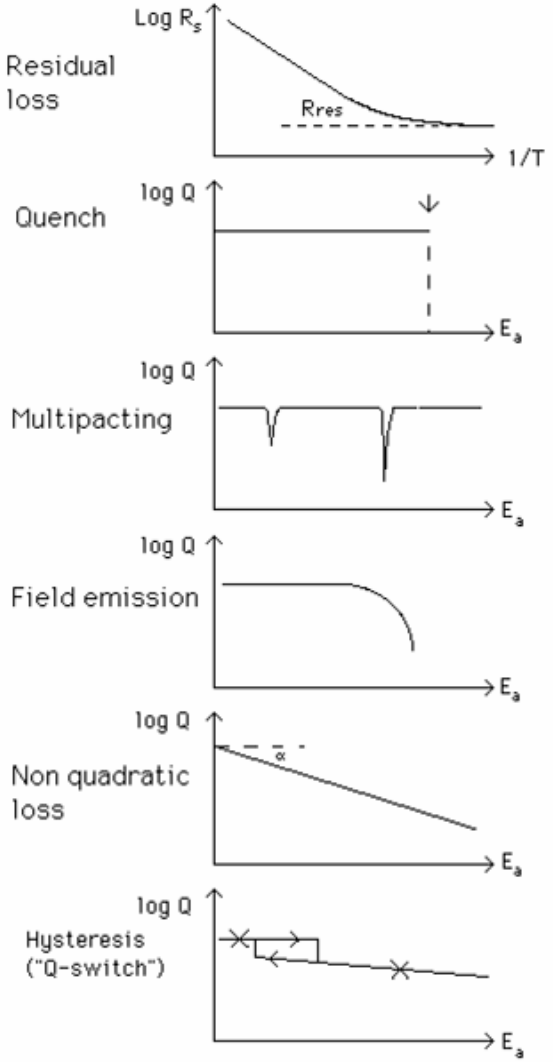

So-called « anomalous losses » account for all contributions to the RF losses that are not described by the intrinsic parameters of the superconducting material (critical temperature, critical field, BCS (or two fluid) surface resistance R_s, etc.).

These anomalous losses show up as heat and are visible in the R_s (T) and $Q_0(E_a)$ plots, as well as in the « temperature maps ».

Diagnostics 1/7

JUAS Lecture Archamps 2008

Diagnostics 2/7

- Temperature mapping equipment (~ 1980)

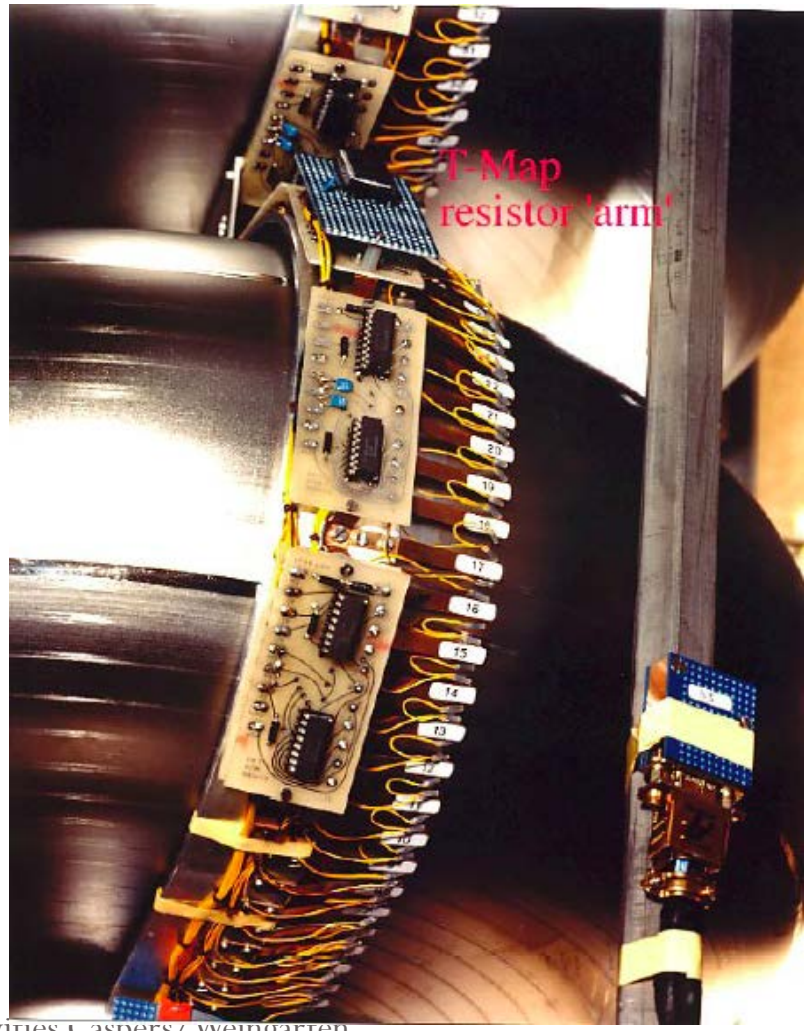

Diagnostics 3/7

- Temperature mapping results (today)

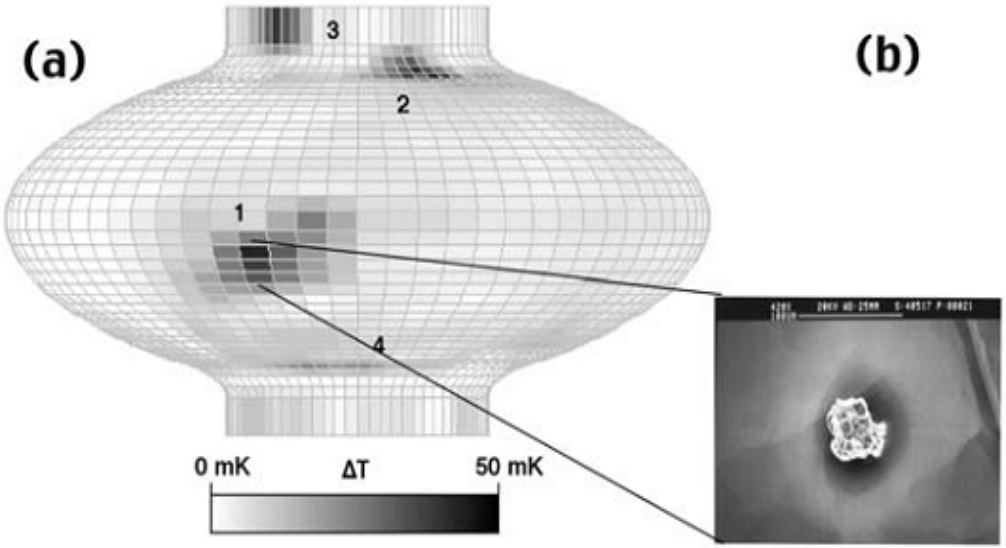

Fig. 16 (Left) Temperature map at 400 Oe of a 1.5 GHz, single cell cavity showing heating at a defect site, labelled #1 and field emission sites labelled #2, 3, and 4. (b) SEM micrograph of the RF surface taken at site #1 showing a copper particle [5].

From H. Padamsee: CERN -2004 - 008

Diagnostics 4/7

- T-mapping for the diagnosis of anomalous losses

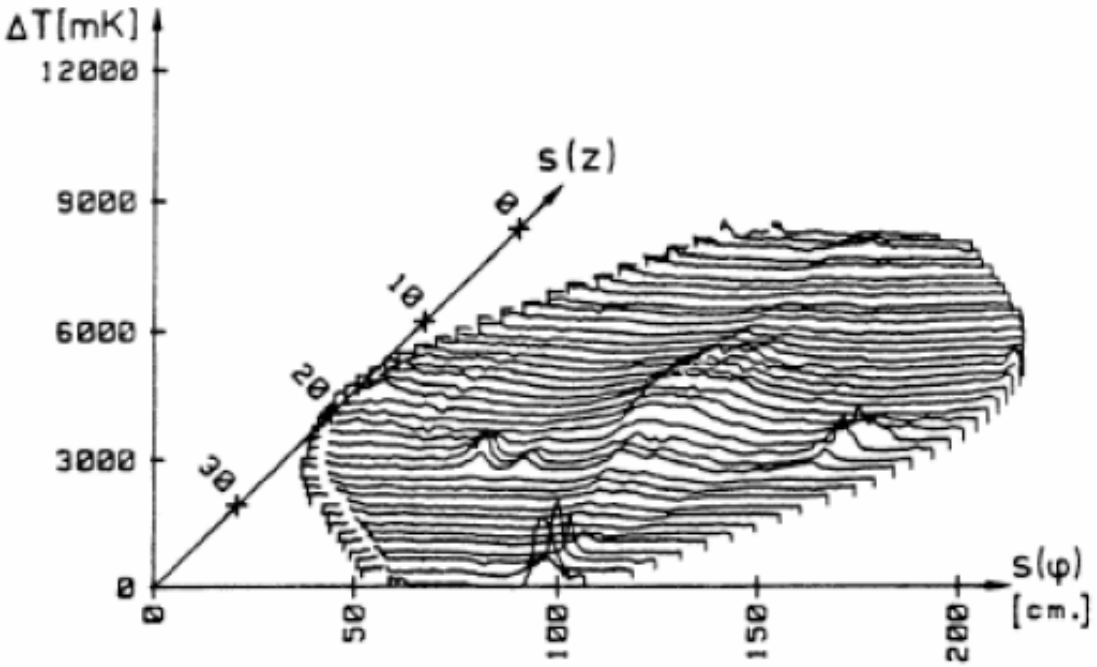

Fig. 4: Temperature map of a 500 MHz cavity at E_{acc} = 12.5 MV/m. The temperature increase ΔT of the outer cavity surface is plotted against the surface coordinates s(z) and s(ϕ)(z=length in arbitrary units along a meridian, ϕ = azimuthal location)

Diagnostics 5/7

- T-mapping for electron field emission diagnosis

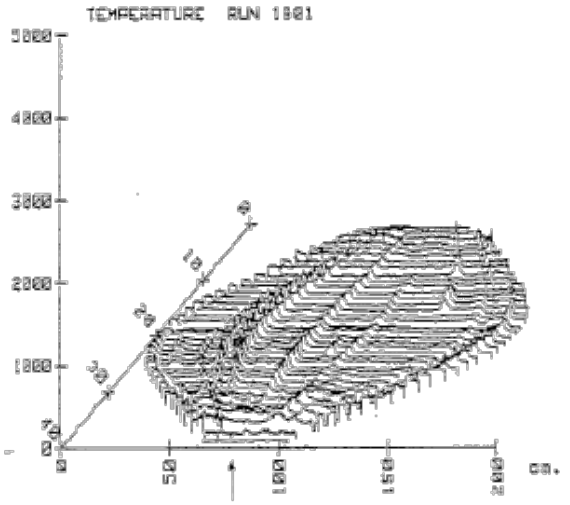

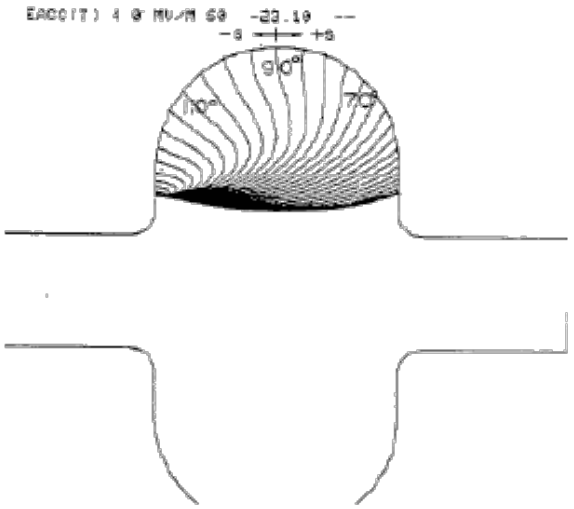

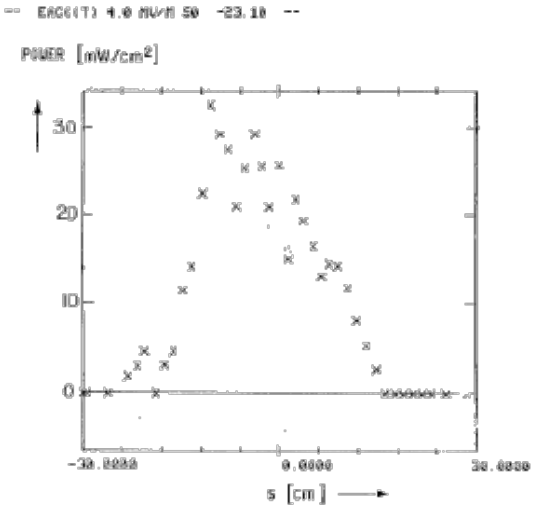

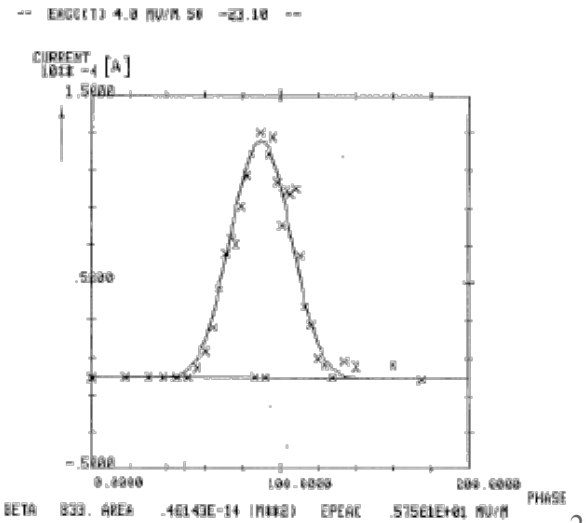

Diagnostics 6/7

- Second sound in superfluid helium

First used by K. Shepard at Argonne NL for detecting the quench location in split ring resonator

Courtesy K. Liao - CERN

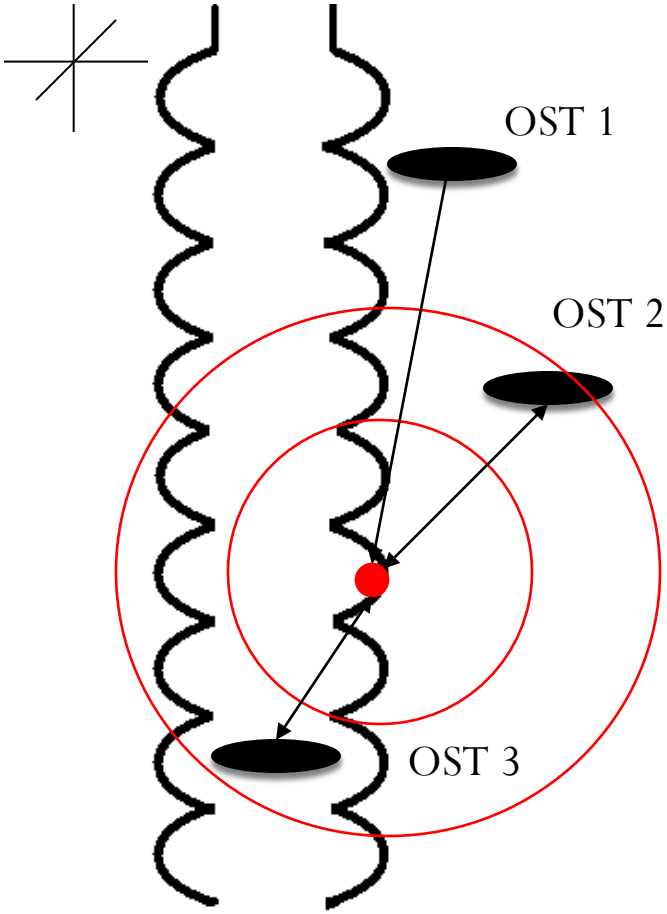

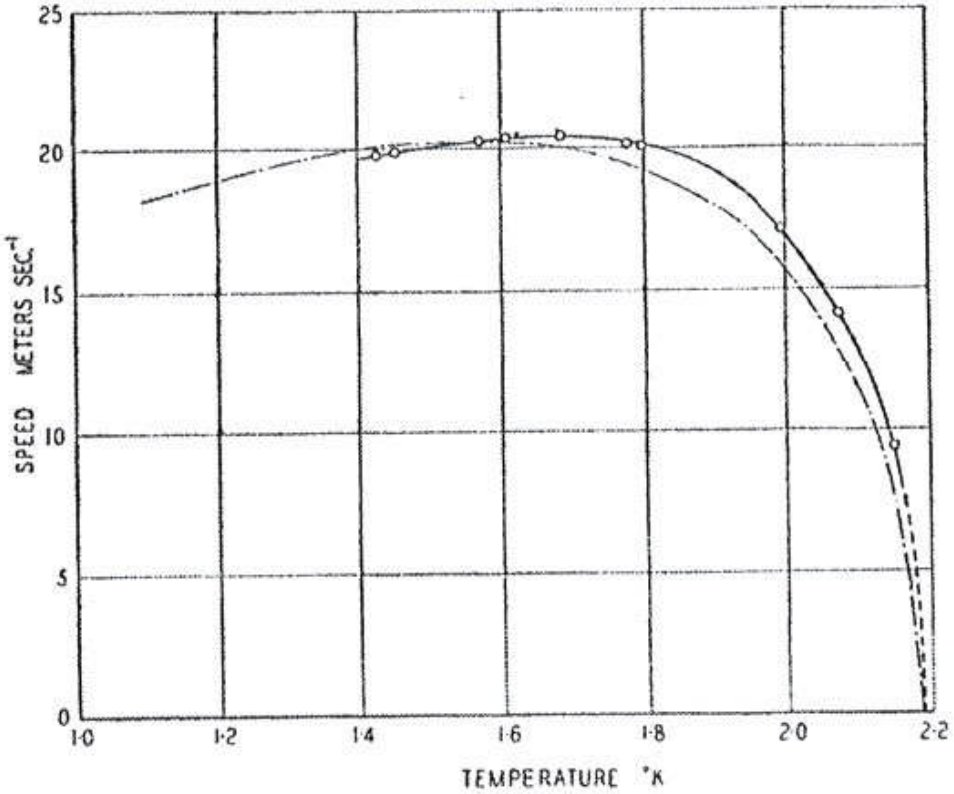

Diagnostics 7/7

- Second sound in superfluid helium: Speed of 2nd sound

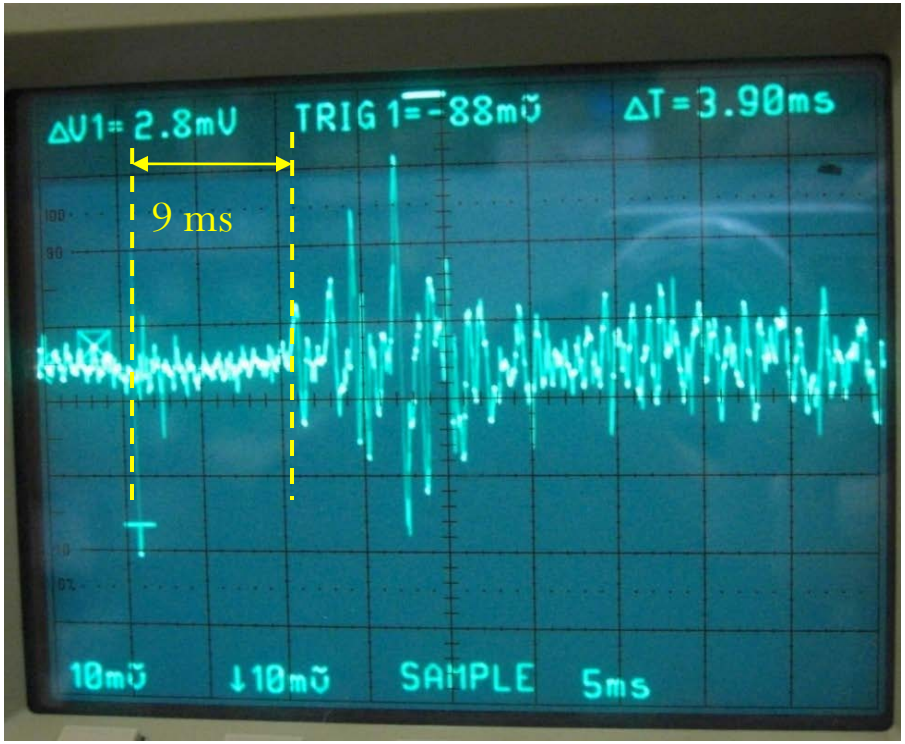

OST 1: 70pF , f=*12kHz* (R.T.)
OST 2: 63.5pF, f=*6.5kHz* (R.T.)
Suppress common mode hum (50Hz)

OST 1 (20 cm) - OST2 (20cm)

V= D/ Δt
=20cm/9ms
=22.2 m/s

Electron field emission 1/5

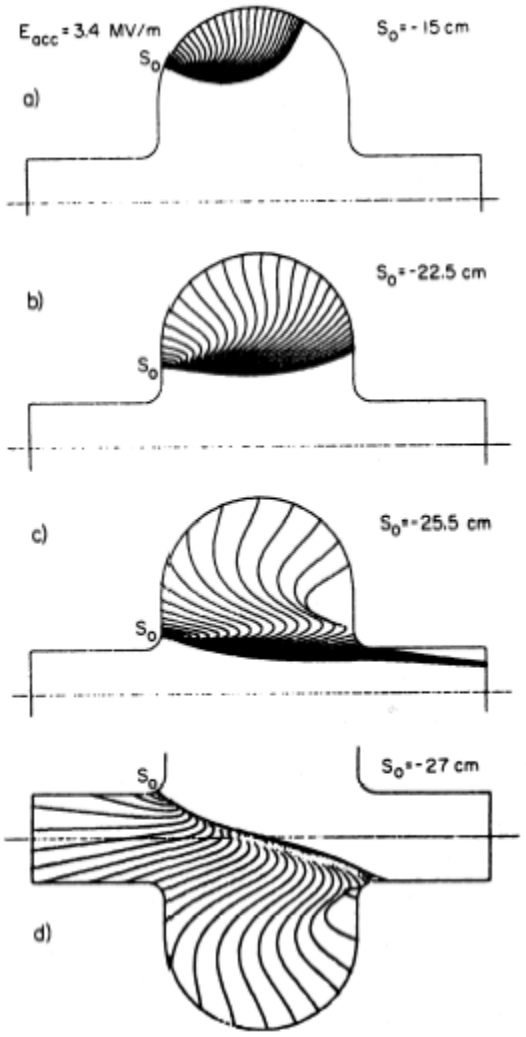

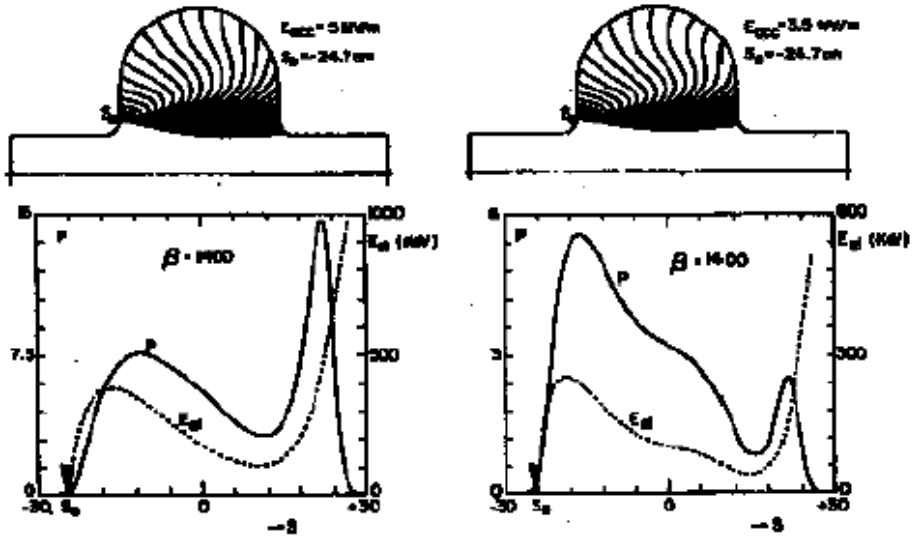

Impact energy and differential heat load

Electron field emission 2/5

The **basic physics** is described by the model calculation due to **Fowler & Nordheim**. The current emitted for a surface area A depends exponentially on the local surface electric field E:

$$I_{FN} = A \cdot \frac{C}{\Phi t^2(y)} E^2 \exp\left(-\frac{B\Phi^{3/2} v(y)}{E}\right)$$

B and C are constants, Φ is the work function, and t and v are slowly varying functions of E close to 1

In reality, the current observed is much larger than described by the FN model. The discrepancy is subsumed in a field enhancement factor β: $E_{local} = \beta E_{applied}$.

Electron field emission 3/5

- Typical particulate emitters containing impurities

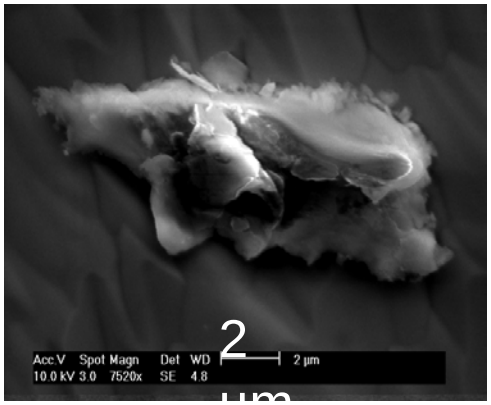

E_{on}(2nA) =140 MV/m
β= 31, S = $6.8 \cdot 10^{-6}$ µm²

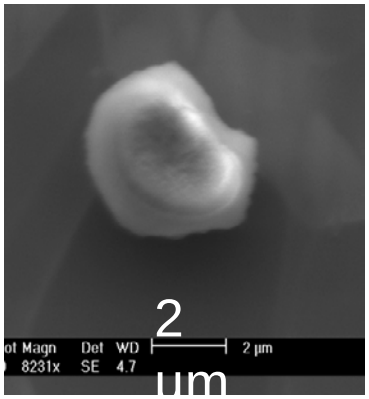

E_{on}(2nA) = 132 MV/m
β = 27, S = $7 \cdot 10^{-5}$ µm²

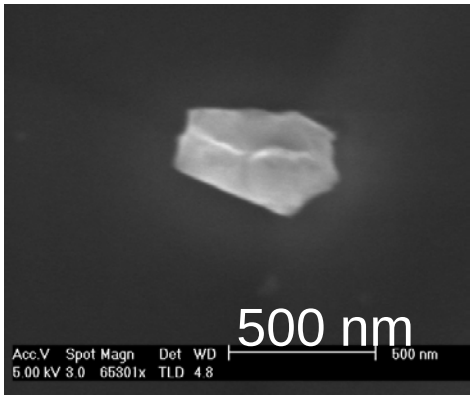

E_{on}(2nA) > 120 MV/m
β = 46, S = $6 \cdot 10^{-7}$ µm²

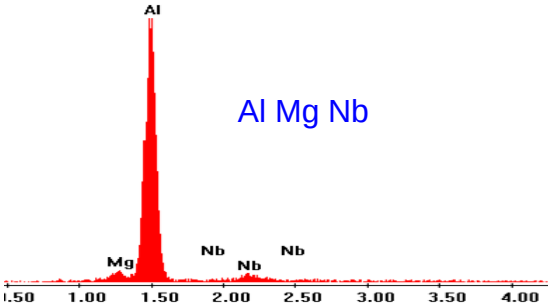

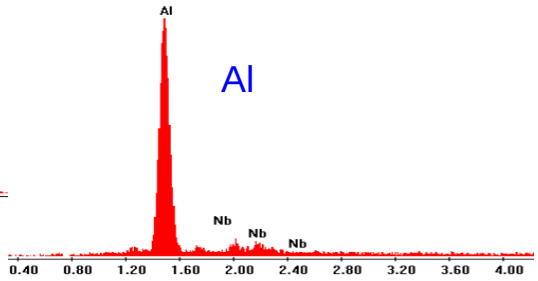

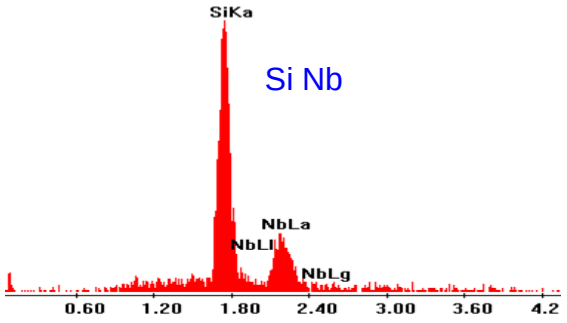

Electron field emission 4/5

- Fowler Nordheim theory

Field emission of electrons from flat metal surfaces

Electron waves of bound states in a metal can tunnel through the potential barrier V(z) at the solid surface into vacuum by means of the quantum mechanical tunnelling effect

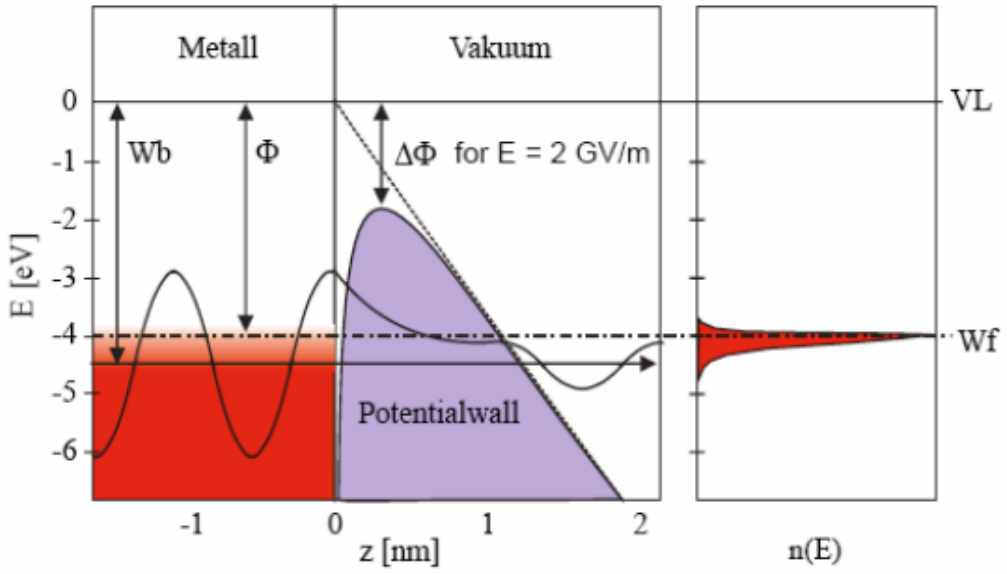

$V(z) = -e \cdot E \cdot z - e^2/(16\pi\varepsilon_0 \cdot z)$

work function Φ of metal

applied field E on surface

image charge correction

$\Delta\Phi = (e^3E/4\pi\varepsilon_0)^{1/2}$

Calculation of the current density j(E) within the Fowler-Nordheim theory results in

$$j(E) = \frac{AE^2}{\Phi t^2(y)} \exp\left(-\frac{B\Phi^{3/2} v(y)}{E}\right)$$

with constants A=154 and B=6830 and slight correction functions t(y) and v(y)

Φ=4eV at **E=2000 MV/m** ⇒ **j= 1nA/μm²**

G. Müller, 15.11.2006 Bergische Universität Wuppertal CARE06, Frascati

Electron field emission 5/5

- Clean room preparation mandatory

Electron multipacting

Localized heating by multiple impact from electron current due to secondary emission in resonance with RF field.

Historically this phenomenon was a severe limitation for the performance of sc cavities.

The invention of the "circular" shape opened up the avenue for higher gradients.

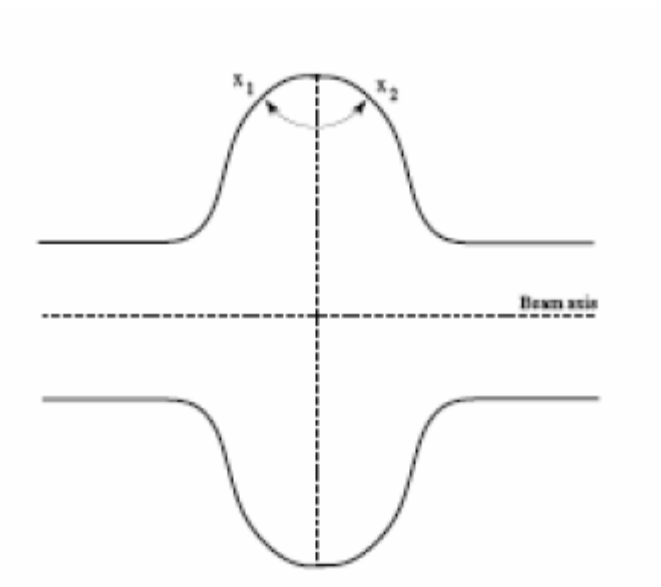

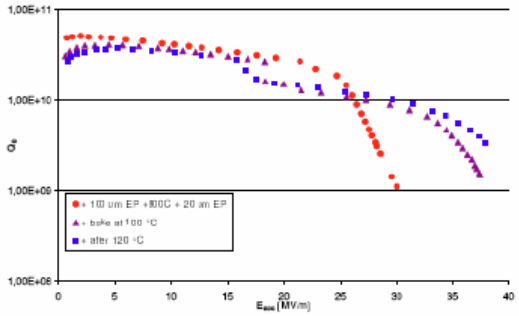

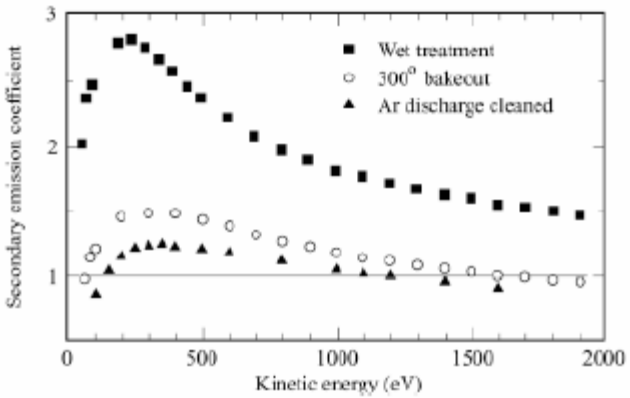

Heat removal 1/2

- Thermal Improvement of thermal conductivity for Niobium sheets

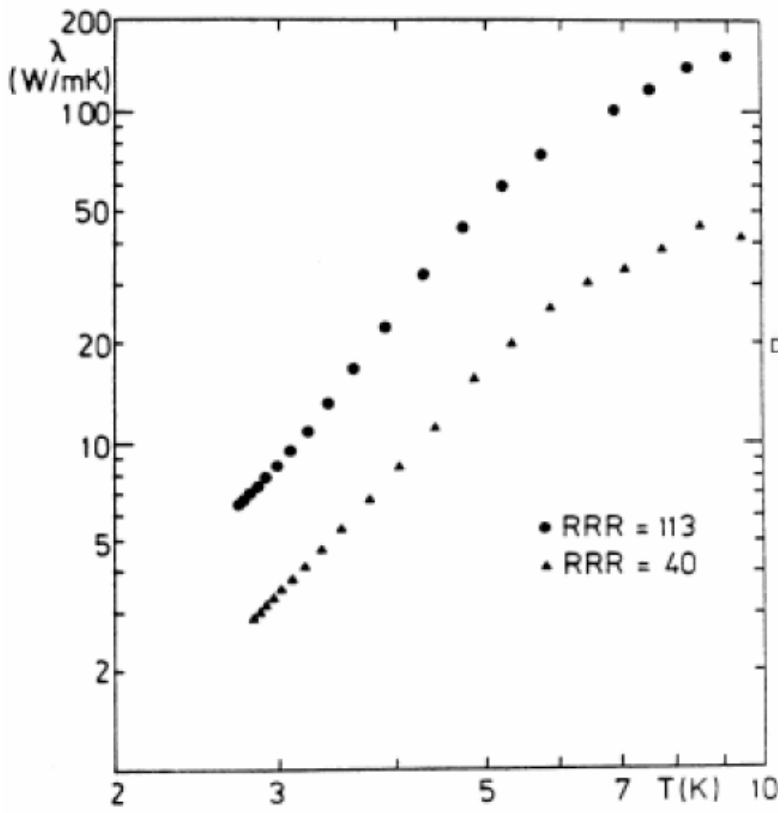

Fig. 1: Thermal conductivity of reactor grade niobium (RRR=40) and niobium of higher purity (RRR=113)

Cause for "quench":

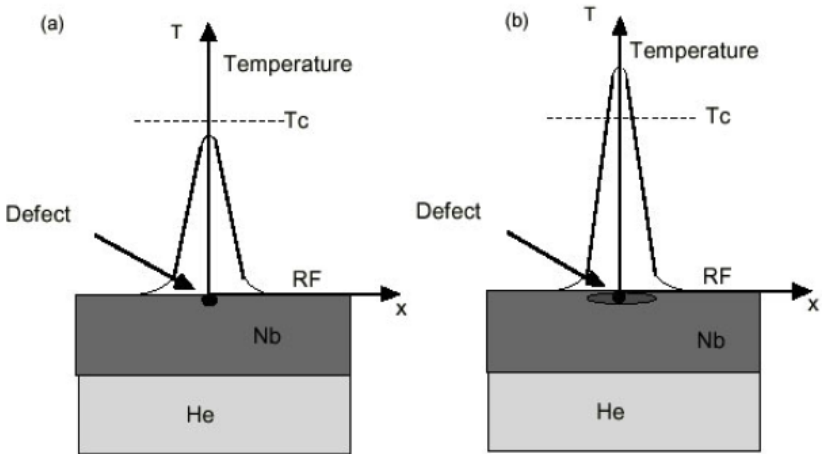

$$H_{max} \approx \sqrt{(4(T_c - T_B)\lambda/(R_n\, r))}\ .$$

Heat removal 2/2

- Role of thermal conductivity on max. RF field for cavities

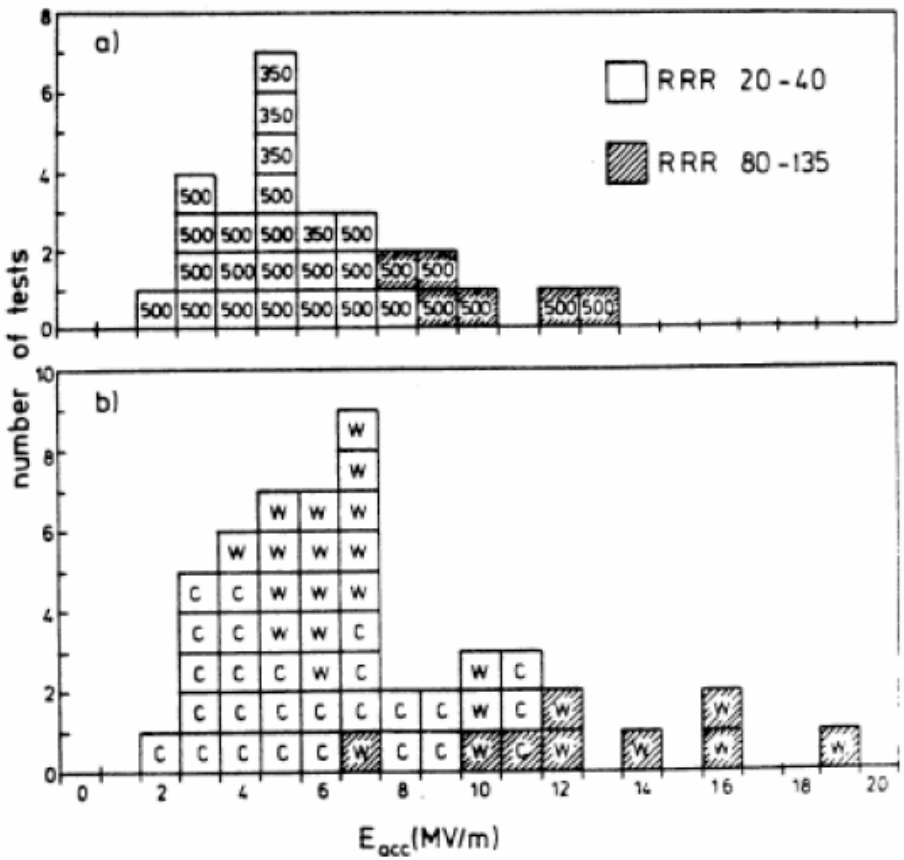

Fig. 3: Histogram of test results for single cell cavities from niobium of different RRR
a) 500 and 350 MHz
b) 3 GHz (CERN and Wuppertal)

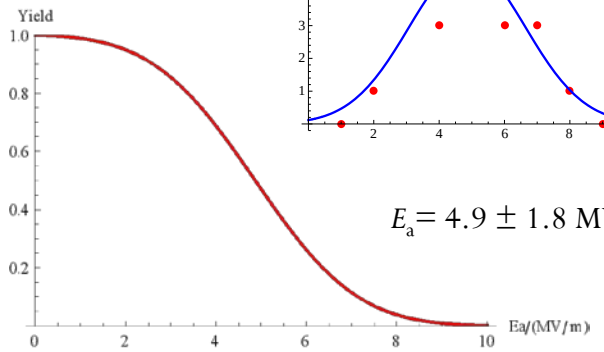

$E_a = 4.9 \pm 1.8$ MV/m

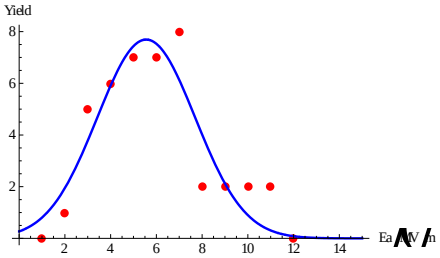

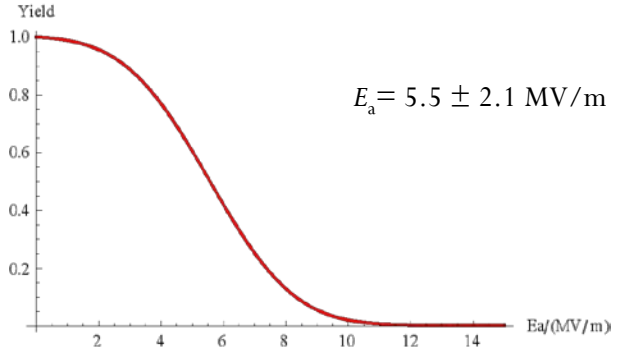

$E_a = 5.5 \pm 2.1$ MV/m

Thin film Nb coating 1/2

- Coating a copper cavity with a thin Nb film

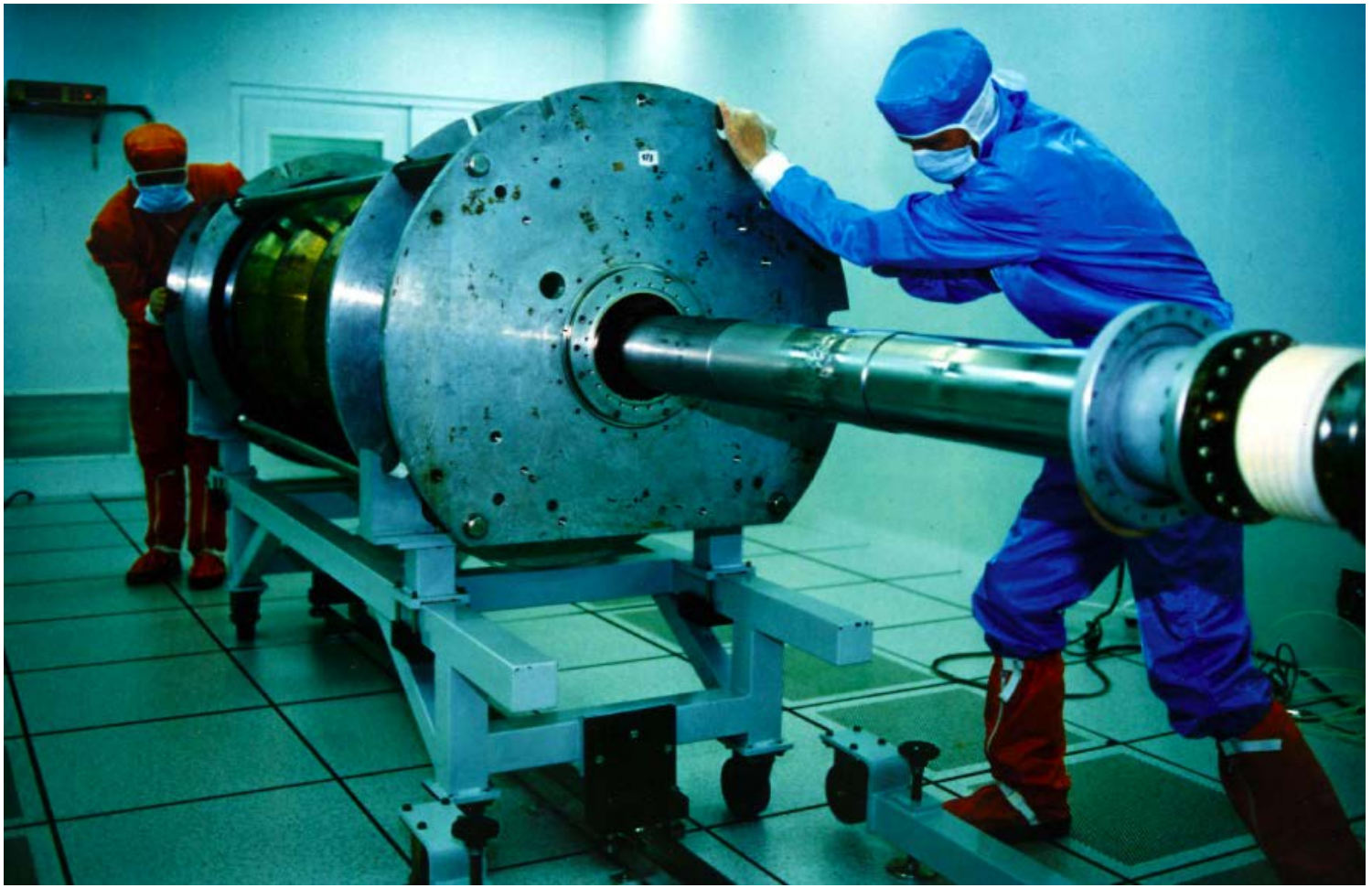

Thin film Nb coating 2/2

- Important role of high thermal conductivity subtrate (Nb/Cu cavity)

Improvement of QA efforts: ORNL/JLAB results

Nevertheless, in spite of all technological efforts, performance of sc cavities is often stochastic

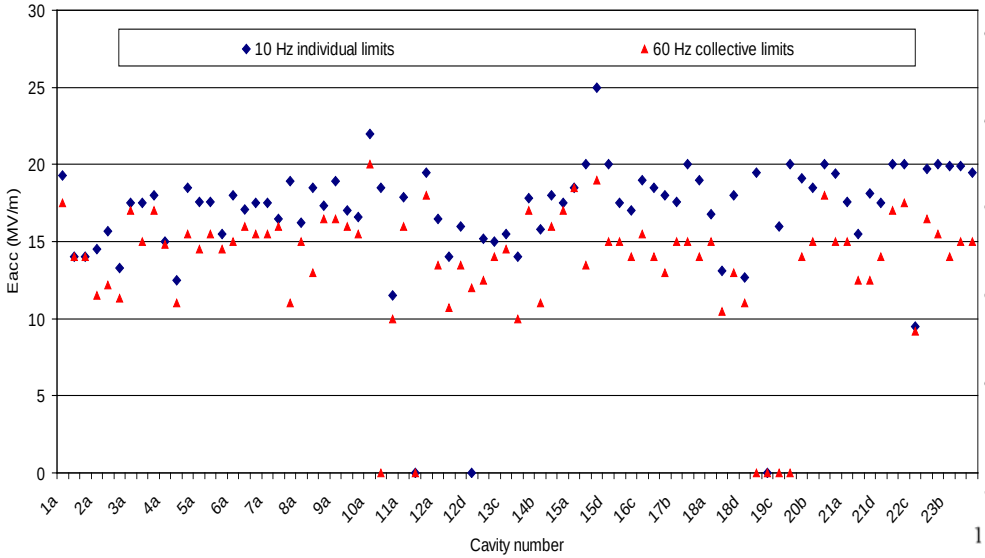

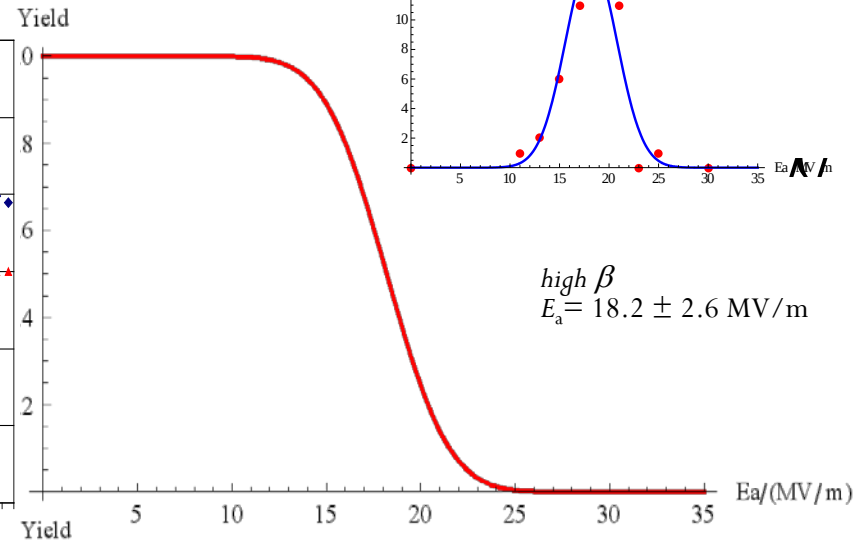

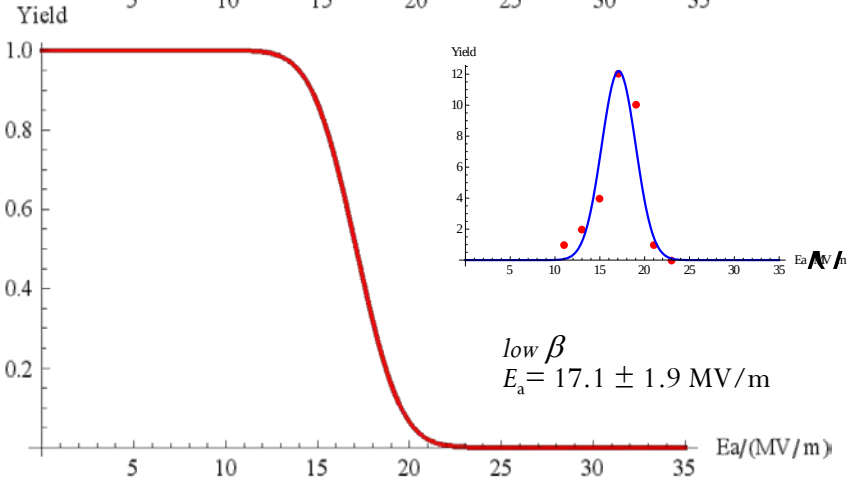

Source: I. E. Campisi and S.–H. Kim, **SNS Superconducting Linac operating experience and issues**,

Accelerator Physics and Technology Workshop for Project X, November 12-13, 2007

http://projectx.fnal.gov/Workshop/Breakouts/HighEnergyLinac/agenda.html

Stochastic parameters

Influencing quantity	Impact quantity	Physical explanation	Cure
Field emission sites (foreign particles sticking to the surface, size, density)	Q – value / acc. gradient γ radiation HOM coupler quench	Modified Fowler-Nordheim-theory	Electro-polishing Assembling in dust-free air Rinsing with ultrapure water (control of resistivity and particulate content of outlet water) and alcohol High pressure ultrapure water rinsing (ditto) "He- processing" Heat treatment @ 800 – 1400 °C
Secondary emission coefficient δ	Electron-multipacting	Theory of secondary electron emission	Rounded shape of cavity Rinsing with ultrapure water Bake-out RF - Processing
Unknown	Q – slope / Q-drop (Q – value / acc. gradient)	***Unknown***	Annealing 150 °C Electro-polishing
Metallic normal-conducting inclusions in Nb	Acc. gradient	Local heating up till critical temperature of Nb	Inspection of Nb sheets (eddy current or SQUID scanning) Removal of defects ($\approx$ 1 µm) Sufficiently large thermal conductivity (30 - 40 [W/(mK)])
Residual surface resistance	Q – value / acc. gradient	***Unknown to large extent***	Quality assurance control of a multitude of parameters

Improvement of cavity performance

Lilje & Schmueser

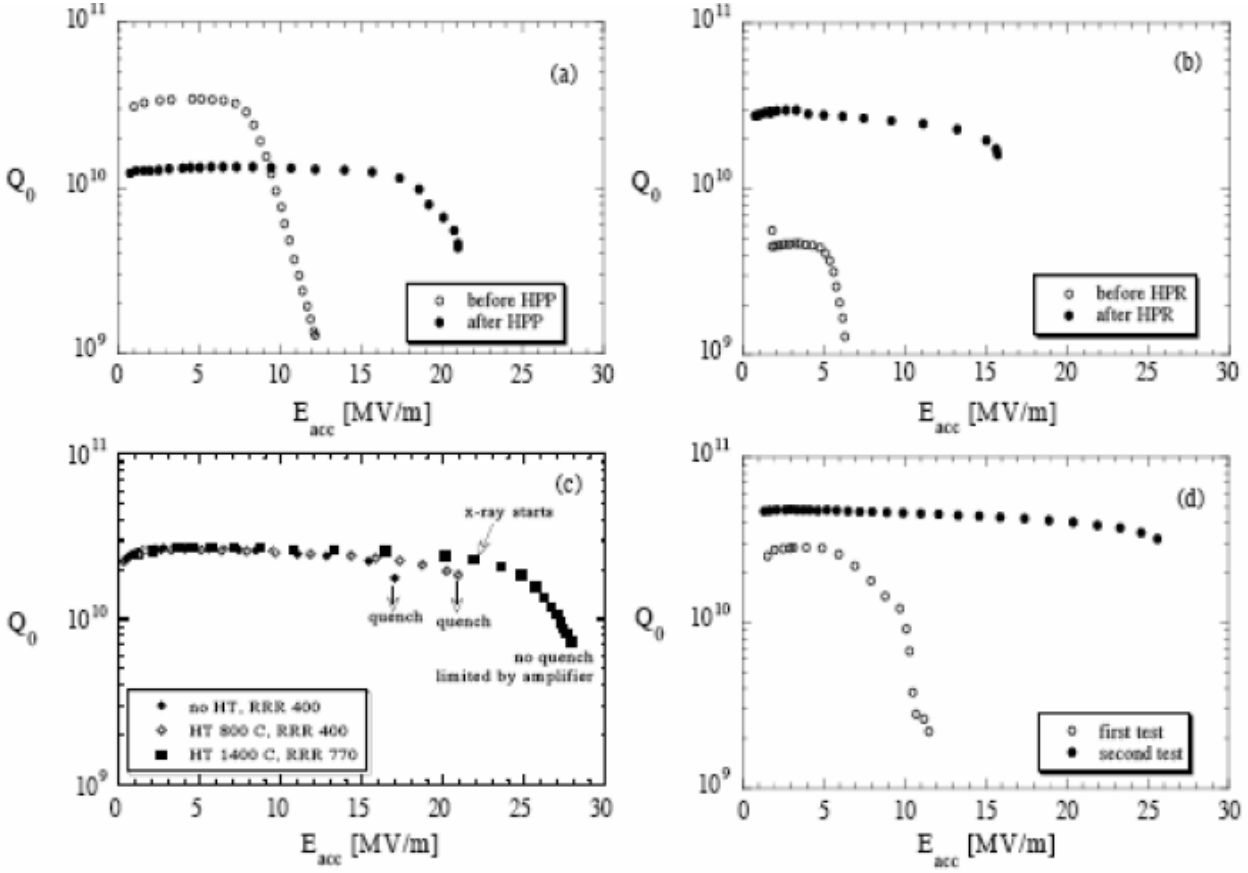

Figure 27: Improvement in cavity performance due to various treatments: (a) high power processing, (b) high pressure water rinsing, (c) successive application of 800°C and 1400°C heat treatment, (d) removal of surface defects or titanium in grain boundaries by additional BCP. All tests were done at 1.8 K [Aune et al. 2000].

Cryomodules 1/2

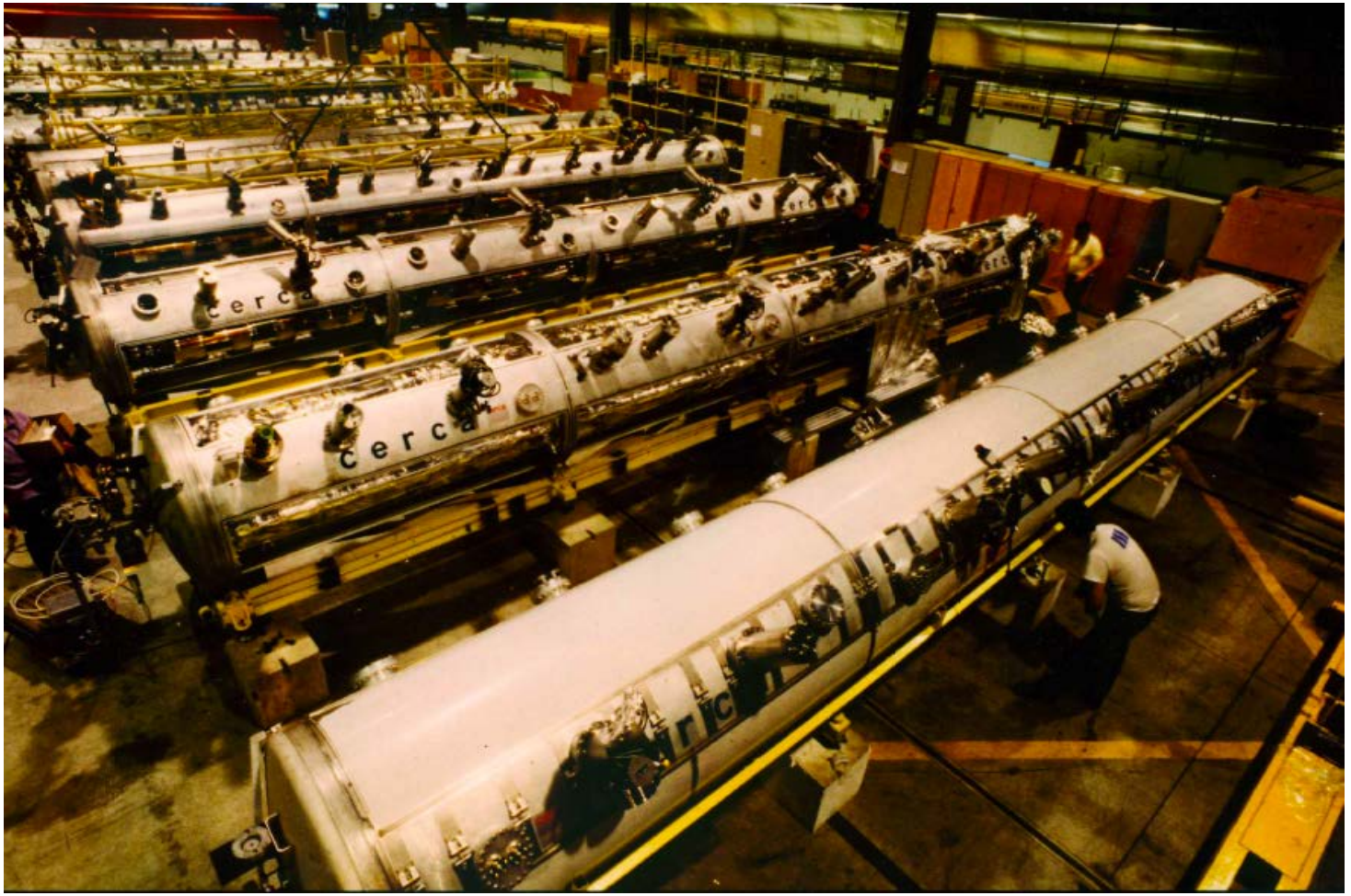

Cryomodules 2/2

- installed in LEP tunnel

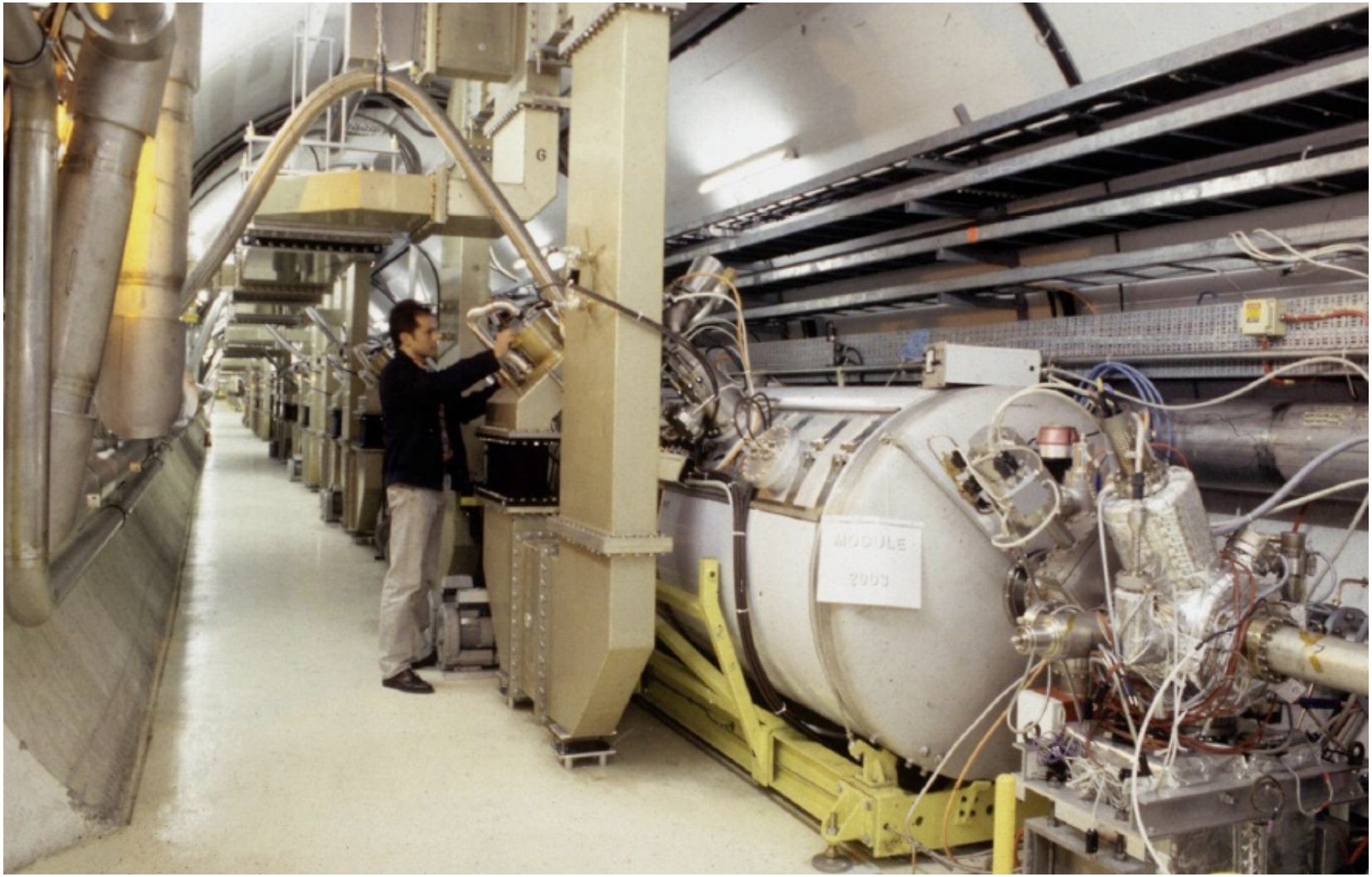

Magnetic shielding 1/2

- Why do we need a magnetic shielding?

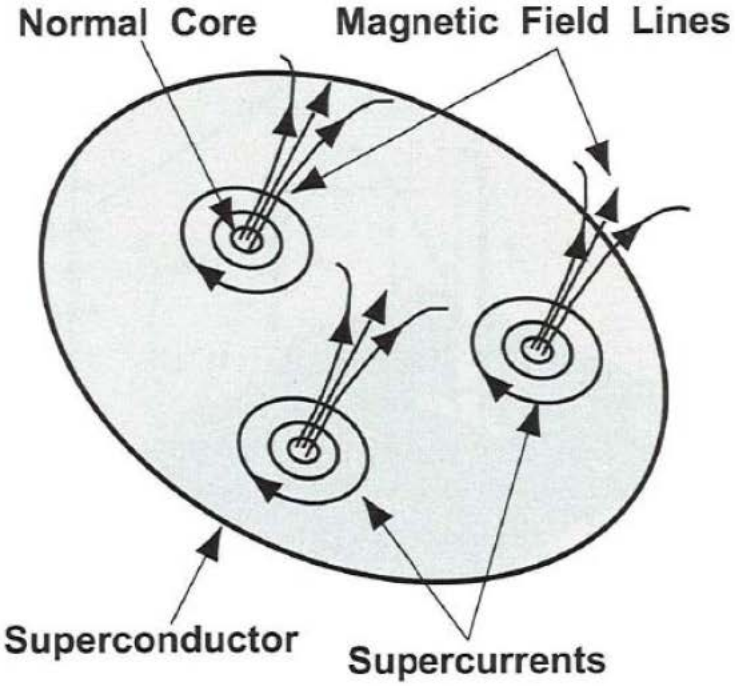

$$R_{mag} = \frac{H_{ext}}{2H_{c2}} R_n$$

$$R_{mag}[n\Omega] = 3H_{ext}[\mu T]\sqrt{f[GHz]}$$

Tobias.Junginger@quasar-group.org

Magnetic shielding 2/2

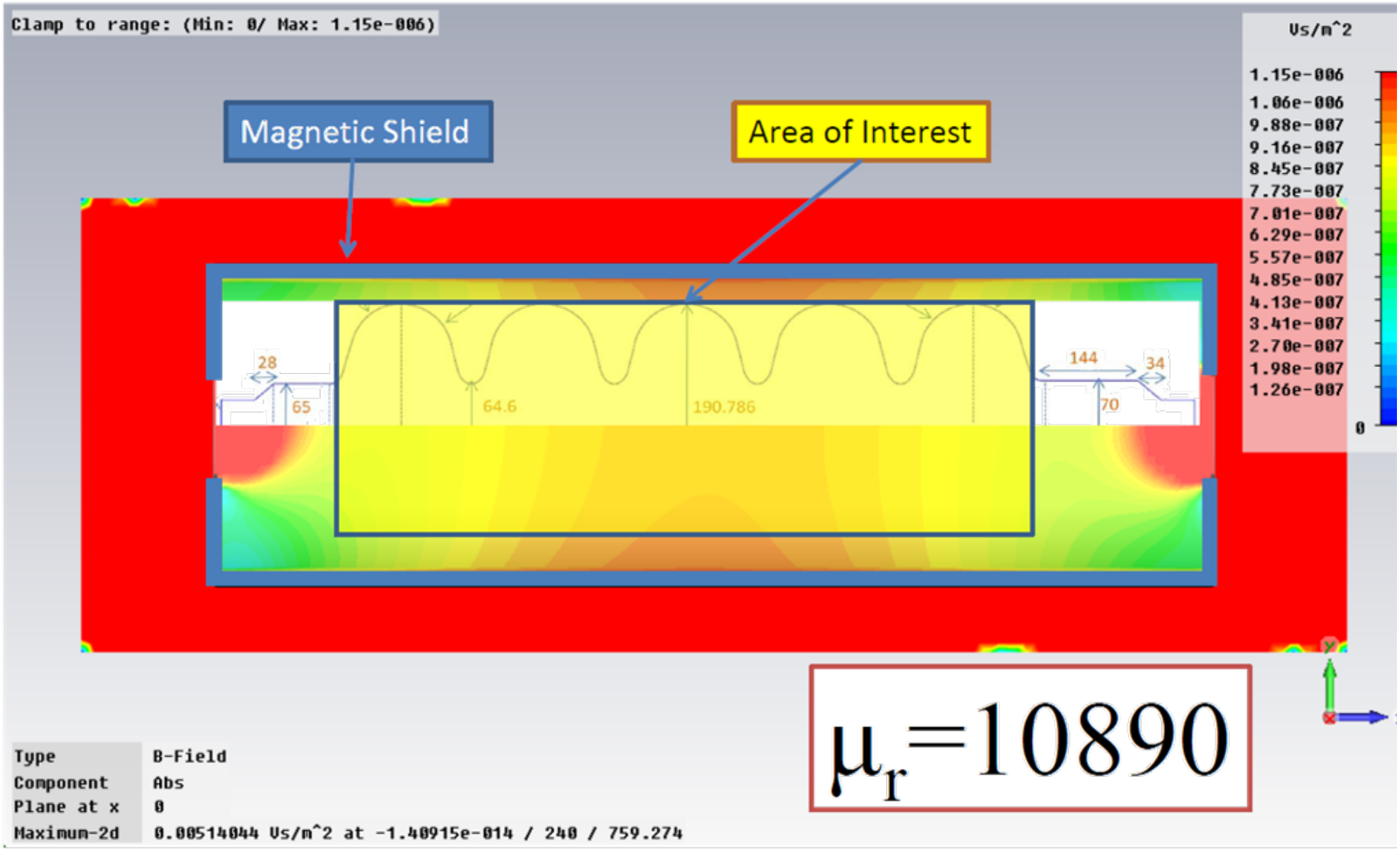

$\mu_r = 10890$

Summary

- The choice of the technology (normal conducting vs.. superconducting) depends on a variety of parameters: mass of accelerated particle, beam energy, beam current, mains power consumption, etc.
- If superconducting, the typical interval of RF frequencies is between 300 MHz and 3 GHz.
- The technically most suitable superconducting material being niobium, choosing lower frequencies allows operation at 4.2 – 4.5 K, the boiling temperature of lHe, higher frequencies request operation at 1.8 – 2 K. However, the cryogenic installation is much more demanding.
- The production of sc cavities requests careful application of quality control measures during the whole cycle of assembly in order to avoid the degradation of performance by « anomalous losses ».
- The « anomalous losses » contribute to an extra heat load, which is expensive to cool and which may limit the performance.
- The cryostats (and cryomodules) comprise the RF cavity, the power and HOM couplers, the frequency tuners, the RF probe connectors, the UHV pumps, and the reservoir for lHe, housed in a thermally isolated vacuum vessel.

Applications and outlook

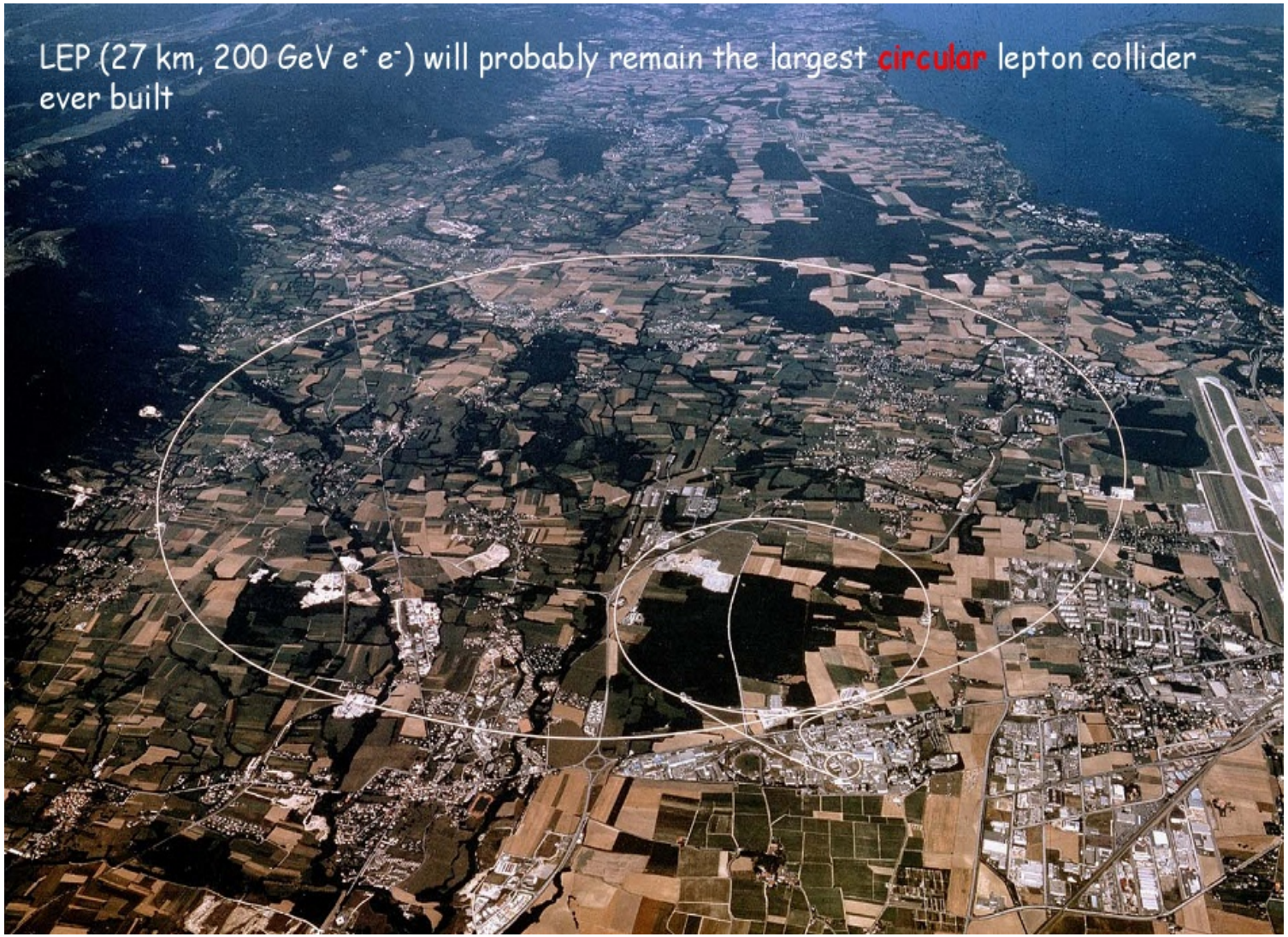

LHC - CERN

XFEL – DESY 1/3

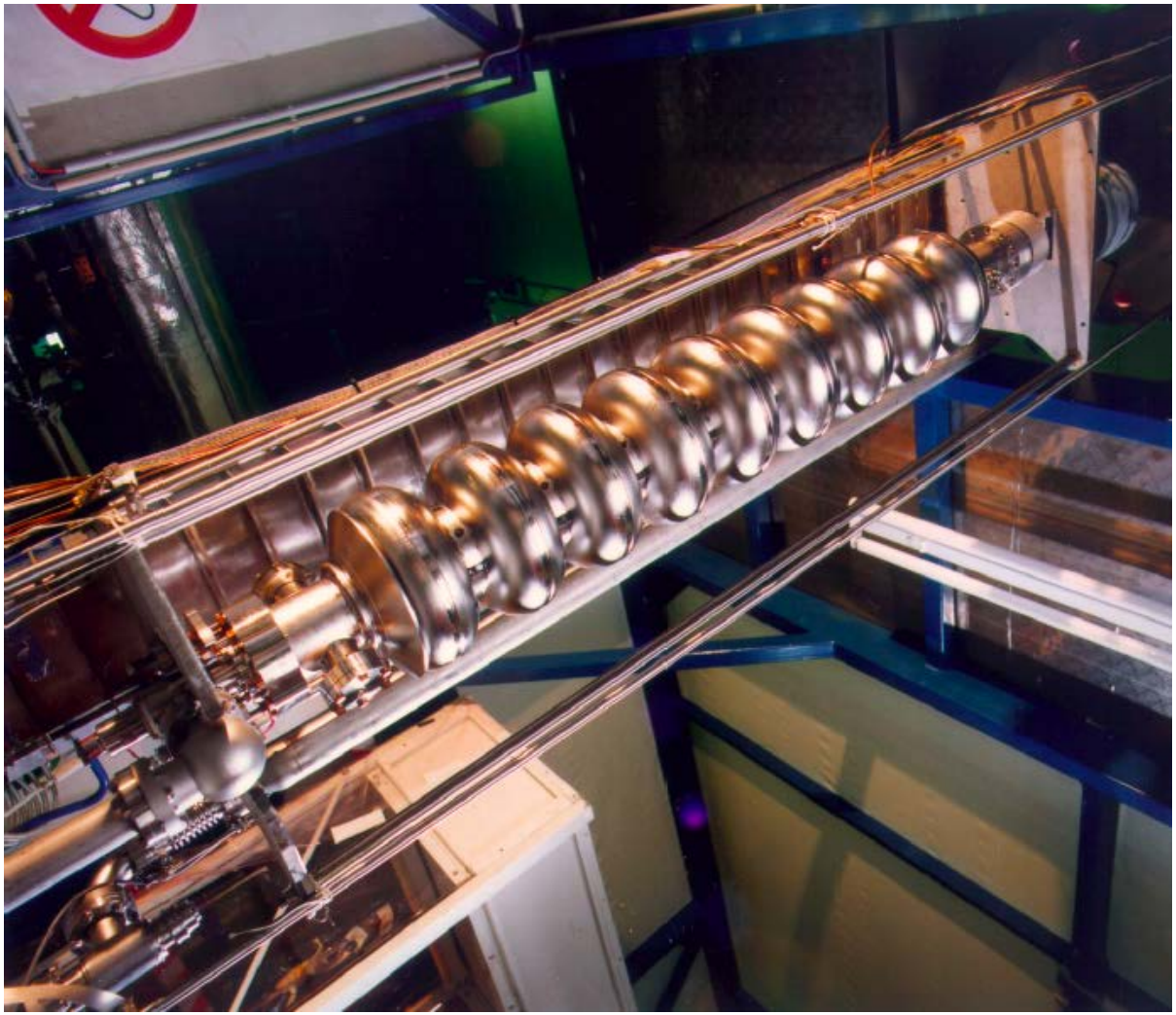

XFEL - DESY 2/3

XFEL - DESY 3/3

CEBAF - JLAB

SPL - CERN/ SNS - ORNL

Prototype Beta 0.61 and .81 Cavities

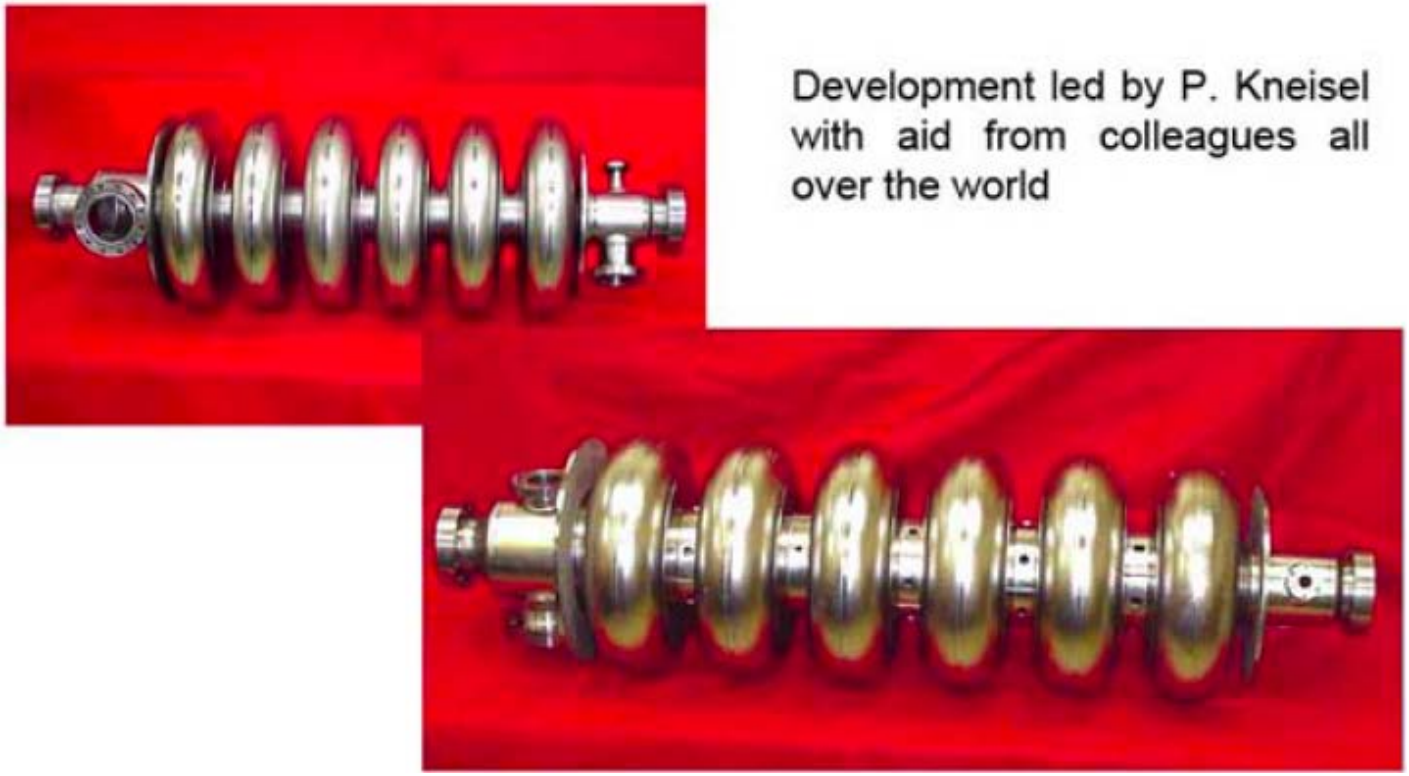

Development led by P. Kneisel with aid from colleagues all over the world

Heavy Ion accelerators ATLAS - ANL

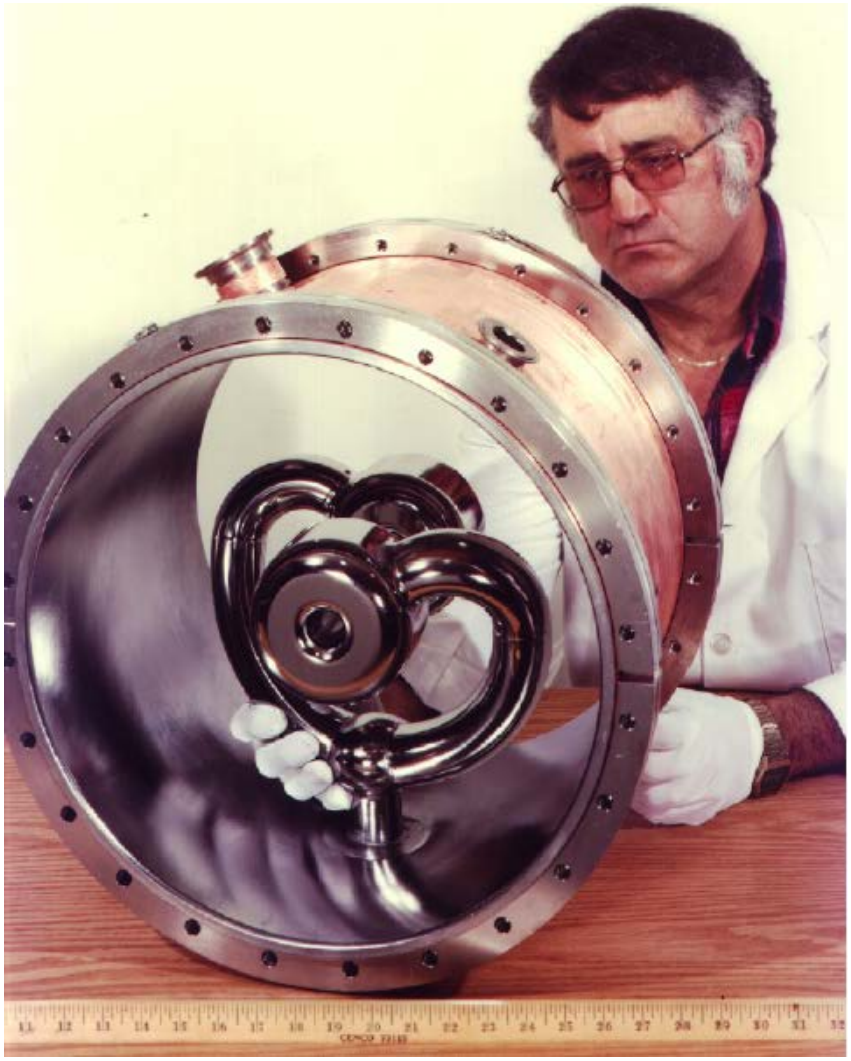

Shapes of heavy ion accelerator cavities

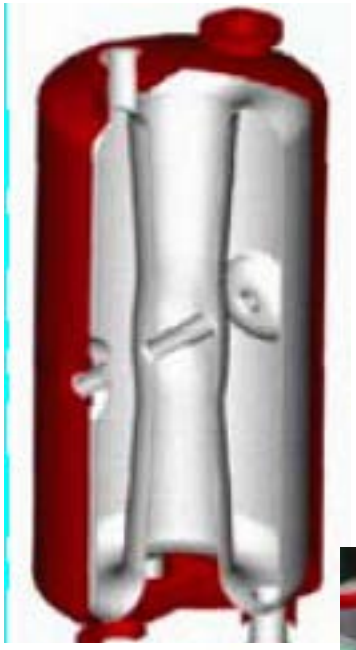

Recent progress of SRF

SRF2009 Contributions to the Proceedings:

http://accelconf.web.cern.ch/AccelConf/srf2009/index.htm

Next SRF "Conference" scheduled for 2011at Chicago, Ill., USA:

http://conferences.fnal.gov/srf2011/index.html